DURABILITY OF NITINOL FOR STRUCTURAL APPLICATIONS

Except where reference is made to the work of others, the work described in this thesis is my own or was done in collaboration with my advisory committee. This thesis does not include proprietary or classified information.

_____
David McCarty

Certificate of Approval:

_____   _____
Robert W. Barnes   Mary L. Hughes, Chair
Associate Professor   Assistant Professor
Civil Engineering   Civil Engineering

_____   _____
Anton K. Schindler   Mark O. Barnett
Gottlieb Assistant Professor   Associate Professor
Civil Engineering   Civil Engineering

_____
Stephen L. McFarland
Acting Dean
Graduate School

DURABILITY OF NITINOL FOR STRUCTURAL APPLICATIONS

David McCarty

A Thesis

Submitted to

the Graduate Faculty of

Auburn University

in Partial Fulfillment of the

Requirements for the

Degree of

Master of Science

Auburn, Alabama
August 7, 2006

DURABILITY OF NITINOL FOR STRUCTURAL APPLICATIONS

David McCarty

_____
Signature of Author

_____
Date of Graduation

VITA

     David McCarty was born March 20, 1982, in Birmingham, Alabama. He graduated from Vestavia Hills High School of Birmingham in 2000 and enrolled at Vanderbilt University. In 2004, he graduated magna cum laude from Vanderbilt with a Bachelor of Science degree in Civil Engineering. The following August, he entered graduate school at Auburn University seeking a Master of Science degree in Civil Engineering with a specialization in structural engineering.

THESIS ABSTRACT

DURABILITY OF NITINOL FOR STRUCTURAL APPLICATIONS

David McCarty

Master of Science, August 7, 2006
(B.S., Vanderbilt University, 2004)

169 Typed Pages

Directed by Mary L. Hughes

Nitinol is a shape memory alloy that has recently been studied for its suitability as a material in energy dissipation devices in structures. The alloy has excellent structural capabilities in terms of strength and elasticity, but it has not been evaluated in terms of durability issues such as corrosion resistance. This thesis investigates the corrosion-related durability of nitinol in environments that are commonly corrosive to civil structures. Furthermore, this research compares the corrosion performance of nitinol to that of A992 and A588 steel, since steel is the metal most abundantly used in structures and is in many ways similar to nitinol. The ultimate objective of this research is to determine whether nitinol is more or less resistant to corrosion than structural steel. If nitinol is shown to have better corrosion resistance than structural steel, it can safely be used in the same environments in which structural steel is currently used.

Since laboratory corrosion test results cannot be easily correlated to real-life performance, this research studies steel and nitinol in identical testing conditions and

compares the performance of the two. The procedure for corroding the specimens is based on ASTM International standards. After the specimens are corroded, their mechanical performance is evaluated by tension testing. Additionally, the solutions used to corrode the specimens are analyzed as another means of comparing corrosion performance. The combination of results is used to determine whether or not nitinol is suitable as a structural engineering material, based on strength degradation due to corrosion.

Testing performed for this research indicates that nitinol resists corrosion much better than structural steel of grades A992 and A588. Therefore, nitinol can be used in the same environments in which these grades of steel are currently used, without undue risk of failure due to corrosion. Based on the results of this research, it can be concluded that nitinol is a safe material for structural engineering in terms of corrosion resistance.

ACKNOWLEDGEMENTS

Style manual or journal used: <u>Guide to Preparation and Submission of Theses</u>

<u>and Dissertations</u>

Computer software used: <u>Microsoft Word, Microsoft Excel</u>

TABLE OF CONTENTS

LIST OF FIGURES

LIST OF TABLES

CHAPTER 1 – INTRODUCTION

1.1 Statement of Problem

Nitinol is a shape memory alloy that has many applications in mechanical engineering, electrical engineering, and the medical field. Recently, structural engineers have begun to experiment with the use of nitinol in civil structures. The appeal of nitinol comes from its unique superelastic property, which allows nitinol to remain elastic within a strain range much larger than traditional civil engineering materials. Additionally, the superelasticity of nitinol leads to enhanced energy dissipation characteristics, which is particularly advantageous for structures prone to seismic loads. The superelasticity and energy dissipation of nitinol have led many engineers to believe that it is an efficient alternative to steel for connections and for other energy dissipation devices.

In the past decade, many studies have been conducted that document nitinol's mechanical performance (Aizawa et al. 1998; DesRoches et al. 2004; Dolce et al. 2001). It has generally been accepted that nitinol's resistance to corrosion, exhibited in medical applications, will render it a durable material for civil applications as well. Very little information is available, though, that shows data related to nitinol's durability characteristics in the types and sizes that would be used in structural components. Before nitinol can be accepted as a viable material for structures, it must first be shown that the material has acceptable durability properties. A primary durability concern for metals in structures is their ability to resist corrosion. To date, several studies performed in the

medical field have investigated the corrosion resistance of nitinol in the human body (Carroll et al. 2003; Rondelli 1996; Shabalovskaya et al. 2003). These studies have mixed results, but several agree that nitinol shows promise as a corrosion resistant material. However, structural use of nitinol differs from medical use of nitinol in terms of environment, function, component sizes, and acceptable levels of corrosion. Therefore, the structural community will benefit from a corrosion study of nitinol that specifically addresses the issues common to civil structures.

Unfortunately, practical corrosion testing of a metal can be problematic. The most accurate method for determining a corrosion rate of structural nitinol would be to measure the depth of corrosion in a structure that has been exposed to the elements for a long-term period such as ten or twenty years. Since nitinol is not currently used in structures, and likely will not be until its corrosion resistance and performance characteristics are proven, this method is impractical. Another option for determining corrosion rates is accelerated corrosion testing. Though these tests are helpful in determining the corrosion potential of a metal, it is difficult to accurately correlate their results to a depth per time corrosion rate. With these limitations, the most practical solution is to perform accelerated corrosion tests on nitinol and structural steel, and to compare the results. If testing shows nitinol to have less potential for corrosion than steel, it can be inferred that nitinol has sufficient corrosion resistance to be used in the same capacity as structural steel.

1.2 Objective

The objective of this research is to compare the corrosion resistance of nitinol with that of structural steel, and the effect of corrosion on the mechanical properties of each. Both materials were corroded in solutions that mimic some of the most common corrosive environments for civil structures. Afterwards, the materials were evaluated to determine the extent of damaged caused by corrosion. The ultimate goal was to conclude whether nitinol performs better or worse than structural steel, in terms of mechanical performance degradation, when subjected to a corrosive environment.

1.3 Work Plan

A brief outline of the work plan to accomplish the research objective is given below.

1. Obtain steel and nitinol specimens.

2. Develop an accelerated corrosion test based on ASTM International standards.

3. Perform tensile tests on uncorroded specimens to quantify their yield strength and ultimate strength.

4. Corrode specimens in solutions that imitate a corrosive environment for civil structures.

5. Perform tension tests on the corroded specimens and note the decrease in yield strength and ultimate strength as compared to the uncorroded specimens.

6. Develop additional methods of measuring corrosion that involve testing of the solutions used to corrode the specimens.

7. Test the solutions to determine which metal is more reactive with a given solution.

8. Use results from the various types of testing to conclude which metal is more prone to corrosion in structures.

1.4 Scope

This investigation is limited to short-term accelerated corrosion tests. The solutions used for corrosion were similar to conditions found in environments that are known to cause corrosion problems in civil structures. Data resulting from this investigation is intended to be used to compare the corrosion resistance of nitinol and steel in civil structures.

CHAPTER 2 – LITERATURE REVIEW

2.1 Shape Memory Alloys

Shape memory alloys (SMAs) are unique materials that can undergo large strains without any permanent deformation. The recoverable elongation of SMAs is in the range of 8-10%, significantly higher than common metals such as structural steel, which typically has a recoverable elongation of less than 1% (Dolce et al. 2001). After the deformation process, SMAs return to their original shape upon removal of the load or by heating. SMAs that return to their original shape by heating exhibit the shape memory effect, whereas SMAs that recover their shape by removal of the load are said to exhibit a superelastic effect. The superelastic effect differs from typical elastic behavior because it involves a phase change, discussed in more detail below (DesRoches et al. 2004).

2.1.1 Austenite and Martensite

The unusual properties of SMAs are due to a reversible solid-to-solid phase transformation (Dolce et al. 2001). The change from the parent phase, known as austenite, to the transformed phase, martensite, is characterized by a shift in the crystal structure. Each phase has its own unique crystal structure, but the chemical nature of the matrix is the same for either phase (Duerig et al. 1990). The austenite phase exhibits a cubic crystal structure, while the martensite phase has an orthorhombic crystal structure (Dolce et al. 2001). The phase transformation from austenite to martensite can be broken down into two types of crystal movements: lattice deformation and lattice-invariant

5

shear. Lattice deformation, depicted schematically in Figure 2.1, refers to the atomic movements necessary to produce the new crystal structure. In Figure 2.1(c), one can see that each atom is only required to move a very small amount, but the net effect is an entirely new geometry. Lattice invariant shear, the second part of martensitic transformation, is necessary to accommodate the original shape of the austenite phase. If the martensitic crystal structure shown in Figure 2.1(d) did not undergo lattice invariant shear, it would be incompatible with the surrounding austenite. Lattice invariant shear can occur by two mechanisms: slip and twinning, shown in Figures 2.2(a) and 2.2(b), respectively. Either of these mechanisms transforms the crystal structure such that it occupies the same space as the austenite from which it was transformed. Twinning is a reversible process, whereas slip results in permanent deformation (Duerig et al. 1990).

At relatively high temperatures and in the stress-free state, SMAs are in the parent austenitic phase. If cooled to a specific temperature, M_s, the SMA will start the transformation to martensite. This process will continue until the temperature drops below M_f, the temperature at which the transformation to martensite finishes. Similarly, the inverse transformation from martensite to austenite is marked by two temperatures: A_s and A_f, the temperatures at which the transformation starts and finishes, respectively (Dolce et al. 2001).
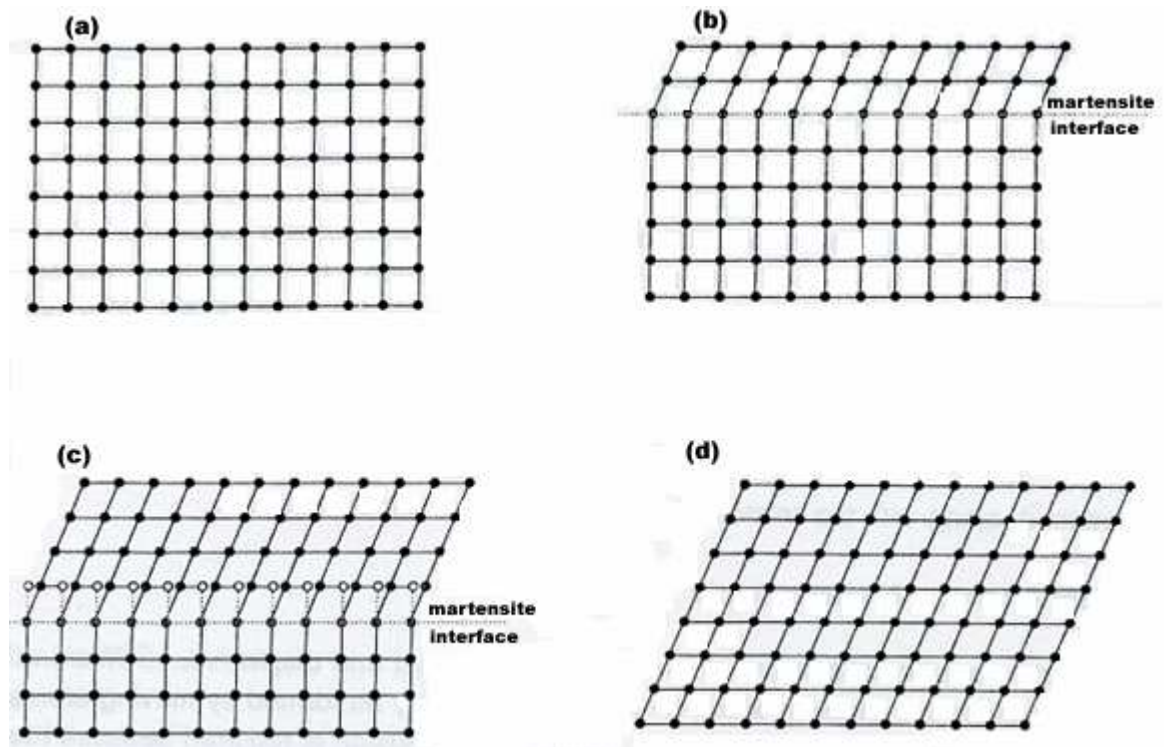
Figure 2.1 Schematic two dimensional drawing of the progressive transformation from
austenite to martensite. In (a) the material is completely austenitic and in (d) the material
is completely martensitic (Duerig et al. 1990).

(a) Accommodation by slip

(b) Accommodation by twinning
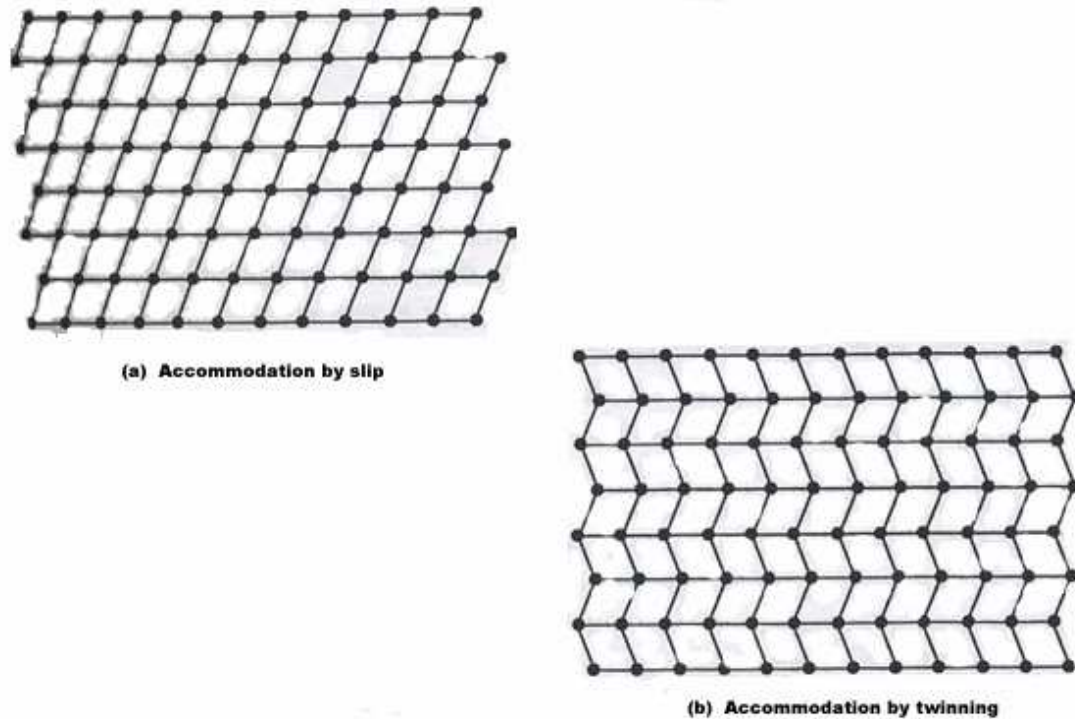
Figure 2.2 The two mechanisms of accommodating shape change due to the atomic shear of a martensitic transformation. Slip results in permanent deformation, but twinning is reversible (Duerig et al. 1990).

2.1.2 Superelastic versus Shape Memory Effect

It is the metallurgy, chemical composition, and heat treatment of a SMA that determine whether the SMA will exhibit the shape memory effect or the superelastic effect. If the shape memory effect is desired, the alloy is chemically engineered so that the M_f and M_s temperatures are higher than the temperature range expected for the environment in which the alloy will be employed. The result is that the SMA alloy will begin in a state of twinned martensite. SMA specimens that demonstrate the shape memory effect are said to be martensitic, since they are typically in their martensitic phase before application of stress or temperature. Conversely, if the superelastic effect is

desired, the alloy is chemically engineered so that the M_f and M_s temperatures are *lower* than the temperature range expected for the alloy's environment. In this case, the alloy begins in the parent austenite phase. Accordingly, these superelastic specimens are said to be austenitic. Though either type of specimen can go through a martensite and austenite phase, standard SMA terminology dictates that a shape memory specimen is called martensitic and a superelastic specimen is called austenitic, because these are the phases in which the specimens exist before any application of stress or heat (Duerig et al. 1990).

When stress is applied to a martensitic specimen, there is a critical value at which "detwinning" occurs. Detwinning refers to the spatial reorientation of the martensitic variants due to the applied stress. Figure 2.3 shows detwinning and slip as they relate to the stress-strain diagram of a SMA alloy (Duerig et al. 1990). During the detwinning process, the stress remains nearly constant until the martensite detwins completely. Further straining beyond this point results in elastic loading of the detwinned martensite (Dolce et al. 2001). At an even higher critical stress value, martensitic variants begin to slip, causing permanent deformation. If the specimen is unloaded before slip, a residual deformation will remain because the martensite is in the detwinned position. However, this deformation is not permanent. When heated above A_f, the material transforms into austenite and the initial shape is recovered. When the specimen cools below M_f, it re-transforms into martensite. Since there is no applied stress at this time, the martensite twins to accommodate the macroscopic shape of the specimen. Thus, a full cycle has been completed, and the specimen is in the same shape and phase as before it was loaded. Figure 2.4 shows the path of this cycle on the stress-strain diagram (Dolce et al. 2001).
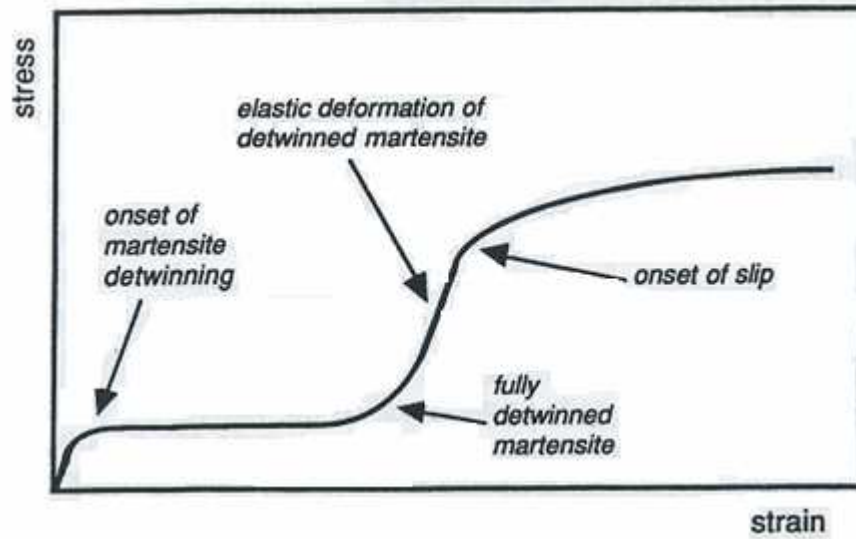
Figure 2.3 A typical stress-strain curve for a twinned martensitic material shows two distinct elastic regions and two distinct plasticity plateaus. The first plateau is due to detwinning, and the second is due to slip (Duerig et al. 1990).

NOTATIONS :

a : austenite

m : twinned martensite

m*: detwinned martensite
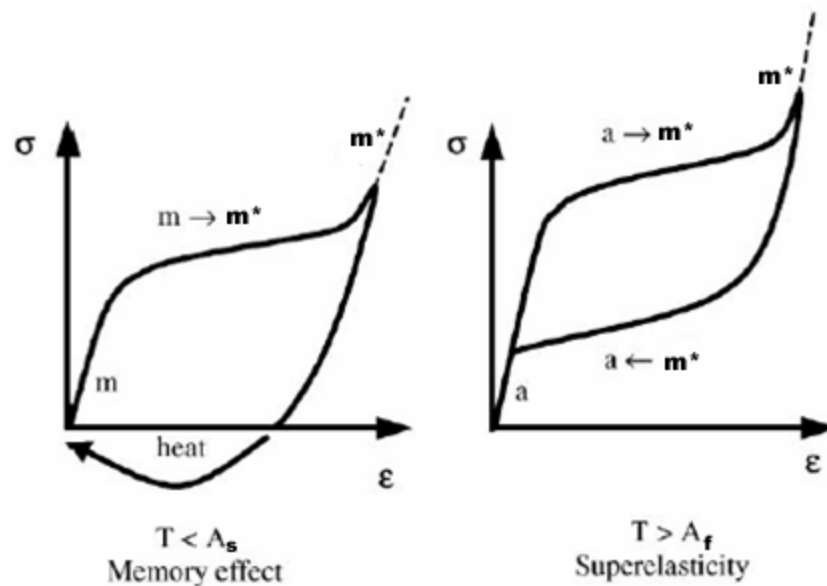
Figure 2.4 Schematic stress-strain curves of an SMA (Dolce et al. 2001).

When stress is applied to an austenitic specimen, there is a critical value at which

the material begins to transform from austenite directly to detwinned martensite. As the

transformation continues, the stress remains practically constant until the transformation

is complete. Further straining leads to the elastic loading of detwinned martensite. If the

load continues to increase, permanent deformation occurs as the martensitic variants

begin to slip. If the specimen is unloaded before slip, a reverse transformation takes

place. This reverse transformation from martensite back to austenite occurs at a lower

stress level than during loading, thereby creating a hysteretic effect. Since the

temperature is already above A_f, this reverse transformation occurs spontaneously, so that

the specimen recovers its original shape without any application of heat. This cycle is

shown in Figure 2.4, as compared to the similar cycle for a martensitic specimen (Dolce

et al. 2001). Figure 2.5 gives another interpretation of the stress-strain diagrams for the

shape memory effect, superelastic effect, and ordinary plastic deformation. Here, it can

be seen that the shape memory effect is temperature dependent, whereas the superelastic

effect and ordinary plastic deformation occur in isothermal conditions (DesRoches et al.

2004). A comparison of these cycles as they relate to the crystal structure of the alloy is

depicted in Figure 2.6.

Both shape memory SMAs and superelastic SMAs can be exploited in a variety of

engineering applications. Electrical connections can be improved by using SMAs to vary

the force applied to the connection at different temperatures (Kulisic et al. 1998). The

medical field has employed SMAs for a myriad of functions including stents, guidewires,

clinical instruments, and even permanent birth control devices (Morgan 2004).

Mechanical applications include safety devices such as over-temperature cut off valves

(Van Humbeeck 2001). In the majority of current applications, the shape memory effect

is used. In structures, however, the superelastic property is more appropriate (DesRoches

et al. 2002). Accordingly, discussion of SMAs in the remainder of this chapter will focus

on the superelastic property.
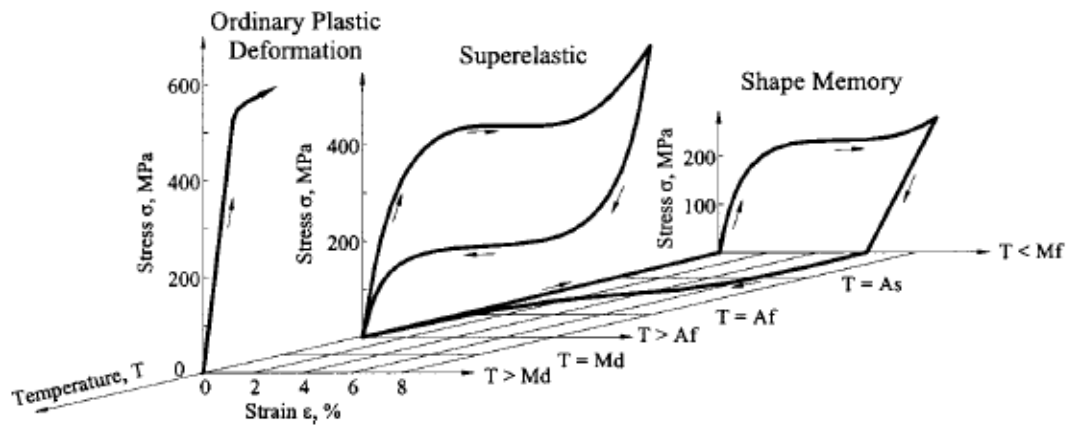
Figure 2.5 Three-dimensional stress-strain temperature diagram showing deformation and shape memory behavior of a SMA (DesRoches et al. 2004)

SHAPE MEMORY

Twinned Martensite, below A_s

Apply load → Martensite detwins

Detwinned Martensite, Below A_s
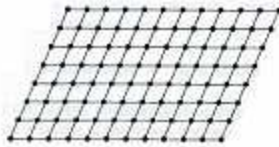
Remove load → Deformation remains

Apply heat → Austenite forms

Austenite, above A_f

Remove heat → Alloy cools below M_f
→ Twinned martensite forms

Twinned Martensite, below A_s

SUPERELASTIC

Austenite, above A_f

Apply load → Martensite forms without twinning

Detwinned Martensite, Above A_f
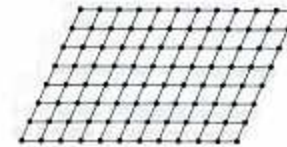
Remove load → Martensite unstable
→ Austenite forms

Austenite, above A_f

Figure 2.6 Comparison of shape memory and superelastic cycles as they relate to the crystal structure of nitinol (adapted from Duerig et al. 1990)

13

2.2 Nitinol

2.2.1 History

Nitinol is a Nickel-Titanium shape memory alloy that was developed in 1958 by William J. Buehler (Ford et al. 1996). At the time, Buehler was working at the Naval Ordnance Laboratory in Maryland, which gave rise to the acronym nitinol, for NIckel TItanium Naval Ordnance Laboratory. Buehler, pictured in Figure 2.7, knew that there was something unique about nitinol because he noticed that the alloy's acoustic properties changed at different temperatures. However, the shape memory property of nitinol was not recognized immediately. In 1961, Buehler's assistant was demonstrating the fatigue-resistance of nitinol by compressing a flat strip into an accordion shape. One of the men in the meeting applied heat to the compressed strip using his pipe lighter, and to everyone's amazement, the strip stretched out longitudinally. This exciting new discovery sparked more interest in the research and development of nitinol (Kauffman et al. 1997).

But the advancement of nitinol was initially slow. Manufacturing processes had not been perfected, which resulted in inconsistencies among batches of nitinol that were intended to perform identically (Johnson 1988). Additionally, material and processing costs were high since the industry was in its infancy (Duerig et al. 1999). Finally, many of the proposed uses for nitinol competed with existing products. Manufacturers were reluctant to experiment with a new material if they could fabricate similar products with technology that had proven to be reliable (Johnson 1988).

Figure 2.7 William J. Buehler demonstrating nitinol wire in 1968. As electricity was passed through a straight piece of wire, the wire would change into the word "innovations" (Kauffman et al. 1997).

Since the mid-nineties, the demand for nitinol has grown tremendously. Precise composition control in the production process has greatly limited the variation of properties between different batches of nitinol (Duerig et al. 1990). Material prices have come down, and potential functions for nitinol are abundant. Though nitinol is used in many engineering disciplines, it is the medical field that has most strongly driven the advancement of nitinol (Duerig et al. 1999).

2.2.2 Properties

Aside from the unique phase change, the properties of nitinol are not unlike those of ordinary engineering metals such as steel. The yield strength falls in the range of 30-

118 ksi and the ultimate tensile strength ranges from 125 ksi up to 155 ksi (Cross et al. 1969; Schuerch 1968; DesRoches et al. 2002; Special Metals 2006). The broad range of reported values can be attributed to variations in chemical compositions and historical advances in nitinol production, but precise composition control ensures that a more exact value can be obtained during production (Duerig et al. 1990). The upper range of yield strength is higher than that of commonly-used structural steels, which typically range from 36 ksi to 70 ksi (McCormac et al. 2003). Even the lower end of the ultimate tensile strength spectrum is higher than typical structural steel values of 65-100 ksi (AISC 2001). The density of nitinol is .234 lb/in^3 (Cross et al. 1969), which is less than the density of steel at .284 lb/in^3 (Hibbeler 2000). Therefore, nitinol has a higher strength-to-weight ratio than steel. In other categories, nitinol and steel perform nearly identically. For example, Poisson's ratio is .33 for nitinol (Jackson et al. 1972) and .32 for steel (Hibbeler 2000). The melting point of nitinol is between 1240º C and 1310º C (Jackson et al. 1972), whereas the melting point of steel is 1370º C (Kross 2006). One property that differs significantly between steel and nitinol is the modulus of elasticity. Nitinol's low modulus of elasticity and unique phase change lead to an elongation at failure that is higher than the elongation at failure for typical structural steel. Table 2.1 compares properties of nitinol and structural steel (DesRoches et al. 2002), and Figure 2.8 provides a thorough list of physical and mechanical properties for an early generation of nitinol (Schuerch 1968).

Table 2.1 Comparison of nitinol properties with typical structural steel (DesRoches et al. 2002)

Property	Ni–Ti shape memory alloy	Steel
Recoverable elongation	8%	0.2%
Young's modulus	8.7E4 MPa (Austenite), 1.4–2.8E4 MPa (Martensite)	2.07×10^5 MPa
Yield strength	200–700 MPa (Austenite), 70–140 MPa (Martensite)	248–517 MPa
Ultimate tensile strength	900 MPa (fully annealed), 2000 MPa (work hardened)	448–827 MPa
Elongation at failure	25–50% (fully annealed), 5–10% (work hardened)	20%
Corrosion performance	Excellent (similar to stainless steel)	Fair

(a) General Physical Properties

Density - 6.45 g/cm^3

Melting point - 1310°C

Magnetic permeability - <1.002

Electrical resistivity - ~80 μ ohm cm at 20°C

                        - ~132 μ ohm cm at 900°C

Mean coefficient of
  thermal expansion   - 10.4 x 10^{-6}/°C (24° - 900°C)

Forming - conventional hot working directly from arc-
         melted ingot at temperatures of 700°C to
         950°C. Room temperature working possible
         with intermediate anneals at 800°C.

(b) Mechanical Properties at Room Temperature
        (below transition temperature)

Ultimate tensile strength - 125 000 psi

Yield strength, 0.2% offset - 30 000 psi

Total elongation - 22%

Reduction in area - 20%

Impact, unnotched - 117 ft-lb (20°C)

                  - 70 ft-lb (-80°C)

                  - 155 ft-lb*(20°C)

                  - 160 ft-lb*(-80°C)

Fatigue - (R.R. Moore - no failure in 25 x 10^6 cycles,
           70 000 psi rotating beam test)

---

* 55.1 weight percent Ni; 44.8 Ti; 0.08 Fe.

Figure 2.8 Typical properties of nitinol (Schuerch 1968)

2.2.3 Corrosion Resistance

The corrosion resistance of nitinol is often touted as being "excellent" (DesRoches et al. 2004; Duerig et al. 1990). Indeed, many studies done in the medical community show that nitinol performs well in human blood, artificial saliva, and artificial physiological solution (Rondelli 1996; Caroll et al. 2003). However, few, if any, studies have evaluated the corrosion resistance of nitinol in an environment typical of civil structures. Furthermore, data obtained from medical studies indicates that the corrosion resistance of nitinol can vary greatly and has been considered to be "poor" in some cases (Shabalovskaya et al. 2004). Studies conducted in environments that mimic corrosive threats to civil structures, such as marine coastal areas and industrial areas (FHWA 1989), could serve to validate the hypothesis that structural nitinol is resistant to corrosion.

2.3 Mechanical Behavior of Nitinol in Structures

Conventional structures are designed to survive strong seismic forces by being ductile enough to undergo plastic deformation without collapse. This design philosophy accepts heavy economical losses during a strong earthquake, because structures will be left with permanently deformed members even if they survive the event, thus requiring retrofit (Dolce et al. 2000). After severe earthquakes in the mid-nineties, such as the 1994 Northridge, California earthquake and the 1995 Kobe, Japan earthquake, engineers began experimenting with the use of new types of passive energy dissipation devices to improve structures' performance during an earthquake (Aizawa et al. 1998; DesRoches et al. 2002). These energy dissipation devices absorb and dissipate large amounts of energy

by connecting different parts of a structure that move reciprocally during earthquakes (Dolce et al. 2000).

Currently, energy dissipation devices exist in the form of visco-elastic devices, elasto-plastic hysteretic devices, friction devices, and viscous devices. Such mechanisms have proven to be advantageous, but they have many limitations. For example, some devices have rubber components that are not durable and deteriorate with age. Other issues include installation complexity, maintenance, and variable performance depending on temperature. Nitinol shows the potential to work as a material suitable for use in an energy dissipation device without any of these limitations (Dolce et al. 2000).

2.3.1 Hysteresis

The energy dissipation capacity of nitinol can be attributed to the solid-to-solid phase transformation inherent in shape memory alloys (Thomson et al. 1995). As the particles slide over each other during the phase change, friction dissipates energy within the material. Such internal energy dissipation is known as hysteresis damping (Tedesco et al. 1999). The phenomenon of hysteresis damping can be seen in the experimental and theoretical stress-strain curves of nitinol wire shown in Figure 2.9. The internal friction of the nitinol causes the reverse phase transformation to take place at a lower stress level than the forward phase transformation, resulting in the hysteresis loop (Thomson et al. 1995). The hysteresis loop is particularly advantageous during cyclic loading such as that experienced during an earthquake. Figure 2.10 is a stress-strain diagram for a nitinol bar as it undergoes cyclic loading (Liu et al. 1999). The cyclic test began with a strain range of +1% to -1% for 50 cycles, then proceeded through 50 cycles of a +2% to -2% strain range and 50 cycles of a +4% to -4% strain range. Results from the test indicated that

the amount of energy dissipated decreased a slight amount during the first few cycles, but then leveled off. The test demonstrates nitinol's ability to continuously dissipate energy through many cycles of loading (Liu et al. 1999).
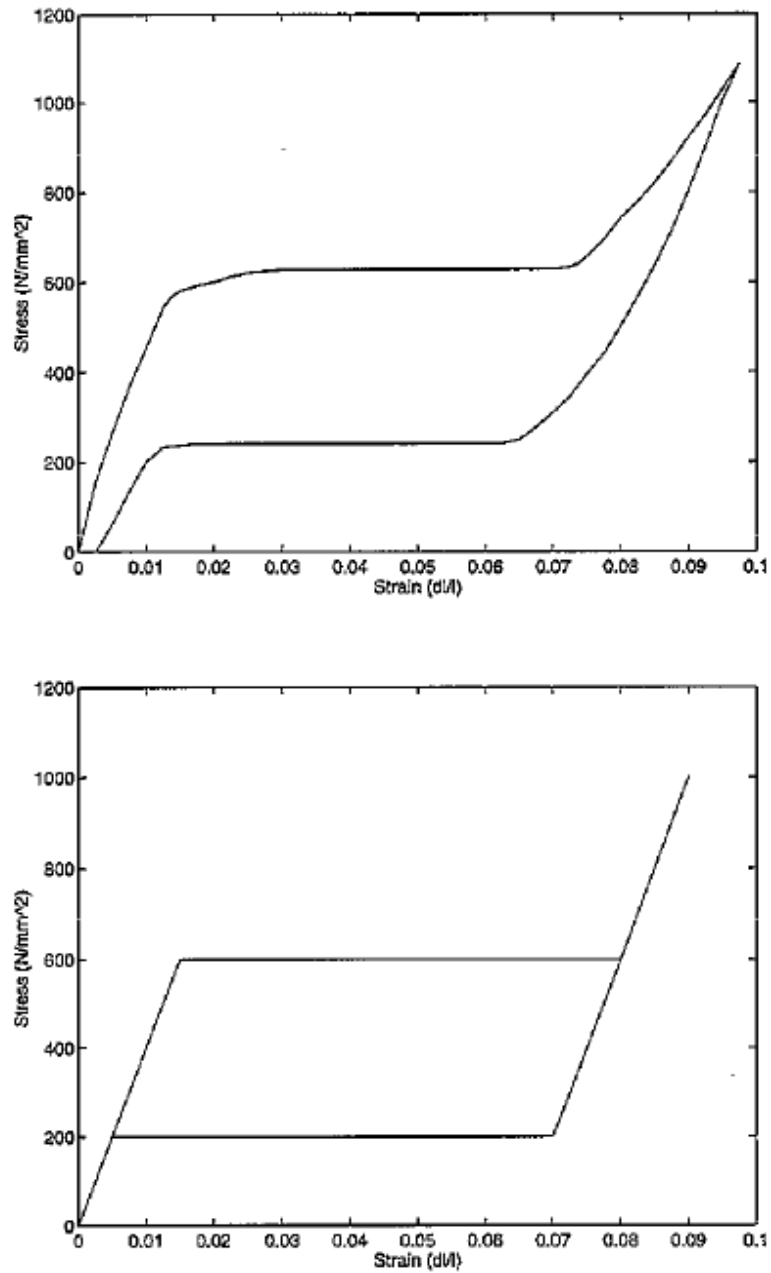
Figure 2.9 Stress-strain curves for nitinol wire. The top figure shows experimental results, and the bottom figure is a piecewise-linear approximation (Thomson et al. 1995).
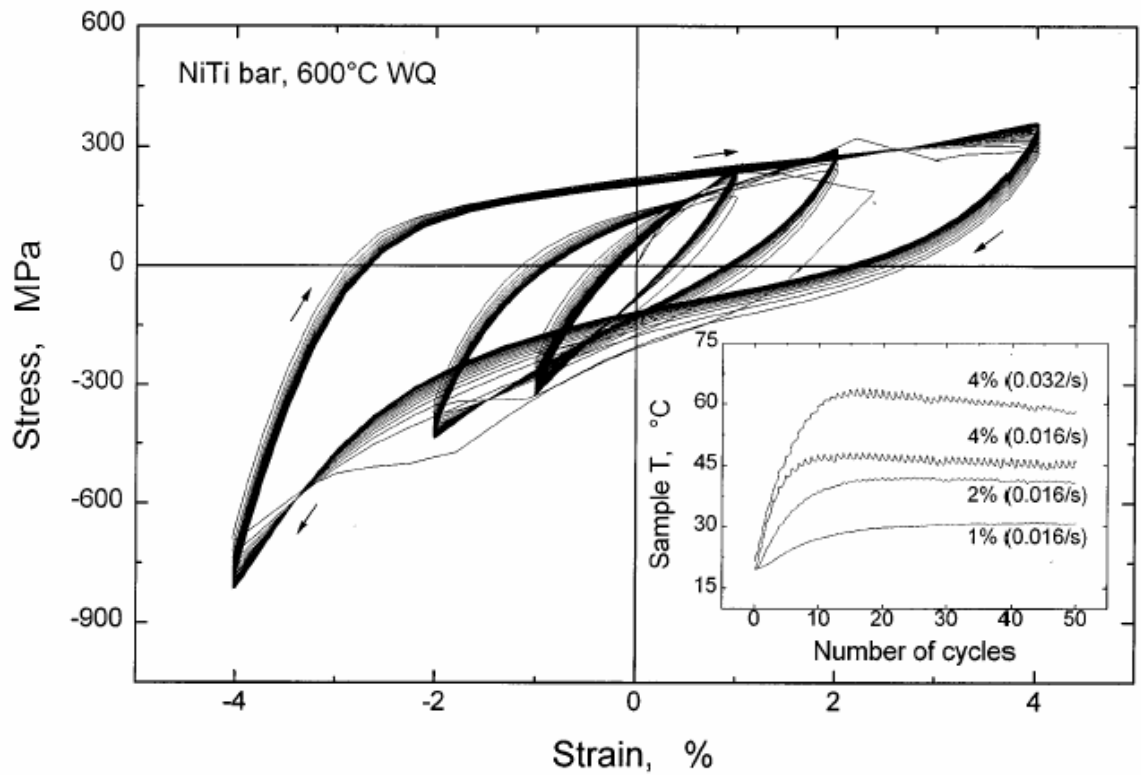
Figure 2.10 Stress-strain curves of a nitinol bar during tension-compression cyclic deformation at a strain rate of 1.6×10^{-2} s^{-1} (Liu et al. 1999)

2.3.2 Examples in Structures

Figure 2.11 displays two examples of proposed applications for nitinol in structures (Tamai et al. 2002). In Figure 2.11(a), a column is welded to a base plate, which is fastened to the footing using anchor bolts. The anchor bolts consist of a length of nitinol coupled with a length of steel. To ensure hysteresis damping will be initiated, the bolt is sized so that the maximum strength of the nitinol piece is lower than that of the steel bolt piece, column end, and base plate. In Figure 2.11(b), nitinol and steel are coupled to produce a braced frame with damping capability. Due to its high strength,

nitinol can easily be applied to these seismic resisting members with practical dimensions

(Tamai et al. 2002). Another example of nitinol's applications to structures is illustrated

in Figure 2.12 (DesRoches et al. 2002). Here, a nitinol bar is used as a bridge restrainer.

DesRoches points out that the effectiveness of nitinol as a bridge restrainer is mainly due

to its ability to remain elastic. An ordinary steel restrainer would be adequate for a few

cycles of loading, but would become far less effective as residual deformation grew.

Nitinol, on the other hand, remains elastic and stays effective for repeated cycles. Figure

2.13 compares the displacement history response of a bridge without restrainers, with

cable restrainers, and with nitinol restrainers using an analytical model (DesRoches et al.

2002). One can see that nitinol greatly reduces the displacement, and continues to limit

displacement through multiple cycles. Figure 2.14 shows yet another example of a

method for employing nitinol in structures. Here, nitinol wire is wrapped around two

cylindrical support posts to form an energy dissipating device (Aizawa et al. 1998). It is

not uncommon to see nitinol in the form of a small diameter wire, because that is how it

is most often produced for the medical field.
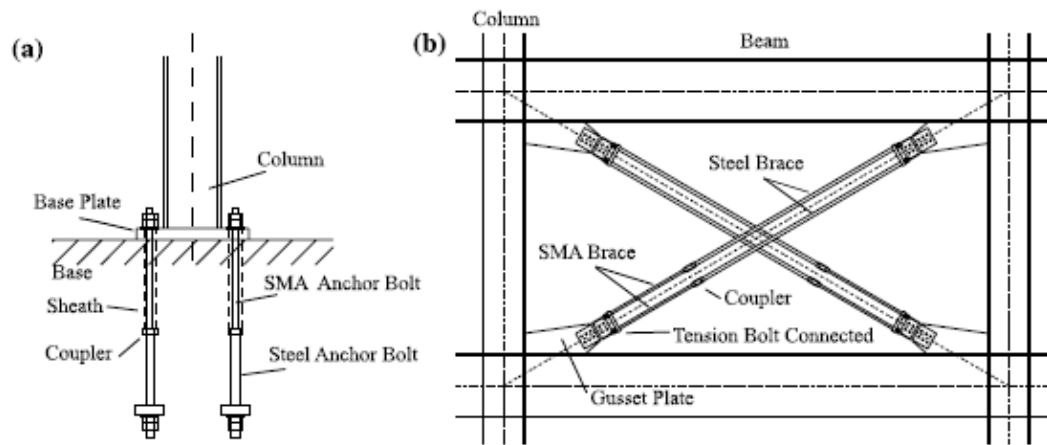
Figure 2.11 Applications of SMA wire to building structures: (a) Exposed-type column base with SMA anchorage, (b) Braced frame with SMA damper (Tamai et al. 2002)
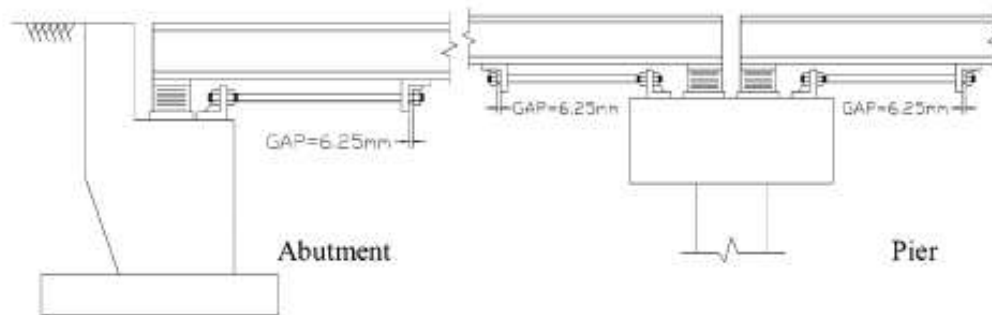
Figure 2.12 Configuration of shape memory alloy restrainer bar used in multi-span simply supported bridge at abutments and intermediate piers (DesRoches et al. 2002)

(a)

(b)
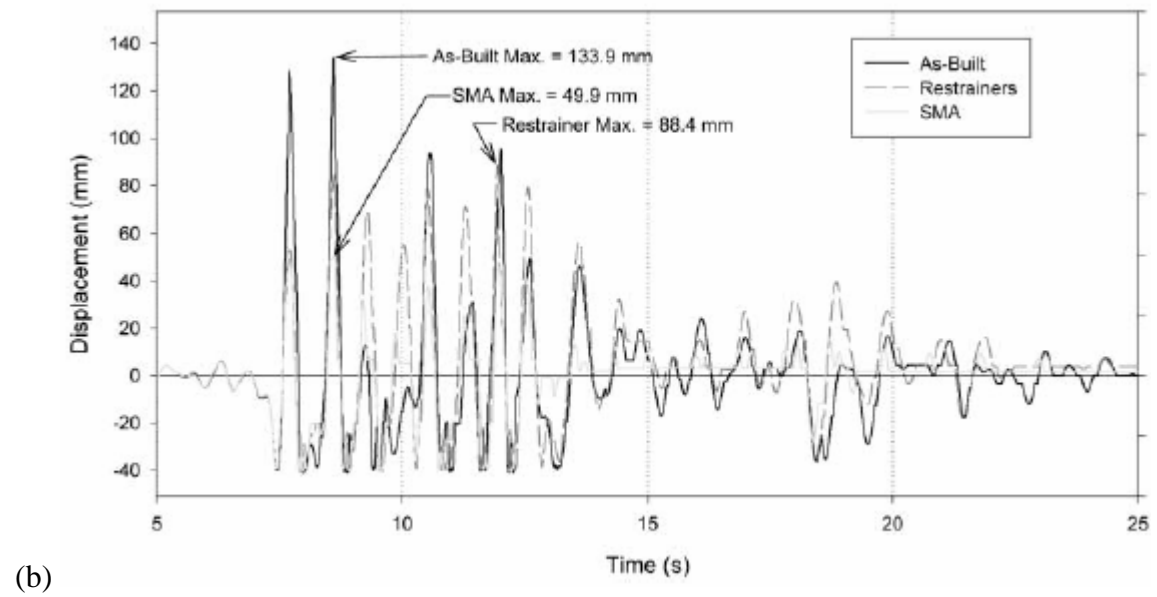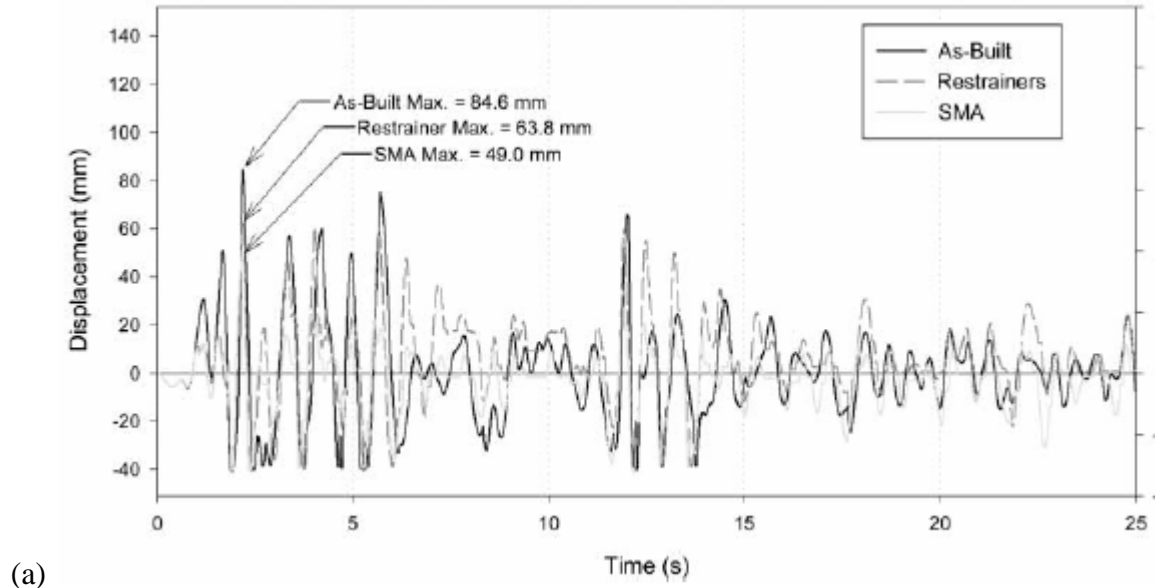
Figure 2.13 Comparison of displacement response history for a bridge in as-built condition, with cable restrainers, and with SMA restrainers. The loads in (a) are from records of the 1940 El Centro earthquake, and the loads in (b) are from records of the 1995 Kobe earthquake (DesRoches et al. 2002).
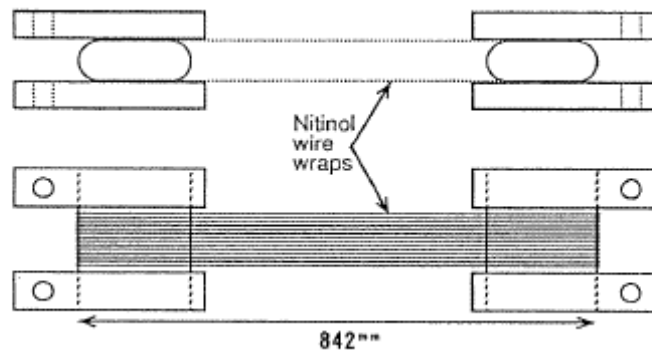
Figure 2.14 Schematic of device design (Aizawa et al. 1998)

The benefits of nitinol extend beyond earthquake protection. An alternative function is vibration control of a stay cable. Cable-stayed bridges are often susceptible to wind-induced vibration or parametric vibration due to the motion of the bridge deck. Since the cables are long and flexible, with little inherent damping, vibration can often lead to very large oscillation amplitude. Adding a nitinol element to laterally brace the cable, as shown in Figure 2.15, can significantly reduce vibration (Li et al. 2004). One more application of nitinol relates to testing of large space structures. Buildings such as the Jet Propulsion Laboratory Phase 0 Testbed and NASA Langley flexible structure have stringent requirements for dimensional stability and vibration control. Studies have shown that these buildings must have some type of inherent passive damping, which can be provided by nitinol (Thomson et al. 1995).
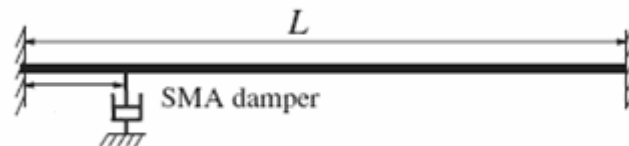
Figure 2.15 Combined cable-SMA damper system (Li et al. 2004).

26

2.4 Corrosion

Corrosion can be defined as the "harmful reaction of the structure of a material with its environment" (Flinn et al. 1981). The effects of corrosion are widespread, and lead to economical loss (Schweitzer 1997). In fact, the United States suffers an annual cost of corrosion and corrosion protection in the range of $8 billion (Flinn et al. 1981). More importantly, corrosion can lead to human injury or loss of life if it causes the premature failure of structures such as bridges (Schweitzer 1997). Accordingly, corrosion should always be a concern for engineers when investigating or designing a new material, device or product.

2.4.1 Corrosion of Metals

Though corrosion can affect many materials, engineers should be most concerned about chemical attack on metals, since it is the most common and most destructive form of corrosion (Diamant 1970). Most metals commonly used for engineering applications are unstable in the atmosphere. They are produced by artificially reducing ores, and they tend to return to their original state when exposed to the atmosphere. They do so by uniting with chemical corrodents to form stable compounds similar to those found in nature. The compound formed is called the corrosion product. Sometimes the corrosion product will form a layer on the metal surface that acts as a protective film, which is sometimes referred to as a passive layer or passivation. If the passive layer stays intact, it prevents further corrosion (Schweitzer 1997). For example, an aluminum wire placed in distilled water will form a protective layer of aluminum oxide that is so adherent that no further corrosion will occur. On the other hand, an iron wire in distilled water will react

27

slower than aluminum, but will continue to react because the corrosion product is non-protective (Flinn et al. 1981).

The chemical principles of corrosion involve anode and cathode reactions between the metal and the surrounding environment. An anode reaction occurs when the metal dissolves into solution as an ion (Flinn et al. 1981). Some common examples of anode reactions for metals used in the building industry are as follows:

$$Mg \rightarrow Mg^{2+} + 2e$$
$$Al \rightarrow Al^{3+} + 3e$$
$$Ti \rightarrow Ti^{2+} + 2e$$
$$Zn \rightarrow Zn^{2+} + 2e$$
$$Cr \rightarrow Cr^{3+} + 3e$$
$$Fe \rightarrow Fe^{2+} + 2e$$
$$Ni \rightarrow Ni^{2+} + 2e$$
$$Cu \rightarrow Cu^{2+} + 2e$$
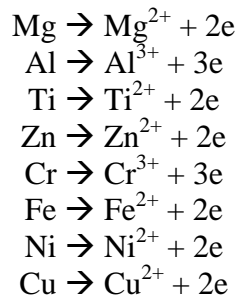
where e = electron (Diamant 1970). These reactions can be shown be the general form,

$$M \rightarrow M^{n+} + ne$$

where M = metal. The electrons produced in the anode reaction flow through the metal until they can be used up in the cathode reaction. The chemical nature of the surrounding environment will dictate the specifics of the cathode reaction. For example, when zinc is placed in acid, the anode reaction results in free electrons that combine with hydrogen atoms during the cathode reaction. The cathode reaction forms atomic hydrogen, which combines to form molecular hydrogen and bubbles off. The chemical equation is as follows:

$$2H^+ + 2e \rightarrow 2H \rightarrow H_2 \text{ (gas)}$$
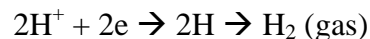
In order for corrosion to continue, it is necessary to have both anode and cathode reactions. The anode reaction generally consists of the metal going into solution,

whereas cathode reactions vary greatly depending on the environment surrounding the metal (Flinn et al. 1981).

Rusting of steel is one of the most common and most thoroughly studied types of metallic corrosion. Although rusting of steel has been studied for at least two centuries, it is still difficult to determine the exact chemical process by which corrosion occurs in complicated environments (Leygraf et al. 2000). In its simplest form, the chemical equation for corrosion of steel can be described by the following equation:

$$2 \text{ Fe} + H_2O + 1\frac{1}{2} \text{ } O_2 \rightarrow 2 \text{ FeO(OH)}$$
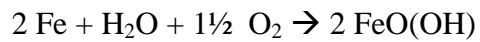
iron + water +oxygen $\rightarrow$ hydrated iron oxide

As can be seen in the equation, water and oxygen are the two main ingredients necessary to cause corrosion of steel. However, the corrosion process is accelerated and complicated by impurities in the atmosphere such as sulfur and chlorides (Knofel 1978). Therefore, corrosion rates of structural steel depend on location. Steel exposed to clean, dry air shows little corrosion. Steel exposed to industrial and marine environments experiences much more corrosion due to the presence of sulfuric acid and chlorides, respectively (Schweitzer 1999). Though corrosion rates can vary tremendously between specific locations, it is generally estimated that structural steel corrodes at rates of 10 micrometers per year in rural air and 100 micrometers per year in industrial air and seawater (Wranglen 1985).

2.4.2 Measurement and Testing

Quantification of a corrosion process is typically discussed in units of inches per year (ipy) or mils per year (mpy), where 1 mil = 0.001 in (Schweitzer 1997). A process that is so slow produces unique challenges in measuring and testing. ASTM standards

for atmospheric testing suggest a time frame of at least several years and recommend that better results are obtained from a corrosion time of up to sixteen years (ASTM G 50 1976). This is obviously unrealistic for most practical purposes. Instead, accelerated corrosion tests such as ASTM's Standard Practice for Laboratory Immersion Corrosion Testing of Materials are used. But even within this very standard, it is noted that "corrosion testing by its very nature precludes complete standardization" and "it is impractical to propose an inflexible standard laboratory corrosion testing procedure for general use" (ASTM G 31 1972). Therefore, it is up to the researcher to use ASTM standards as a guide to assist in the development of a corrosion test that is suitable for the goals of the test.

CHAPTER 3 – LABORATORY TESTING PROGRAM

3.1 General

Since corrosion testing "standards" are quite flexible, one of the challenges of this research was to develop an appropriate method for measuring and studying the corrosion of nitinol. This included selecting the size and shape of nitinol product to be investigated, devising a method of corroding the specimens, and formulating a plan for measuring the amount of corrosion. Choices were influenced by requirements such as size compatibility of equipment, product availability, and time factors.

3.2 Specimens

In choosing appropriate specimens for this research, several criteria had to be met. The nitinol specimens needed to be in dimensions typical of proposed uses for nitinol in structures, but they also had to be compatible with all equipment used for corrosion and corrosion measurement. The decision was made to use nitinol bar and wire, 12 inches long, with diameters of .5, .25, and .085 inches. These sizes were chosen for the following reasons:

- They are long enough to fit in the grips of the Tinius Olsen 60-kip Universal Test Machine (UTM) (see Section 3.4.1 for a detailed description of tensile testing with the Tinius Olsen UTM).

- They are thin enough to fit through the top of a 2000-mL kettle (see Section 3.3 for information on equipment used to corrode the specimens).

31

- These nitinol product sizes were studied in recent research of the mechanical and cyclic properties of nitinol bars and wires, including work done by Dr. Reginald DesRoches at the Georgia Institute of Technology (DesRoches et al. 2004).

- Nitinol is readily available in bar and wire form of these sizes.

- Most proposed structural uses of nitinol involve bars or wires of these sizes.

Nitinol specimens were purchased from Special Metals in the sizes noted. The .5 inch diameter bars were delivered ready-to-use, whereas the smaller diameter wires were delivered as one single coil of wire, and had to be cut to length. The .5 and .085 specimens were cold drawn and 30% cold worked, and the .25 inch specimens were hot rolled and given an oxide surface. Test certificates for nitinol specimens are found in Appendix A.

Steel specimens were also chosen for comparison with nitinol. The steel specimens needed to meet the same size criteria as the nitinol, and also be of the same grade and shape of steel commonly used in structures. Therefore, the decision was made to buy steel in normal structural shapes and proportions, and cut smaller specimens from the original pieces. The steel pieces chosen were a W8×40 section and a flat plate 6 inches x .5 inches. The W8×40 had a web thickness of .36 inches and a flange thickness of .56 inches. With help from Auburn's engineering machine shop, specimens were cut from both the web and flange that were 12 inches long and 1 inch wide. To eliminate surface irregularities that affected precise dimensioning, the specimens were surface ground, leaving them thinner than previously noted. The final cross sectional dimensions of the specimens were .310 x 1.000 inches for the web, and .450 x 1.000 inches for the flange. The accuracy in both cases was within ±.001 inches. The W8×40 was grade

32

A992, typical of structural steel. Typically, grade A992 steel consists of approximately 97% iron with a carbon content less than 0.5% and small concentrations of other elements such as copper, manganese, silicon, molybdenum, vanadium, and nickel (Cattan 1999). The flat plate, on the other hand, had a grade of A588, which has slightly higher concentrations of alloying elements included to increase corrosion resistance, most notably copper, nickel, chromium, silicon, and phosphorus (McCuen et al. 2005). Grade A588 steel is often used in areas where corrosion is a concern. This corrosion-resistant steel provided a higher mark of performance to compare to the nitinol. After machining specimens from the flat plate, the final dimensions were .410 x 1.000 inches, also with an accuracy of ±.001 inches. In summary, the steel specimens were taken from typical structural elements, but were made to be similar in size to the nitinol specimens. A list of specimens is given in Table 3.1, and a picture of these different shapes and sizes is shown in Figure 3.1.

Table 3.1 List of Specimens

Specimen Designation	Source	Length (in)	Width (in)	Thickness or Diameter (in)
Steel-Flange	Flange of W8x40	12	1.000	0.450
Steel-Web	Web of W8x40	12	1.000	0.310
Steel-A588	A588 Flat	12	1.000	0.410
Nitinol-.5"	Round Bar	12	-	0.500
Nitinol-.25"	Round Wire	12	-	0.250
Nitinol-.085"	Round Wire	12	-	0.085

Figure 3.1 Specimen sizes, from left to right: Steel-Flange, Steel-Web, Steel-A588, Nitinol-.5", Nitinol-.25", Nitinol-.085"

3.3 Corroding the Specimens

ASTM International has many standards and guides for corrosion testing, but few are applicable and practical for studying the corrosion of nitinol in structures. Experience has shown that a metal's corrosion resistance can vary greatly depending on the corrosive environment. Accordingly, many ASTM corrosion standards only apply to a specific metal and environment, but no such standard exists for a nickel-titanium alloy. The most appropriate standard for evaluating nitinol is ASTM's "Standard Practice for Laboratory

Immersion Corrosion Testing of Metals," which acts as a guideline for creating a unique

corrosion experiment, instead of imposing a rigid standard for a particular metal (ASTM

G 31 1972). This standard, also known by the designation G 31 – 72, offers suggestions

for equipment, sample size, duration, and sample preparation, and alerts the researcher to

potential pitfalls in corrosion testing. However, the standard allows a researcher to tailor

the experiment to the goals of the research, noting that its use as a guide is more sensible

than following an inflexible standard.

3.3.1 Corrosive Solutions

ASTM G 31 – 72 can apply to any metal being immersed in any solution. It is up

to the researcher to choose a solution that will mimic the environment encountered in the

service life of the metal. The most corrosive environments for structures are marine

coastal areas, which attack a metal with salt-laden air or seawater splash, and industrial

areas, which corrode a metal with chemicals such as sulfur that create acid rain when

pumped into the air. Therefore, the two solutions chosen for this research were seawater

and sulfuric acid. The seawater was taken directly from the Gulf of Mexico, near Gulf

Shores, Alabama, and was filtered to remove debris. The chloride ion concentration of

the seawater was measured to be 19,400 mg/L, which is typical of seawater that is not

diluted with freshwater. The sulfuric acid solution was purchased from Fisher Scientific,

who describes the solution as "simulated acid rain." The solution was approximately

0.0003% sulfuric acid and 99.99% water, and had an initial pH between 3.0 and 3.7,

which is more acidic than typical acid rain. Choosing highly corrosive environments

allowed the duration of the test to be practical, and choosing solution types that are

similar to typical structural environments ensured that the results would be applicable to structural engineering.

3.3.2 Test Size

Another important consideration in an immersion corrosion experiment is the size of the specimen in relation to the volume of the solution. ASTM G 31 – 72 suggests that a minimum solution volume to specimen area ratio should be used to make sure that a chemical reaction will continue throughout the duration of the experiment. The standard advises that a minimum ratio near 125 mL/in^2 is appropriate. A similar ratio was achieved for the specimens of this research by using a 2000 mL kettle for the corrosion test. When the kettle was filled with 2000 mL of solution, the specimen was partially submerged so that a length of approximately 6.5 inches of the specimen was in contact with the solution. For the largest specimen size, this yielded a specimen area of 18.9 in^2 and a solution volume to specimen area ratio of 105.8 mL/in^2. Table 3.2 lists the specimen area and volume to area ratios for all six specimen sizes. Note that the broad range of specimen sizes resulted in some very high volume to area ratios. A high ratio did not negatively affect the results of the experiment; it simply meant that there was a surplus of solution for the smaller specimens.

Table 3.2 Surface area corroded and solution volume to surface area ratios for the six specimens in a 2000 mL kettle

Specimen	Surface Area Corroded (in^2)	Solution Volume / Surface Area (mL/in^2)
Steel-Web	17.0	117.6
Steel-Flange	18.9	105.8
Steel-A588	18.3	109.3
Nitinol-.5"	10.2	196.1
Nitinol-.25"	5.1	391.4
Nitinol-.085"	1.7	1149.4

3.3.3 Duration of Test

It was important to choose an exposure time that was long enough to see significant corrosion, but short enough to allow a reasonable number of specimens to be corroded. ASTM G 31 – 72 advises a test duration of 48 to 168 hours (2 to 7 days). The standard also indicates that it is best to run a trial test to determine if the duration chosen is appropriate. Clearly, a longer test leads to more corrosion, which makes measuring the corrosion easier and more accurate. However, practical time and equipment considerations precluded very long-duration testing. A limited number of preliminary tests were run to determine the minimum test time needed to corrode the steel. These preliminary tests demonstrated that the steel specimens showed visible signs of some corrosion within a day, and more thorough corrosion after five days. Therefore, the test duration chosen was five days.

3.3.4 Test Matrix

A test matrix, shown in Table 3.3, was developed to establish the combinations of specimens and solutions. The test matrix was influenced by the number of available specimens, the time required to corrode the specimens, and the specified goals of the research effort.

Table 3.3 Test matrix

		Solution			
		Sulfuric Acid	Seawater	None	Total
Specimen	Steel-Flange	2	1	2	5
	Steel-Web	2	1	2	5
	Steel-A588	2	1	2	5
	Nitinol-.5"	2	1	2	5
	Nitinol-.25"	2	1	2	5
	Nitinol-.085"	2	1	2	5
	Total	12	6	12	30

3.4 Measuring Corrosion

After the specimens were corroded, a variety of techniques were used to measure the amount of corrosion that had occurred. Although corrosion is often discussed in terms of a thickness per time rate, it is rarely measured in units of thickness per time. One reason is that short-term corrosion tests are unlikely to corrode a specimen enough to accurately measure the change in thickness. Also, the corrosion product on a metal can actually *increase* the thickness of a specimen, thereby causing misleading measurements that do not accurately reflect the depth of the metal that has been damaged. In fact, experience has shown that titanium, which is an element of nitinol, often forms a tightly bonded layer that cannot be easily removed. One technique often used for measuring corrosion is mass loss. However, this method would be more accurate for smaller

38

specimens, which would lose a much higher percentage of their mass in a five day

corrosion test. Also, a mass loss measurement would be deceptive if the corrosion

product was tightly bonded. Therefore, corrosion measurement for this research required

some more uncommon techniques.

The original method chosen for comparing the detrimental effects of corrosion on

the different specimen types was tension testing. By measuring the tensile forces

required to yield and fracture a corroded specimen, and comparing those values to the

tensile forces needed to yield and fracture an uncorroded identical specimen, the amount

of strength lost to corrosion can be calculated. Since tension testing provided a means to

measure the strength lost due to corrosion, it was not adversely affected by an adherent

corrosion product. Furthermore, the data obtained from a tension test is in units of

measure that are more familiar to structural engineers, who are accustomed to force and

strength but rarely deal with corrosion rates. But tension testing posed a potential

problem; a five-day corrosion test may not be long enough to produce an appreciable

decrease in strength. Therefore, it was decided that additional test methods should be

employed for quantifying the corrosion effects. The methods chosen involved evaluating

the solutions used to corrode the specimens. By measuring changes in the solutions, it

was possible to gather information about the corrosion process for structural steel and

nitinol and to determine which metal was more reactive with the solutions.

The decision to use multiple methods for measuring corrosion was important for

several reasons. First, it ensured that specific results would be established, even if

tension testing proved inconclusive. Secondly, data from various tests could be analyzed

and compared to form a stronger conclusion than would be possible with just one form of

corrosion measurement. Finally, by evaluating the metal specimens and the solutions, a

more accurate understanding of the corrosion process for nitinol could be obtained.

Tension testing and other corrosion measuring techniques are discussed in more detail

below.

3.4.1 Tension Tests

Tension testing of the specimens conformed to ASTM's "Standard Test Methods

for Tension Testing of Metallic Materials", also referred to as ASTM E 8 – 04. This

standard is typically used to determine the yield strength and ultimate tensile strength of a

metal, so it is ideal for measuring the lowered strength of a corroded specimen. Tension

testing was performed using a Tinius Olsen 60-kip Super "L" Universal Testing Machine

(UTM) with Model 398 Display and CMH 496 Controller, pictured in Figure 3.2.
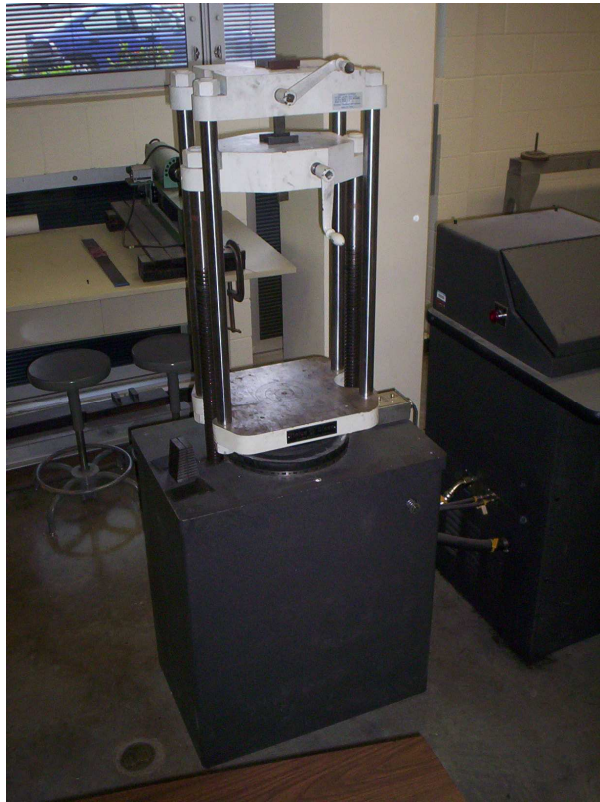
Figure 3.2 Tinius Olsen Super "L" Universal Testing Machine

One of the most critical parameters of tension testing is the speed of the test. In accordance with ASTM E 8 – 04, test speed can be defined in terms of rate of straining of the specimen, rate of stressing of the specimen, rate of separation of the two crossheads of the testing machine, or elapsed time for completing all or part of a test. Rate of straining was chosen as the method for controlling test speed. ASTM E 8 – 04 states that an appropriate test speed is between 10,000 and 100,000 psi/min when determining yield strength, and between .05 and .5 in/in/min when determining ultimate tensile strength. Since both yield strength and ultimate tensile strength were desired for this research, two testing speeds were required. The tests were begun at a test speed appropriate for determining yield strength, and then changed to a speed appropriate for determining ultimate tensile strength after the specimen yielded. The range of test speeds for yield strength is given as a stress rate (psi/min), but can be converted to a strain rate (in/in/min) by dividing by the material's nominal modulus of elasticity. Since the nominal modulus of elasticity for steel is 29,000 ksi, the range of acceptable test speeds for determining yield strength is given by the following equation:

$$\text{Test Speed Range} = \frac{10 ksi / \min}{29,000 ksi} \text{ to } \frac{100 ksi / \min}{29,000 ksi} = .000345 \text{ to } .00345 \text{ in/in/min}$$

The modulus of elasticity for nitinol can vary between 4,400 and 12,000 ksi and is not specified by the manufacturer for the nitinol used in this research. Therefore, the test speed range was calculated using the lower nominal modulus for the lower limit and the higher nominal modulus for the upper limit:

$$\text{Test Speed Range} = \frac{10 ksi / \min}{4,400 ksi} \text{ to } \frac{100 ksi / \min}{12,000 ksi} = .00227 \text{ to } .00833 \text{ in/in/min}$$

41

After calculating the appropriate range of test speeds, it was decided to begin tests at a strain rate of .003 in/in/min and to increase the strain rate to .3 in/in/min after yield. Since these speeds are acceptable for testing both steel and nitinol, all specimens were tested at rates of .003 and .3 in/in/min to determine yield strength and ultimate tensile strength, respectively.

ASTM E 8 – 04 also contains advice about measuring the extension of the specimen. Acceptable methods include measurement of change in crosshead displacement or the use of an extensometer. Crosshead displacement can be affected by slip of the grips, but use of an extensometer requires that failure will take place within the gage length, which was not guaranteed for the specimen geometry used. Since a comparison of yield strength and ultimate strength for different specimens were the desired results, rather than specific strain values, crosshead displacement was an acceptable means of measuring elongation.

The testing machine was connected to the 398 Display and CMH 496 Controller, which were connected to a computer equipped with a program called Test Navigator. Test Navigator allows the operator to set test parameters such as testing speed, gage length, and size of specimen. It also provides a means for displaying results in the form of a stress versus strain diagram.

3.4.2 pH Tests

Use of a pH meter provided a simple way to determine the extent of reaction between the metals and solutions. A solution's pH value is a measure of the hydrogen ion activity within the solution and is defined by the equation

$$pH = -\log\{H+\}$$

where H+ is the hydrogen ion activity in mol/L and pH is unitless. Therefore, a high

activity of hydrogen ions leads to a low pH value and a low activity causes the pH to be

high. For this research, change in pH of the solutions was noted by measuring the pH of

the solutions before and after using them to corrode the specimens. If the pH level

changed significantly, it meant that the hydrogen ion activity had changed, and it could

be inferred that a chemical reaction had damaged the metal. Conversely, a steady pH

level indicated that little or no chemical reaction took place. Measuring pH levels is not a

sufficient method for determining a corrosion rate, but by comparing the change in pH

levels for tests involving steel and nitinol, it could be determined which metal reacted

more to the solutions.

3.4.3 Atomic Absorption Spectrometer Tests

Use of an Atomic Absorption Spectrometer (AAS) provided further information

about the corrosion of steel and nitinol. The AAS, pictured in Figure 3.3, is outfitted with

an element lamp that uses light of a specific wavelength to detect the presence of a

particular element in a solution. For samples taken while corroding steel, an iron lamp

was used with the AAS since iron is the predominant element in steel. For samples taken

while corroding nitinol, a nickel lamp was used. Nitinol is approximately 50% nickel and

50% titanium, so the amount of nickel dissolved in a solution should be roughly

equivalent to the amount of titanium lost to corrosion, but is dependent upon the specific

chemical reaction. Since titanium corrosion product has been shown to stay tightly

bonded to the surface (ASTM G 31 1972), it is more efficient to test for the presence of

nickel within the solution. In either case, the lamp was used to shine light through the

solution sample. The AAS measured the amount of light that was not absorbed by the

element, and converted this information into milligrams of the element per liter of solution (mg/L). The AAS is connected to a computer and controlled with a computer program called SpectrAA. SpectrAA guides the operator through the collection of data and provides an outlet for displaying results.

Figure 3.3 Atomic Absorption Spectrometer

3.4.4 Mass Loss Tests

As previously discussed, mass loss was not an appropriate measure of corrosion for this research. Most of the specimens were too large to accurately measure minute changes in mass, and it was possible that an adherent corrosion product could interfere with results. The smallest nitinol specimens, however, were small enough to test for mass loss. And since the goal of this research was to study the damaging effects of

corrosion of nitinol, it was beneficial to measure the change in mass, and to use the results to learn about the way nitinol is affected by corrosion, even though the results were not used to compare nitinol to steel. Specimen mass was measured before and after the corrosion period using an analytical balance. Specimens were dried after the corrosion period, to ensure that mass measurements were not affected by wetting from the solution.

3.4.5 Visual Evaluation

Since corrosion attacks the surface of a metal, the process is often visible to the naked eye. Much can be learned about the corrosion of a metal by simply observing the changes over time. While the results of visual evaluation are not as objective as numerical data obtained from meticulous testing, thorough inspection of a metal's condition can provide information about the corrosion product and aid in explanation of test results. For this research, pictures were taken of the specimens in the solutions at 24-hour intervals. These pictures capture the surface of the metal as well as the color of the solution. Pictures were also taken at the end of a corrosion test as the specimen was being wiped clean of corrosion product. Additionally, the specimens were carefully examined at various times throughout the corrosion test, and any abnormalities or notable observations were recorded.

3.5 Labeling and Nomenclature

With testing being conducted on both the metal specimens and the solution samples, it was important to have a system to label each test piece. Note that throughout this thesis, the word "specimen" always refers to a piece of steel or nitinol, and the word "sample" always refers to a volume of solution extracted during the corrosion process.

These distinctions serve to clarify the type of data or test piece being discussed. Figure 3.4 demonstrates the system used for labeling. This system can apply to the specimens and samples, so that each is labeled according to the kind of metal, size, solution, number, and time of corrosion. For example, using Figure 3.4, a sample labeled N-.25-A-2-96 would be a sample of sulfuric acid taken 96 hours into the second corrosion test involving a .25 inch diameter nitinol wire placed in sulfuric acid. This system also applies to metal specimens, so that a specimen labeled S-F-W-1-120 would be the first piece of steel from the flange of the W8x40 that had been corroded for 120 hours in seawater. An uncorroded specimen would be labeled S-F-0-1-0, indicating that it is the first steel flange piece to be tension tested with zero hours of corrosion. In addition to the labeling options listed in Figure 3.4, it was necessary to distinguish a second solution sample taken at 120 hours. Just after collecting the first 120 hour sample, the specimens were wiped with a glove in order to ensure that all corrosion product was dissolved into the solution instead of clinging to the surface of the specimen. This second 120 hour sample, collected just after the wipe, was designated "120W".
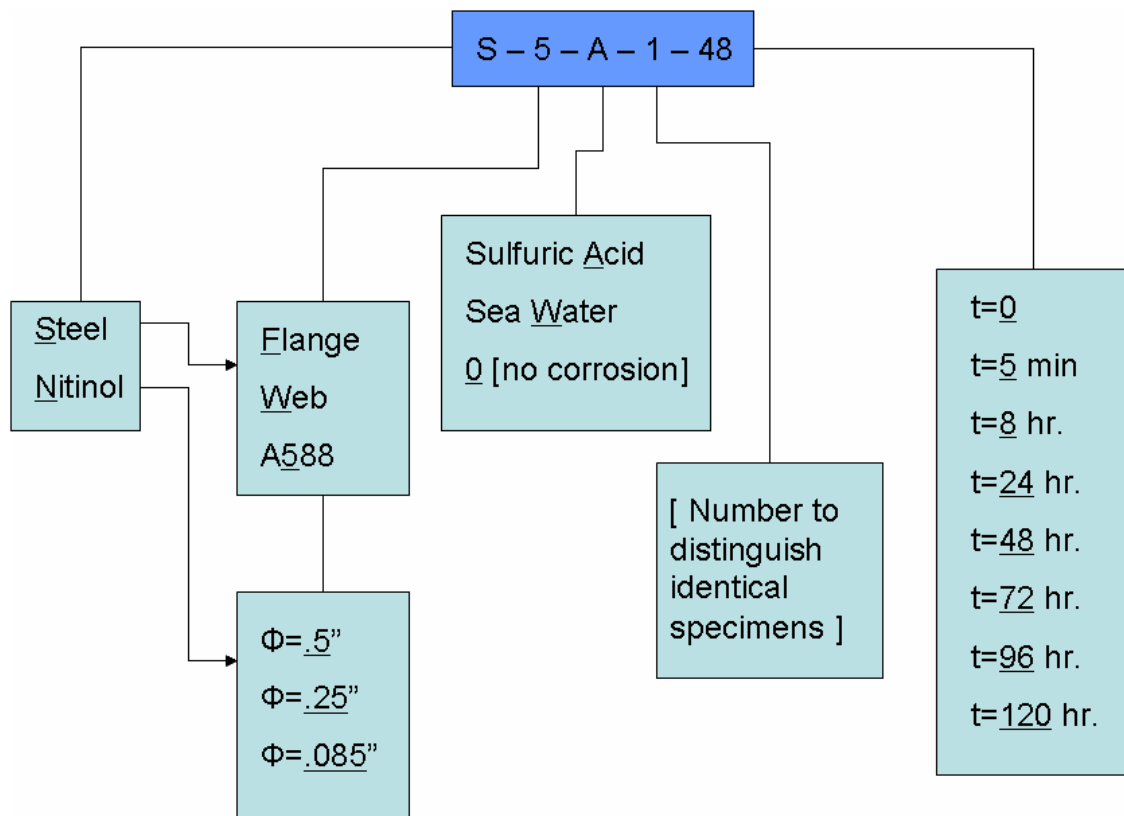
Figure 3.4 Labeling system

CHAPTER 4 – LABORATORY EQUIPMENT AND PROCEDURES

4.1 General

The laboratory procedures for this research consisted of two primary procedures: corroding the specimens and measuring the amount of corrosion. Corroding the specimens was a relatively easy task that simply required time and collection of solution samples for later use. Measuring the amount of corrosion was a much more arduous task due to the complications discussed in Chapter 3. The intent was to use a variety of measuring techniques in order to get an accurate picture of the corrosion process for nitinol and a solid comparison of the corrosion resistance of nitinol and steel.

4.2 Corroding Specimens

4.2.1 Preparation for Corroding Specimens

After acquiring the necessary specimens, solutions, and lab equipment, a small amount of preparation was needed before corrosion testing could begin. Most notably, the seawater needed to be filtered with .45 micrometer filter paper to remove debris. To do this, a large funnel was connected to the filtering device using a clamp. The funnel and filtering device were placed on top of a 2000-mL volumetric flask. Finally, a hose ran from the nozzle of the volumetric flask to the nozzle of a vacuum. When the seawater was in the funnel and the vacuum was turned on, the seawater was pulled through the filter into the flask. Figure 4.1 shows this process.

Figure 4.1 Filtering seawater

4.2.2 Corrosion Procedure

The corrosion procedure for this research was based on ASTM G 31 – 72.

Equipment included a stirring hot plate, stir bar, 1000 mL volumetric flask, 2000 mL

kettle, kettle clamp, 10 mL pipette, bulb, several 20 mL vials, several 125 mL jars, and

parafilm. The corrosion procedure was as follows:

1. Thoroughly wash the flask, kettle, pipette, and stir bar with water.

2. Rinse the flask, kettle, pipette, and stir bar with a small amount of the solution to be used for corroding the specimen (sulfuric acid or seawater).

3. Use the flask to measure exactly 1000 mL of solution. Pour this into the kettle and repeat the process to result in 2000 mL of solution in the kettle.

4. Use the pipette to measure a 100 mL sample of solution into a jar. This sample is set aside for later use with AAS testing.

5. Place the kettle onto the stirring hot plate and set the stirrer to 90 rpm. Put the stirrer bar in the kettle so that stirring begins. The solution is left at room temperature, which the hot plate measures as 24° C.

6. Place the metal specimen into the solution. Orient the kettle and specimen so that the stir bar will stir freely without magnetically attaching to the specimen.

7. Use the kettle clamp to secure the top onto the kettle so that the specimen protrudes through the large hole in the kettle top. Place parafilm over the smaller three holes and over the gaps of the large hole.

8. After five minutes, use the pipette to measure a 10 mL sample of the solution into a vial. This sample is set aside for later use with AAS testing.

9. Continue to take 10 mL samples at times of 8, 24, 48, 72, 96, and 120 hours.

10. Immediately after taking the final 10 mL sample, remove the specimen and use a glove to thoroughly wipe the corrosion product back into the solution.

11. Use the pipette to measure a 100 mL sample of solution into a jar.

12. Empty the kettle and repeat the process beginning with washing the equipment.

Wiping the surface of the metal at the end of the corrosion process was an important step for accurate testing of the solutions. During preliminary tests, it was noted that the corrosion product adhered to the metal surface. Wiping this corrosion product back into the solution ensured that AAS and pH testing could measure the full extent of corrosion.

Keeping the stir bar free of the specimen was sometimes tricky, but necessary for quality results. If the stir bar bumped the specimen, it would prematurely knock some of the corrosion product off of the specimen. Also, the stir bar could become attached to the specimen and stop spinning, thereby leaving the solution stagnant. To prevent or limit collisions between the stir bar and specimen, the specimen was propped at an angle so that the bottom of the specimen was at the very edge of the kettle. Additionally, the kettle could be positioned off-center on the stir plate, so that the stir bar was farther from the specimen. The experimental setup is pictured in Figure 4.2. The specimen and kettle are positioned to give the stir bar ample room to spin without contacting the specimen.

The volume of the solution was an important consideration because it changed slightly as samples were taken. In order to maintain a nearly constant volume, sample size was limited to 10 mL, the minimum amount of solution needed for AAS testing. Therefore, the total change in solution volume throughout the corrosion procedure was small enough to be considered negligible, as shown in the following calculations:

$$(2000 \text{ mL}) - (7 \text{ samples}) \text{ x } (10 \text{ mL/sample}) = 1930 \text{ mL}$$

$$(7 \text{ samples}) \text{ x } (10 \text{ mL/sample}) \text{ x } (100\%) / (1930 \text{ mL}) = 3.6 \text{ \%}$$

Figure 4.2 Experimental setup

Figure 4.3 Collecting a sample

4.3 Tension Testing

Tension testing was performed in accordance with ASTM's "Standard Test Methods for Tension Testing of Metallic Materials", also called ASTM E 8 – 04. The standard recommends using specimens with a thicker cross-section on the ends, in order to ensure that failure occurs between the grips of the testing machine. However, nitinol specimens were only available in sizes with a constant cross-section, and could not be conveniently or precisely machined into specimens of the recommended shape. Steel specimens were also cut with a constant cross-section in an effort to keep all specimen shapes similar.

The standard cautions that the test machine should be warmed up to normal operating temperatures following a period of inactivity, in order to minimize errors. This was accomplished by running the machine through a few cycles in which an extra steel specimen was stressed to just below its yield strength. After warming up the machine, the procedure used for each specimen was as follows:

1. Turn on the power and press the "Pump On" button on the 398 Display.

2. Press and hold the "Home" key until the display advances to the next screen.

3. Mount the specimen in the upper grips of the machine.

4. Use the "Up" or "Down" buttons to position the lower crosshead in an appropriate location for gripping the specimen.

5. If necessary, use the keypad to zero the load and position readings.

6. Place the lower grips on the specimen and tighten both sets of grips with the hand cranks. Any load reading is now due to stress on the specimen, and should not be zeroed.

7. Turn on the computer and open Test Navigator.

8. Within Test Navigator, click "File", "Edit Test Setting", and choose "Corrosion Samples".

9. Edit test settings such as specimen shape, gage length, and test speeds.

10. Input the name of the specimen and click "Start Test".

11. After the specimen yields, push the designated key to switch to the higher test speed.

12. After ultimate load is achieved, end the test to prevent damage to the grips that can occur when the specimen fails.

13. Unload the specimen, remove it from the grips, and reset the crossheads to begin a new test.

During the test, test speed changes were controlled by keyboard input. The tests were begun at low strain rates, in order to accurately measure yield strength, and then sped up to capture the ultimate load. The initial distance between the grips was approximately 3.6 inches for all specimens. Tests were ended after observing ultimate load on the stress-strain diagram and necking of the specimen, as pictured in Figure 4.4.

Figure 4.4 Specimen S-F-A-1-120 prior to failure

4.4 pH Testing

Measurement of pH values was the first step in evaluating the corrosive solutions. The pH of the solutions was taken at three specific times:

- Just before the metal was immersed.

- At the end of the corrosion period, before the corrosion product was wiped.

- At the end of the corrosion period, after the corrosion product was wiped.

The pH was measured using a pH meter with a probe, as pictured in Figure 4.5. The steps for measuring the pH were as follows:

1. Remove the probe from the buffer solution and wipe it clean with a laboratory tissue.

2. Place the probe in at least 50 mL of solution and wait for the display to indicate the pH.

55

3. After recording the pH value, remove the probe from the solution, rinse it with

   de-ionized water, wipe it clean, and replace it in the buffer solution.

Figure 4.5 pH meter taking a reading

4.5 Atomic Absorption Spectrometer Testing

4.5.1 Preparation of Samples

Before a sample could be tested with the Atomic Absorption Spectrometer (AAS),

it was first necessary to acidify the sample. This ensured that any clumps of iron or

nickel within the sample would be dissolved into the solution. The samples were

acidified by adding concentrated nitric acid in an amount equal to 2-4% of the sample

size. Many of the samples had such high iron concentrations that they needed to be

diluted with de-ionized water before they could be tested with the AAS. This was

particularly true for samples collected after wiping the corrosion product off of the steel

specimens. Samples were considered to be sufficiently diluted and acidified if the

solution was clear of any visible particles. Figure 4.6 pictures a sample after being

acidified and after being diluted. The bottle on the left contains sample S-W-A-1-120W

after being acidified with 4% nitric acid. The bottle on the right contains 3 mL from the

bottle on the left, plus 84 mL of de-ionized water and 3 mL of nitric acid. The result is

sample S-W-A-1-120W diluted 30:1 and acidified with a total of 3.47% nitric acid.

Figure 4.6 Sample S-W-A-1-120W acidified and diluted

4.5.2 Preparation of Working Standards

Another prerequisite to AAS testing was to prepare standard solutions with a

known quantity of iron or nickel. These standards were used to calibrate the AAS for

each test. The following procedure was used to prepare the standard iron solutions:

1. Using a pipette, place 20 mL of a 1000 mg/L iron reference solution into a
   200 mL volumetric flask.

2. Add 4 mL of nitric acid.

3. Add 176 mL of de-ionized water in order to obtain a solution that is 100 mg/L iron and is acidified with 2% nitric acid.

4. From the 100 mg/L solution, use a pipette to place quantities of 2, 4, and 6 mL into 3 separate 100 mL volumetric flasks.

5. Fill the remainder of these flasks with de-ionized water to obtain working standards of 2, 4, and 6 mg/L of iron.

This procedure was repeated to obtain working standards of nickel solutions from the nickel reference solution.

4.5.3 Measuring Iron and Nickel Concentrations

After all of the samples were acidified and the working standards were prepared, iron and nickel concentrations could be measured with the AAS. The procedure for AAS testing was as follows:

1. Open the computer program SpectrAA, and specify the number of samples to be tested.

2. Within SpectrAA, click "Add Method" and choose "Fe" or "Ni" for steel or nitinol, respectively.

3. Set appropriate preferences within SpectrAA such as lamp position, concentrations of standard solutions, and printing options.

4. Edit the names of the samples so they can be identified in SpectrAA's results.

5. Turn on the air and acetylene, which connect to the AAS.

6. Turn on the element lamp via SpectrAA and allow a few minutes for it to warm up.

7. Push and hold the ignition button on the AAS until the flame is ignited.

8. Put the tube in de-ionized water.

9. Click "Start" within SpectrAA.

10. Follow the prompts on the computer screen, which first instruct the operator to place the tube in the standard solutions.

11. Continue to follow prompts as they alert the operator when one sample has been sufficiently tested and the tube should be moved to the next sample.

12. Upon completion of testing for a set of samples, the flame shuts off automatically, but the AAS, air, and acetylene should all be turned off by the operator.

The tube mentioned above is depicted in Figure 4.7 as it draws the solution sample from the vial into the flame. The AAS usually required the tube to be left in each sample for 5 to 10 seconds to get a reading, which did not require more than 10 mL.

When a test was finished, SpectrAA printed out results in terms of element concentration, or mg/L. In many cases, SpectrAA returned a reading of "OVER", which indicated that the concentration of iron or nickel in a sample was higher than the concentrations of the standard solutions. When this occurred, samples were diluted further with de-ionized water and retested. It was important to keep track of the ratio of total solution volume to original solution volume so the results could be adjusted accordingly. For example, if 10 mL of de-ionized water were added to 5 mL of a sample, the sample would be diluted 3:1. Therefore, results indicating a concentration of 4.77 mg/L would be multiplied by 3, to give a true reading of 14.31 mg/L.

Figure 4.7 Measuring nickel concentration with the AAS

4.6 Mass Loss Testing

Mass loss testing was performed on the smallest nitinol samples using a high

precision analytical balance. Since little change in mass was expected, it was of

paramount importance to measure mass with as little interference as possible. The

analytical balance used has sliding glass doors to eliminate minute influences of air

movement, but the 12 inch specimens were too long to allow the doors to be closed, and

were also difficult to keep steady on the surface of the analytical balance. These

problems were solved by placing the specimen in a beaker and angling it so that one glass

door could be shut and the other door could be almost shut. This delicate procedure,

pictured in Figure 4.8, allowed the mass of the specimens to be accurately measured to

the thousandth of a gram. For each specimen, the following procedure was performed

before and after the specimen was corroded:

1. Turn on the analytical balance.

2. Place the beaker on the surface and press the "Tare" button to zero the

   reading.

3. Close one glass door completely and leave the opposite door cracked open.

4. Place the specimen through the cracked door and into the beaker.

5. Record the mass to the thousandth of a gram.
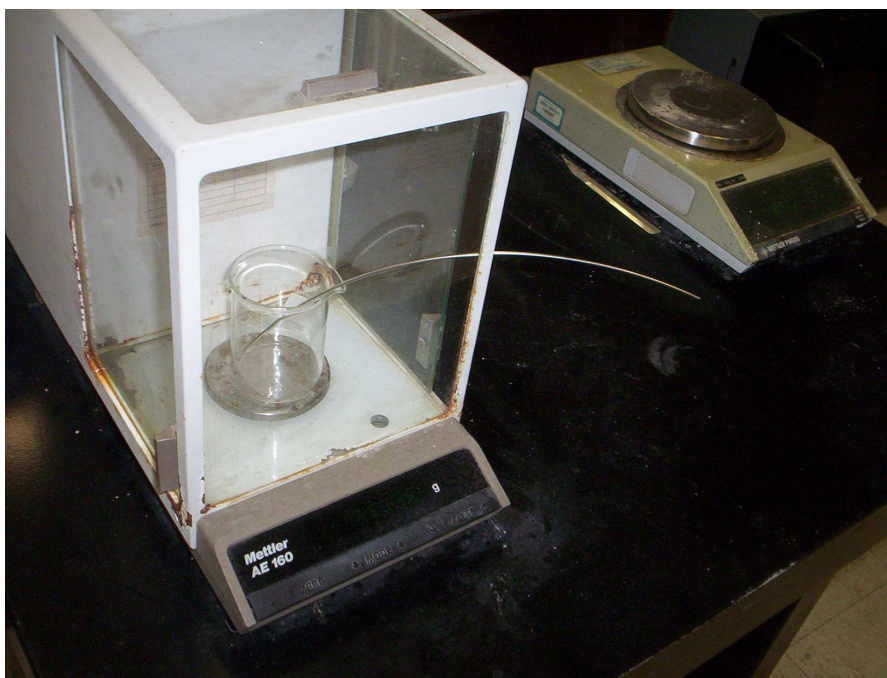
Figure 4.8 Analytical balance with specimen

4.7 Visual Evaluation

Visual evaluation was performed by taking pictures of the specimens in the solutions at the same intervals at which solution samples were taken. Additionally, the specimens were monitored multiple times a day, and any changes or irregularities were recorded.

CHAPTER 5 - RESULTS

5.1 Visual Examination Results

Visual examination was clearly the most subjective and least precise method for evaluating the corrosion of nitinol. However, making notes of the condition of the specimens and taking pictures at various stages provided clues about the corrosion process, as well as reinforced test results. Since visual examination was available before any tests were performed, it could also be used to predict test results.

The most obvious conclusion drawn from visual evaluation was that steel showed signs of corrosion in both sulfuric acid and seawater, whereas nitinol showed no visible change at all. The difference was so dramatic that even the casual observer would hypothesize that nitinol has less tendency to corrode than steel. Each combination of metal and solution is discussed below.

5.1.1 Steel in Sulfuric Acid

Within just eight hours of placing steel in sulfuric acid (for both grades of steel), the steel began to blacken and the acid showed a yellow tint. At twenty-four hours, the steel specimen was even darker and the solution was more yellow. Interestingly, this trend did not continue for the entire corrosion period. From twenty-four to forty-eight hours, the acid showed virtually no change in color, but the steel began to form a yellowish film. It appeared that the small yellow particles within the solution were attaching to the surface of the steel. For the remainder of the corrosion test, the solution

color changed very little and the surface of the steel built up more of the yellow film. In some cases, the solution appeared to even clear up some as the particles attached to the surface of the steel. These observations held true for both A992 and A588 steel specimens. The progression can be seen in Figure 5.1, which chronicles sample S-W-A-2-120 at various time intervals.

Occasionally, a clump of the film would break off from the surface of the steel and dissolve back into the solution. This would happen if the steel was bumped by the stir bar or the pipette, but could also happen due to the movement of the solution. When some of the film broke off, the area of exposed steel underneath was black, but would begin to turn yellow again as particles from the solution reattached themselves.

The corrosion product was wiped into the solution at the end of the corrosion period. After wiping the steel, the surface was discolored but showed no surface irregularities. The sulfuric acid instantly changed from a pale yellow to an opaque black as the corrosion product was wiped from the steel. Figure 5.2 shows a comparison of the steel and sulfuric acid for specimen S-5-A-1-120 before and after wiping it.

Figure 5.1 Specimen S-W-A-2-120 at various time intervals
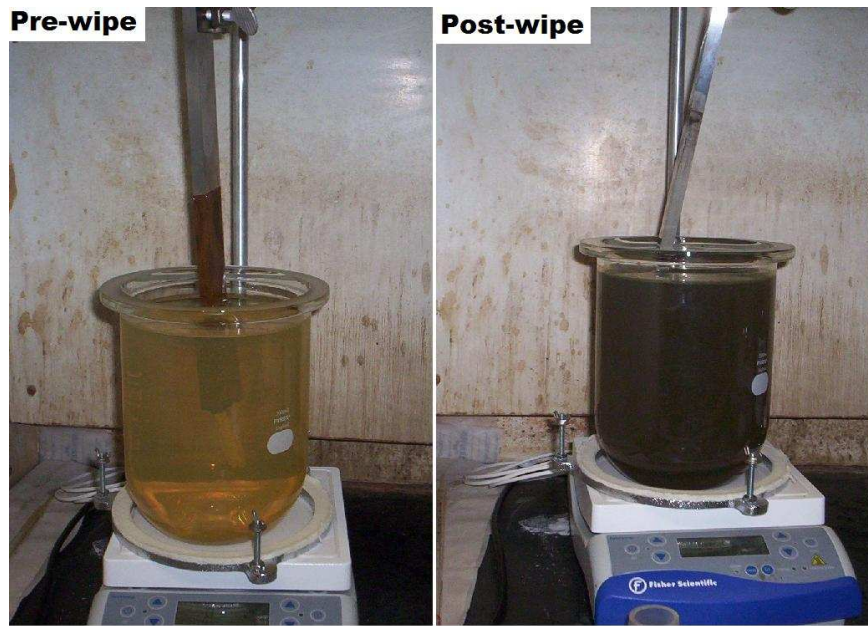
Figure 5.2 Specimen S-5-A-1-120 pre-wipe and post-wipe

5.1.2 Nitinol in Sulfuric Acid

Contrary to the steel, nitinol showed no visible signs of change when placed in sulfuric acid. The sulfuric acid remained clear throughout the remainder of the test, and the surface of the nitinol specimens showed no discoloration or abnormalities. To remain consistent, the specimens were wiped at the end of the corrosion period. But there was no visible corrosion product on the surface of the specimen, and neither specimen nor solution showed any change when wiped. Figure 5.3 compares steel and nitinol specimens after a five-day corrosion test. On the steel specimen, it is easy to determine what part of the steel was submerged, whereas the nitinol specimen looks identical throughout. Note that in Figure 5.4, which shows specimen N-.5-A-1-120 at various times, all pictures look nearly identical.

Figure 5.3 Comparison of steel (top) and nitinol (bottom) after five days in sulfuric acid

Figure 5.4 Specimen N-.5-A-1-120 at various time intervals

5.1.3 Steel in Seawater

Corrosion tests involving steel in seawater proceeded similarly to steel in sulfuric acid, except that the corrosion product and solution color were more orange. Again, the most noticeable change occurred within the first twenty-four hours. For the remainder of the corrosion period, the surface of the steel continued to develop an orange film, and the seawater kept the same orange tint. When the corrosion test was finished and the corrosion product was wiped back into the seawater, the seawater turned deep orange and the surface of the steel was left with orange discoloration. A comparison of the solution color at each interval can be seen for specimen S-5-W-1-120 in Figure 5.5. Note that the final sample, taken after the corrosion sample was wiped from the steel, is significantly darker than any other sample.

One interesting observation about the steel in seawater corrosion tests is that the steel showed mild corrosion on the section above the solution but below the parafilm. This indicates that steel is susceptible to corrosion when exposed to salt-laden air for a few days, even if it does not contact the seawater.

It was also interesting to note that the steel specimens showed initial visible signs of corrosion faster in seawater than in sulfuric acid. Figure 5.6 is a steel specimen that was exposed to seawater for no more than twenty minutes. Even after such a short corrosion time, the specimen is discolored.

Figure 5.5 Solution samples for specimen S-5-W-1-120

Figure 5.6 Steel specimen after less than twenty minutes in seawater

5.1.4 Nitinol in Seawater

Again, nitinol did not appear to change when submerged in seawater for five days. The seawater remained clear, and the nitinol showed no damage or discoloration. Figure 5.7 compares steel and nitinol specimens after five days in seawater. The nitinol specimen looks identical to specimens that were not corroded.

Figure 5.7 Comparison of steel (top) and nitinol (bottom) after five days in seawater

5.2 pH Testing Results

Results from pH testing, displayed in Table 5.1, support the hypothesis that nitinol experiences less corrosion than steel. For nitinol in sulfuric acid tests, the average change in pH from time zero to 120 hours was only +0.06, an amount considered almost negligible in pH testing. By comparison, the pH change for steel in sulfuric acid over the same time period was +2.35. Since pH and hydrogen ion activity are related on a logarithmic scale, a change of +2.35 is equivalent to a 99.55% decrease in hydrogen ion activity, whereas a change of +0.06 corresponds to a 12.90% activity decrease. The pH

was also measured after wiping the metal specimens, and compared to the original pH of the solutions. For steel in sulfuric acid, the average change from time zero to just after the wipe was +1.72; and for nitinol in sulfuric acid, the change was +0.04. Since nitinol specimens were smaller than steel specimens, it was expected that impact on pH would be less for nitinol than steel. However, the negligible change in pH for the nitinol specimens, even for the .5 inch diameter specimens, indicates that the sulfuric acid has a stronger reaction with steel than with nitinol, in terms of hydrogen ion activity.

The pH of seawater showed little change after reacting with either metal. Still, nitinol specimens changed the pH of the seawater less than steel specimens. For nitinol in seawater tests, the average change in pH from time zero to 120 hours was +0.03, and the average change from time zero to after the wipe was +0.06. For steel in seawater, the average change in pH was -0.24 from time zero to 120 hours, and -0.22 from time zero to after the wipe.

The pH results for each individual corrosion test are displayed in Table 5.1. Note that the pH values of the starting solutions were not identical, but were close to 3.33 for sulfuric acid and 8.14 for seawater. It is also interesting to note that two of the corrosion-resistant steel specimens, S-5-A-1-120 and S-5-W-1-120, impacted the pH level of solutions noticeably less than the other steel specimens. However, specimen S-5-A-2-120 caused pH changes similar to those experienced for typical steel specimens.

Table 5.1 pH results for each corrosion test

Specimen/Solution	pH			Change in pH	
Designation	Start	Pre-wipe	Post-wipe	Start to Pre-wipe	Start to Post-wipe
S-F-A-1-120	3.21	5.36	5.10	2.15	1.89
S-F-A-2-120	3.69	5.95	5.39	2.26	1.70
S-W-A-1-120	3.20	5.97	5.40	2.77	2.20
S-W-A-2-120	3.61	5.99	5.23	2.38	1.62
S-5-A-1-120	3.33	5.26	4.21	1.93	0.88
S-5-A-2-120	3.17	5.78	5.18	2.61	2.01
Average	3.37	5.72	5.09	2.35	1.72
N-.5-A-1-120	3.48	3.59	3.55	0.11	0.07
N-.5-A-2-120	3.48	3.58	3.57	0.10	0.09
N-.25-A-1-120	3.54	3.67	3.67	0.13	0.13
N-.25-A-2-120	3.29	3.31	3.26	0.02	-0.03
N-.085-A-1-120	2.89	2.88	2.86	-0.01	-0.03
N-.085-A-2-120	3.10	3.10	3.11	0.00	0.01
Average	3.30	3.36	3.34	0.06	0.04
S-F-W-1-120	8.10	7.81	7.88	-0.29	-0.22
S-W-W-1-120	8.20	7.92	7.95	-0.28	-0.25
S-5-W-1-120	8.13	7.99	7.95	-0.14	-0.18
Average	8.14	7.91	7.93	-0.24	-0.22
N-.5-W-1-120	8.12	8.12	8.13	0.00	0.01
N-.25-W-1-120	8.14	8.14	8.23	0.00	0.09
N-.085-W-1-120	8.20	8.28	8.29	0.08	0.09
Average	8.15	8.18	8.22	0.03	0.06

5.3 Atomic Absorption Spectrometer Testing Results

For each solution sample, the Atomic Absorption Spectrometer (AAS) was used to determine the concentration of either iron or nickel, and these results were used to plot time versus element concentration within the solution. Data for each grouping of metal and solution are discussed in the following sections, and SpectrAA printouts for all AAS testing can be found in Appendix B. The AAS data provided further evidence to prove that steel corrodes more readily than nitinol in corrosive environments typical of civil structures. Additionally, the data collected from AAS testing strongly corresponds to visual observations made during each corrosion test.

5.3.1 Steel in Sulfuric Acid

In the case of steel corroded with sulfuric acid, the concentration of iron in sulfuric acid began increasing as soon as the corrosion period began. After just five minutes, the iron concentrations were between 0.3 and 0.6 mg/L. After eight hours, the iron concentrations ranged from 3 to 11 mg/L. This early increase in iron concentration did not continue throughout the corrosion period. Instead, the iron concentration usually peaked between 24 and 48 hours, and then began to actually decrease. Initially this was surprising, because it was expected that the iron concentrations would increase up to a maximum value and then hold steady. However, the decrease in iron concentration can be attributed to particles reattaching to the steel surface, as was observed and recorded during visual examination.

Solution samples taken after the corrosion product was wiped back into the solution had a very high iron concentration. Again, this is supported by visual evidence which demonstrated that iron seeps out from the steel, but stays close to the surface

74

instead of completely dissolving within the sulfuric acid. Therefore, it can be concluded that the iron concentrations measured prior to wiping the corrosion product are low because the samples do not include the iron collected on the steel surface. Iron concentrations in samples taken after wiping the corrosion product were as high as 229 mg/L, as seen in Table 5.3.

Iron concentrations for each solution sample, and time versus concentration plots for each corrosion test can be seen in Tables 5.2-5.7 and Figures 5.9-5.14 on the following pages. Some of the plots have a seemingly random curve with more than one peak. This can be attributed to pieces of the film breaking off of the steel surface and dissolving back into the solution. For example, in Figure 5.8, it can be seen that the orange film of specimen S-W-A-1-120 is missing a piece near the upper left edge. This addition of iron to the solution is likely the cause of the second peak in Figure 5.11. For the time versus concentration plots, the iron concentration for the post-wipe sample is not plotted because the value is in some cases much higher than the values at other times. However, it should be noted in the tables that the post-wipe sample, designated "120W", is always significantly higher than the 120 hour sample taken just before wiping the corrosion product.

Figure 5.8 Specimen S-W-A-1-120

Table 5.2 Iron concentrations for samples from specimen S-F-A-1-120

Time (hr)	Iron Concentration (mg/L)
0	0.013
0.08	0.603
8	10.302
24	11.348
48	9.364
72	19.197
96	9.39
120	9.258
120W	21.36

Figure 5.9 Time versus concentration plot for S-F-A-1-120

Table 5.3 Iron concentrations for samples from specimen S-F-A-2-120

Time (hr)	Iron Concentration (mg/L)
0	0
0.08	0.364
8	3.5454
24	8.079
48	6.591
72	6.051
96	5.277
120	4.626
120W	229.32
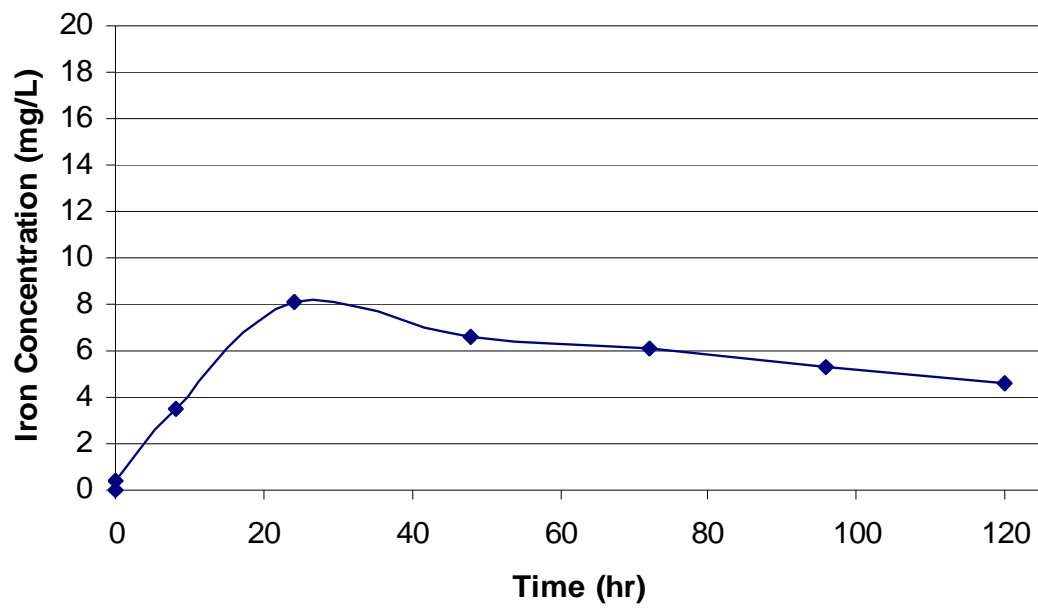
Figure 5.10 Time versus concentration plot for S-F-A-2-120

Table 5.4 Iron concentrations for samples from specimen S-W-A-1-120

Time (hr)	Iron Concentration (mg/L)
0	0
0.08	0.514
8	7.542
24	7.758
48	7.65
72	8.532
96	10.122
120	7.476
120W	36.9

Figure 5.11 Time versus concentration plot for S-W-A-1-120

Table 5.5 Iron concentrations for samples from specimen S-W-A-2-120

Time (hr)	Iron Concentration (mg/L)
0	0.002
0.08	0.377
8	5.253
24	7.872
48	6.957
72	6.363
96	5.535
120	4.905
120W	170.01

Figure 5.12 Time versus concentration plot for S-W-A-2-120

Table 5.6 Iron concentrations for samples from specimen S-5-A-1-120

Time (hr)	Iron Concentration (mg/L)
0	0
0.08	0.327
8	5.22
24	6.738
48	8.367
72	9.177
96	9.069
120	6.741
120W	14.31

Figure 5.13 Time versus concentration plot for S-5-A-1-120

Table 5.7 Iron concentrations for samples from specimen S-5-A-2-120

Time (hr)	Iron Concentration (mg/L)
0	0
0.08	0.6
8	10.887
24	12.132
48	13.848
72	10.866
96	9.669
120	8.49
120W	41.58
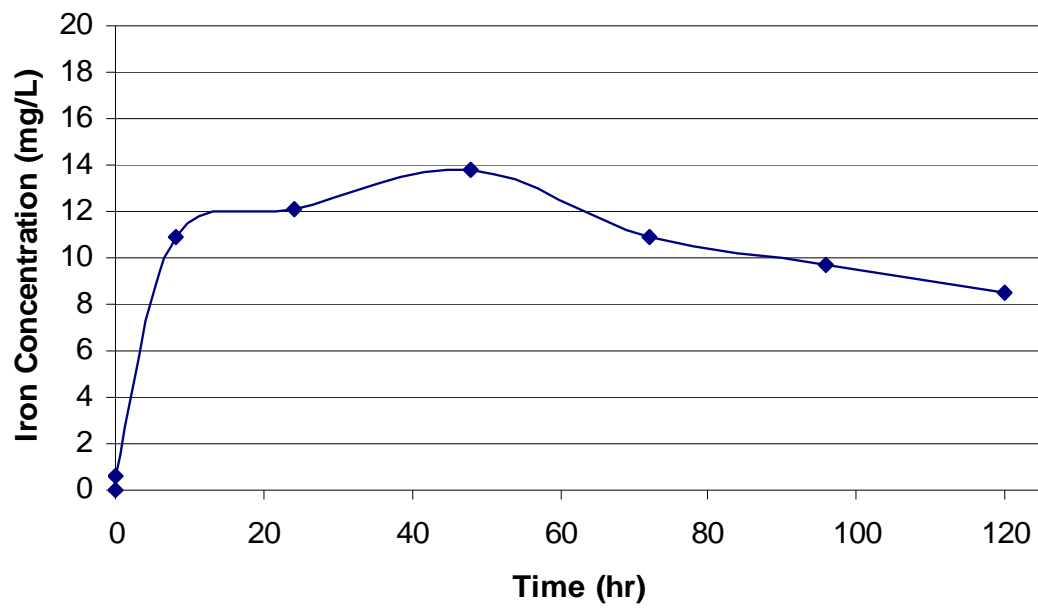
Figure 5.14 Time versus concentration plot for S-5-A-2-120

5.3.2 Nitinol in Sulfuric Acid

Solution samples taken from nitinol in sulfuric acid tests had very low nickel concentrations. In fact, the maximum nickel concentration at any time for all six tests was just 1.0 mg/L, considerably less than iron concentrations for steel in sulfuric acid tests. However, it should be pointed out that total nitinol mass affected by corrosion could be twice the amount of nickel loss, since nickel only accounts for half of nitinol.

Nickel concentrations and time versus concentration plots are shown in Tables 5.8-5.13 and Figures 5.15-5.20 on the following pages. The plots are shown on the same scale as the previous iron concentration plots. Additionally, the plots are shown on a smaller scale in Figure 5.21. Plots for the .5 inch diameter specimens are most similar to the plots for steel specimens because they show an increase in concentration over the first 24 hours, then level off. The plots for the .25 inch diameter specimens are unusual because they appear almost linear, without any upper plateau. Still, the nickel concentrations are extremely low compared to iron concentrations from steel specimens. The .085 inch diameter specimens had concentrations so close to zero that they were often read as negative values by the AAS. This simply means that concentrations were below the detectable limit and were therefore recorded as zero.

The plots for time versus nickel concentration include values for the solution sample collected after wiping the corrosion product. As expected, this sample shows little deviation from the 120 hour sample, because there was not a corrosion product to be wiped into the solution.

Table 5.8 Nickel concentrations for samples from specimen N-.5-A-1-120

Time (hr)	Nickel Concentration (mg/L)
0	0.022
0.08	0.004
8	0.635
24	0.908
48	0.966
72	0.962
96	1.007
120	0.937
120W	0.935

Figure 5.15 Time versus concentration plot for N-.5-A-1-120

Table 5.9 Nickel concentrations for samples from specimen N-.5-A-2-120

Time (hr)	Nickel Concentration (mg/L)
0	0
0.08	0
8	0.285
24	0.454
48	0.547
72	0.547
96	0.567
120	0.594
120W	0.523

Figure 5.16 Time versus concentration plot for N-.5-A-2-120

Table 5.10 Nickel concentrations for samples from specimen N-.25-A-1-120

Time (hr)	Nickel Concentration (mg/L)
0	0
0.08	0
8	0.015
24	0.155
48	0.259
72	0.335
96	0.396
120	0.453
120W	0.45
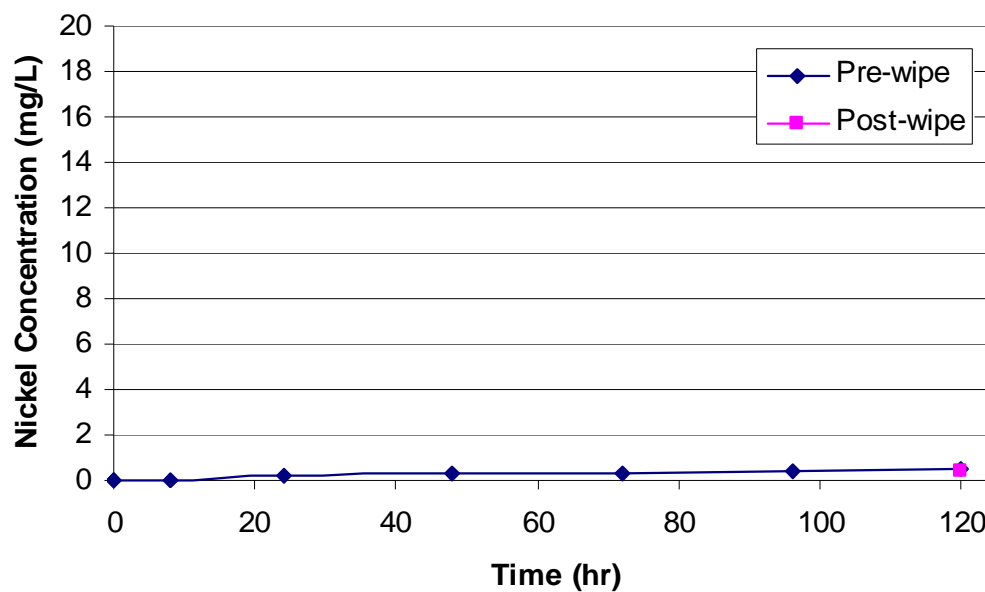
Figure 5.17 Time versus concentration plot for N-.25-A-1-120

Table 5.11 Nickel concentrations for samples from specimen N-.25-A-2-120

Time (hr)	Nickel Concentration (mg/L)
0	0.02
0.08	0.01
8	0.02
24	0.059
48	0.102
72	0.145
96	0.207
120	0.273
120W	0.271
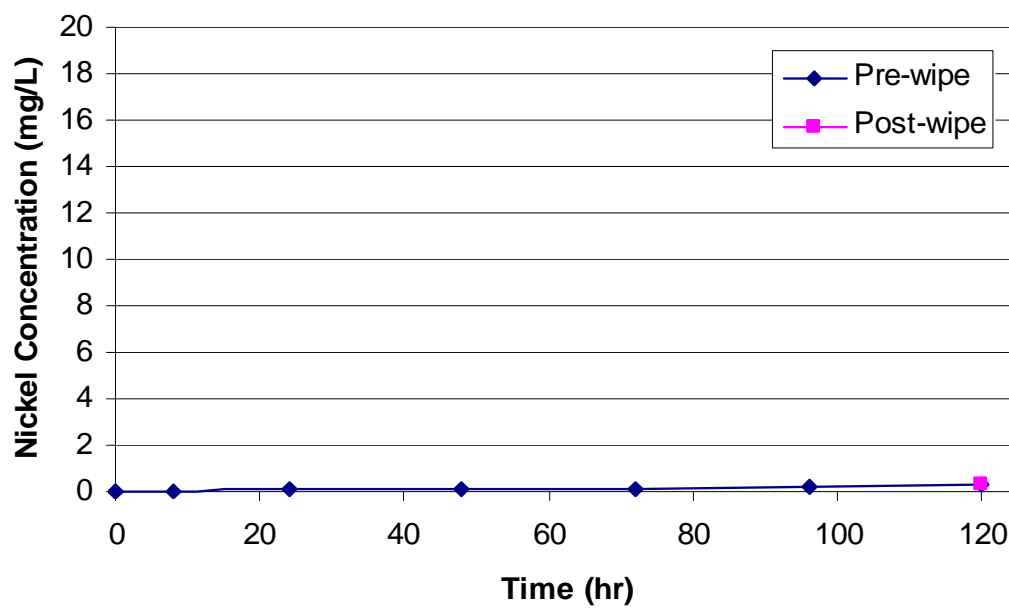
Figure 5.18 Time versus concentration plot for N-.25-A-2-120

Table 5.12 Nickel concentrations for samples from specimen N-.085-A-1-120

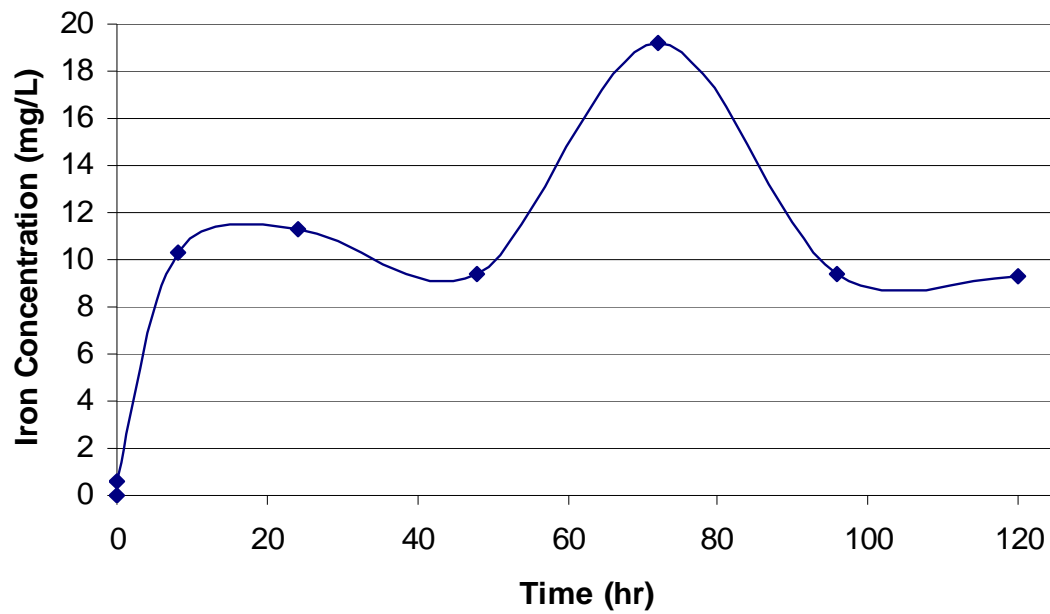| Time (hr)	Nickel Concentration (mg/L)
0	0
0.08	0.014
8	0
24	0
48	0.003
72	0
96	0
120	0.008
120W	0.01
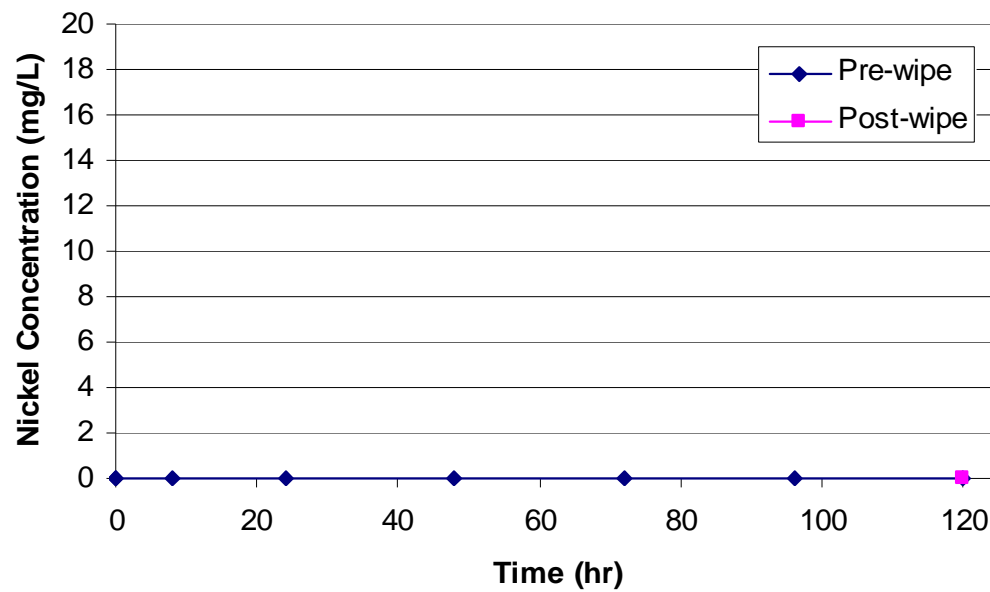
Figure 5.19 Time versus concentration plot for N-.085-A-1-120

Table 5.13 Nickel concentrations for samples from specimen N-.085-A-2-120

Time (hr)	Nickel Concentration (mg/L)
0	0.005
0.08	0.01
8	0
24	0
48	0.009
72	0
96	0.025
120	0.028
120W	0.012
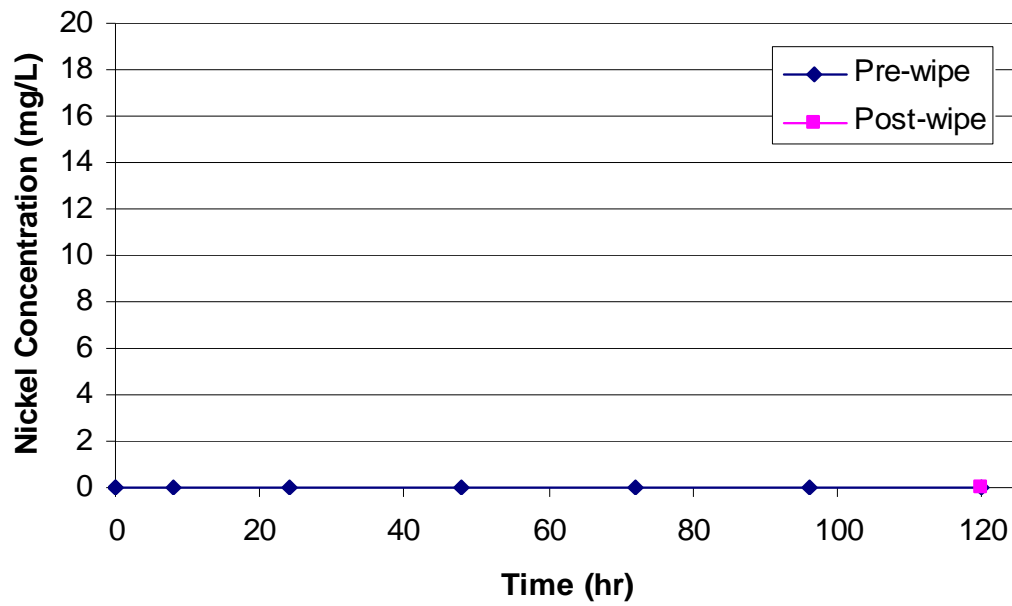
Figure 5.20 Time versus concentration plot for N-.085-A-2-120
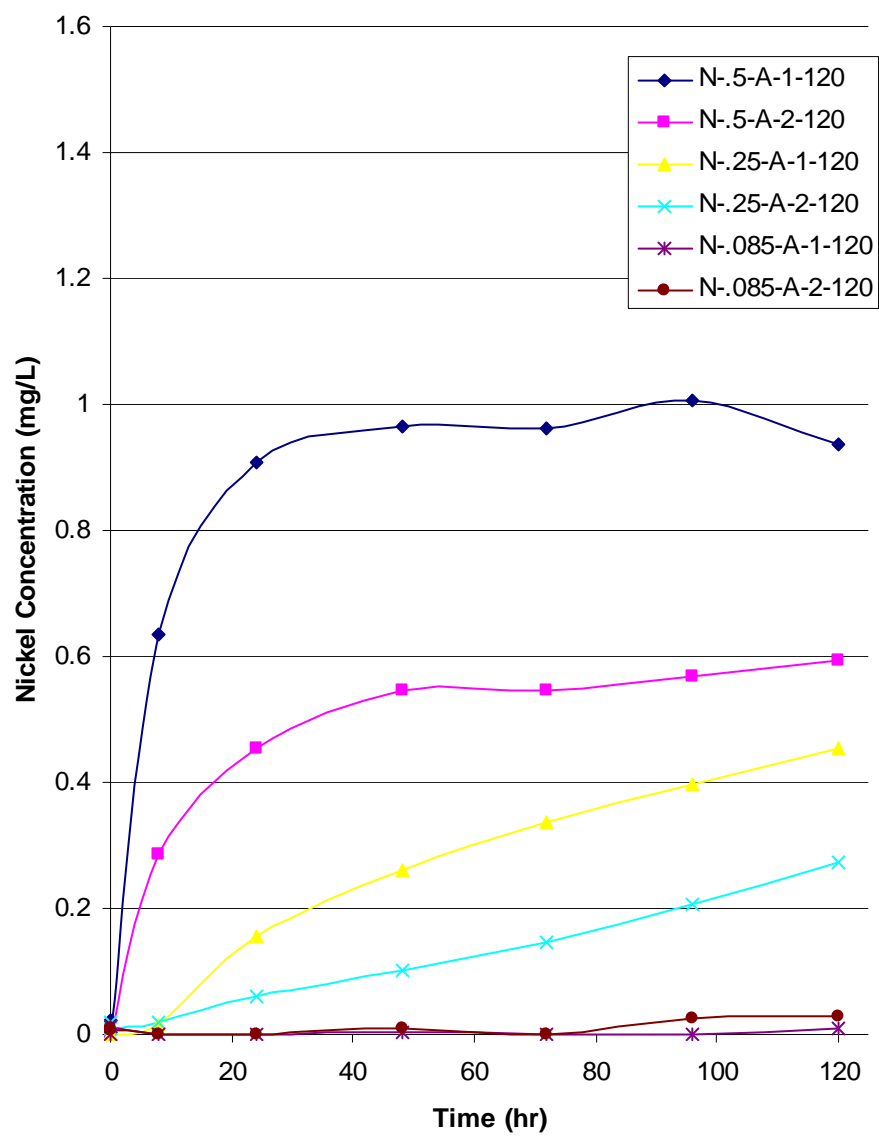
Figure 5.21 Time versus concentration plots for all nitinol specimens in sulfuric acid

5.3.3 Steel in Seawater

For steel in seawater, time versus concentration plots look similar to the plots for steel in sulfuric acid, except that the iron concentrations are lower. For all samples taken prior to wiping the corrosion product, the maximum iron concentration is about 7 mg/L. Again, iron concentrations for the post-wipe solution samples are much higher, up to 130 mg/L for sample S-5-W-1-120W. Results for the three corrosion tests are displayed in Tables 5.14-5.16 and Figures 5.22-5.24. The plots show a quick initial increase in iron concentration, followed by lower values, but with additional crests due to pieces of the film breaking off of the surface of the steel. The post-wipe samples are not plotted because they are too high to be shown on the same scale. High iron concentrations in the post-wipe sample indicate that the iron was concentrated in the surface film, much like the case of steel in sulfuric acid. Therefore, concentrations for samples prior to the wipe can be misleading because they do not measure the full amount of iron that has dissolved from the specimen.

Table 5.14 Iron concentrations for samples from specimen S-F-W-1-120

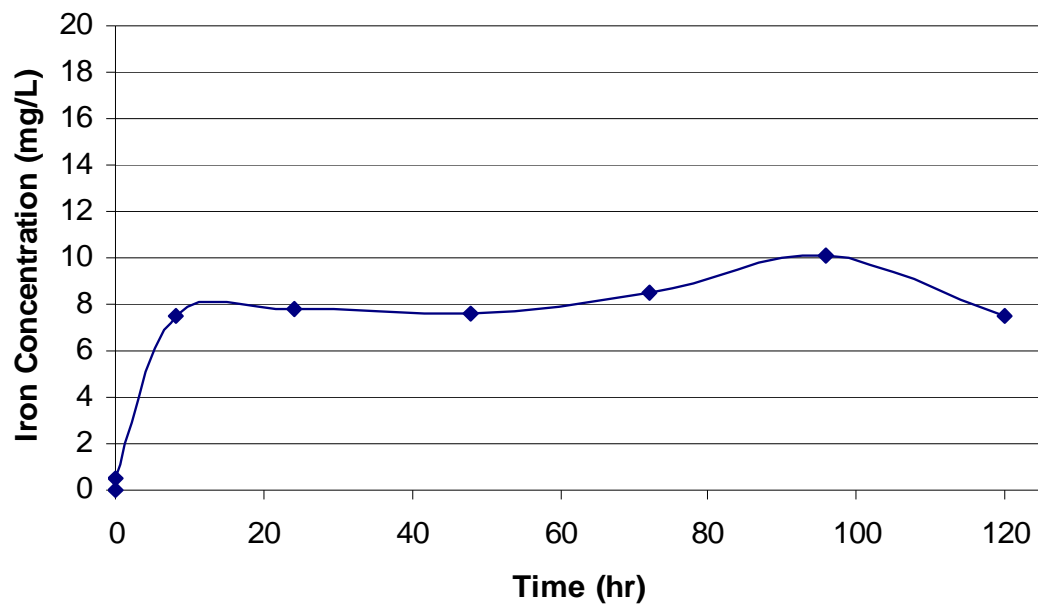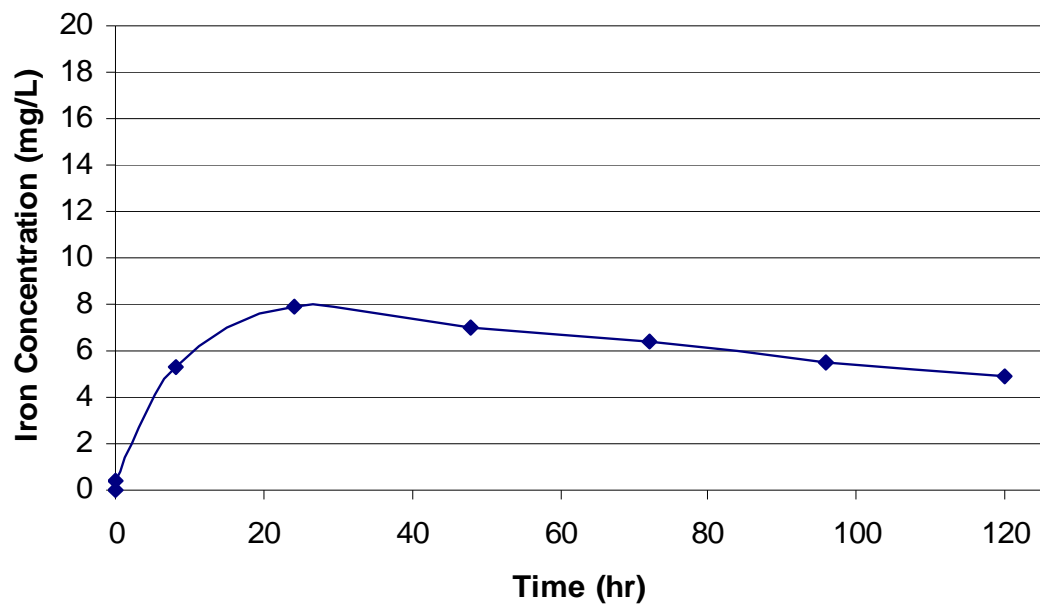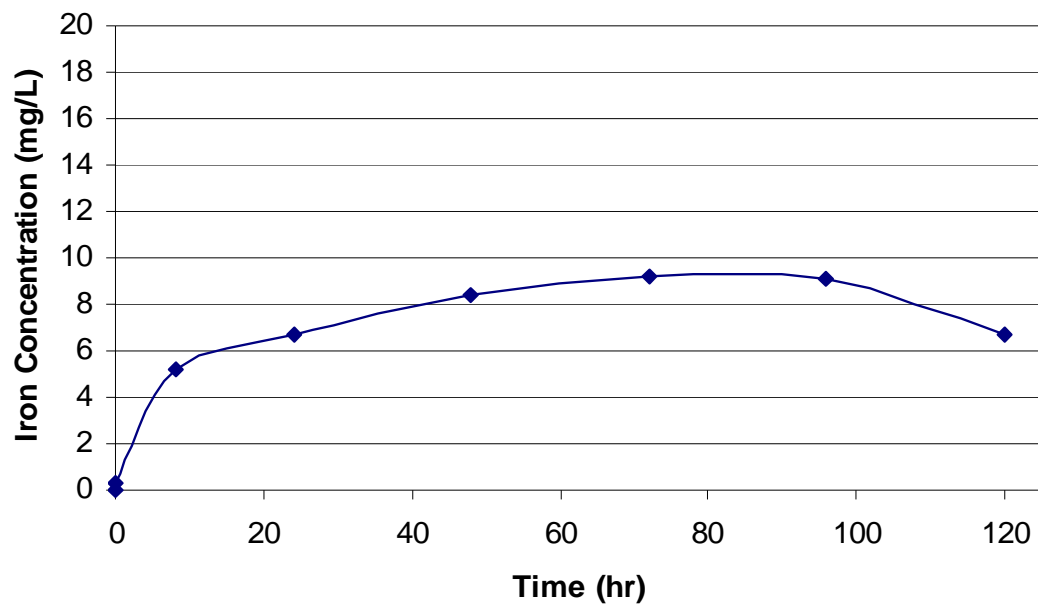| Time (hr)	Iron Concentration (mg/L)
0	0.315
0.08	0.566
8	7.056
24	3.695
48	1.374
72	1.517
96	1.314
120	0.948
120W	106.68
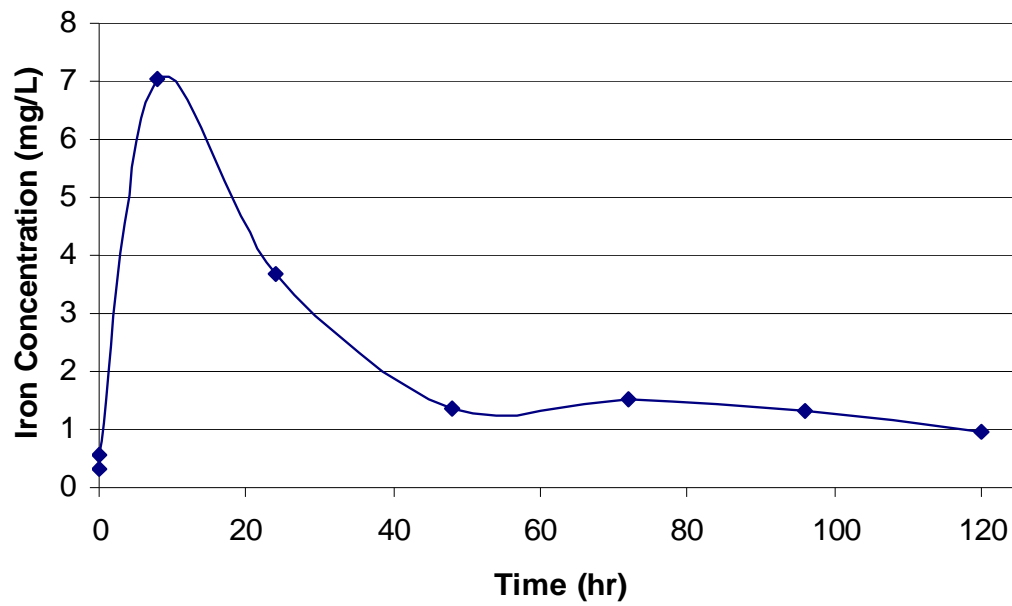
Figure 5.22 Time versus concentration plot for S-F-W-1-120

Table 5.15 Iron concentrations for samples from specimen S-W-W-1-120

Time (hr)	Iron Concentration (mg/L)
0	0.331
0.08	0.63
8	5.16
24	4.204
48	3.275
72	2.493
96	2.033
120	5.282
120W	94.74
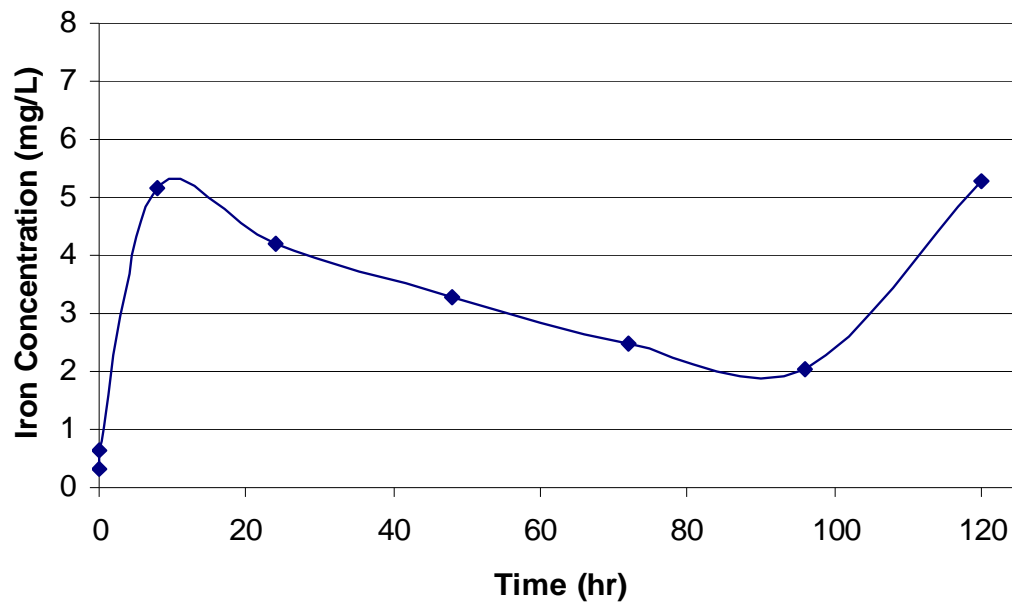
Figure 5.23 Time versus concentration plot for S-W-W-1-120

Table 5.16 Iron concentrations for samples from specimen S-5-W-1-120

Time (hr)	Iron Concentration (mg/L)
0	0.334
0.08	0.47
8	5.465
24	4.413
48	5.957
72	2.846
96	1.654
120	3.56
120W	130.77
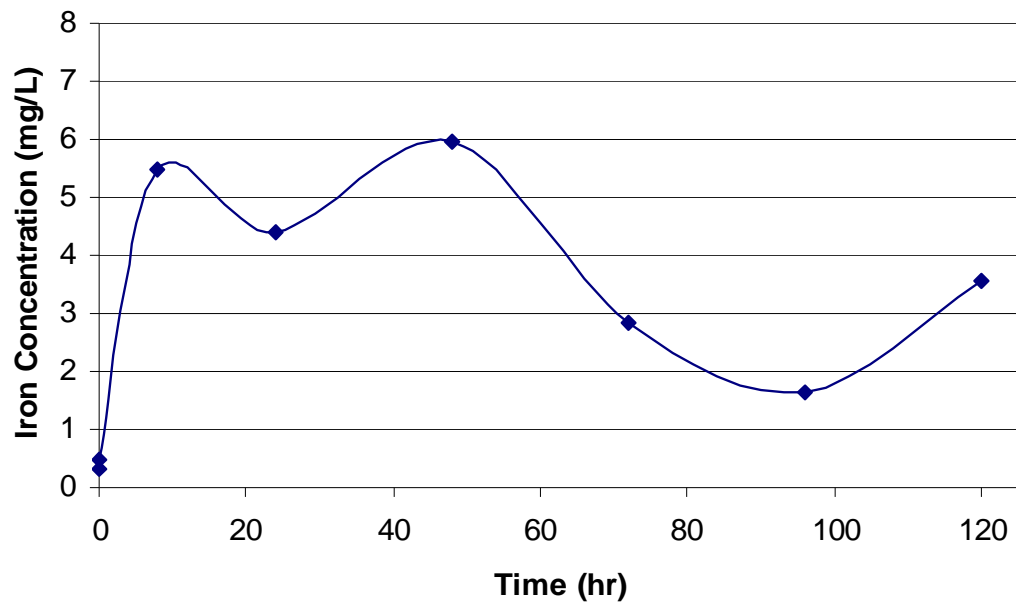
Figure 5.24 Time versus concentration plot for S-5-W-1-120

5.3.4 Nitinol in Seawater

Nickel concentrations from samples of nitinol in seawater tests were even lower than the concentrations from nitinol in sulfuric acid tests. The highest nickel concentration was .621 mg/L, found in sample N-.5-A-1-120. However, the measured nickel concentration for sample N-.5-A-1-0 was .324 mg/L, indicating that the seawater already had a small trace of nickel in it before combining it with the nitinol specimen. AAS data for each nitinol and seawater corrosion test is presented in Tables 5.17-5.19 and Figures 5.25-5.27. Again, time versus concentration plots are shown on a smaller scale in Figure 5.28. Nickel concentrations are often so low that they are recorded to be less than the amount of nickel in the seawater alone. Concentrations for the post-wipe solution samples, which are shown on the plots, are almost identical to the 120 hour samples taken just before wiping the corrosion product.

Table 5.17 Nickel concentrations for samples from specimen N-.5-W-1-120

Time (hr)	Nickel Concentration (mg/L)
0	0.324
0.08	0.326
8	0.37
24	0.184
48	0.477
72	0.54
96	0.591
120	0.621
120W	0.621
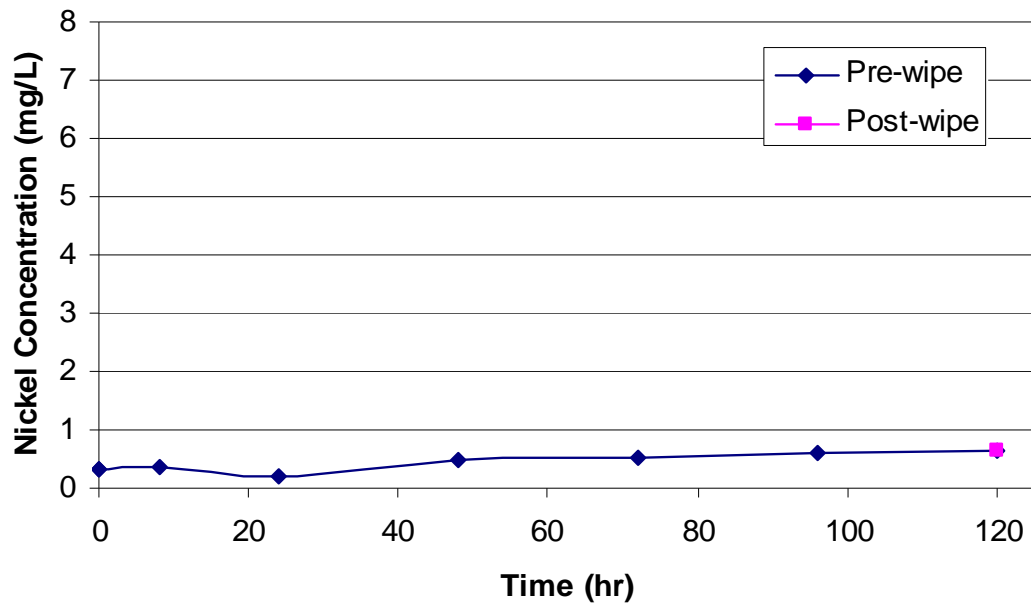
Figure 5.25 Time versus concentration plot for N-.5-W-1-120

Table 5.18 Nickel concentrations for samples from specimen N-.25-W-1-120

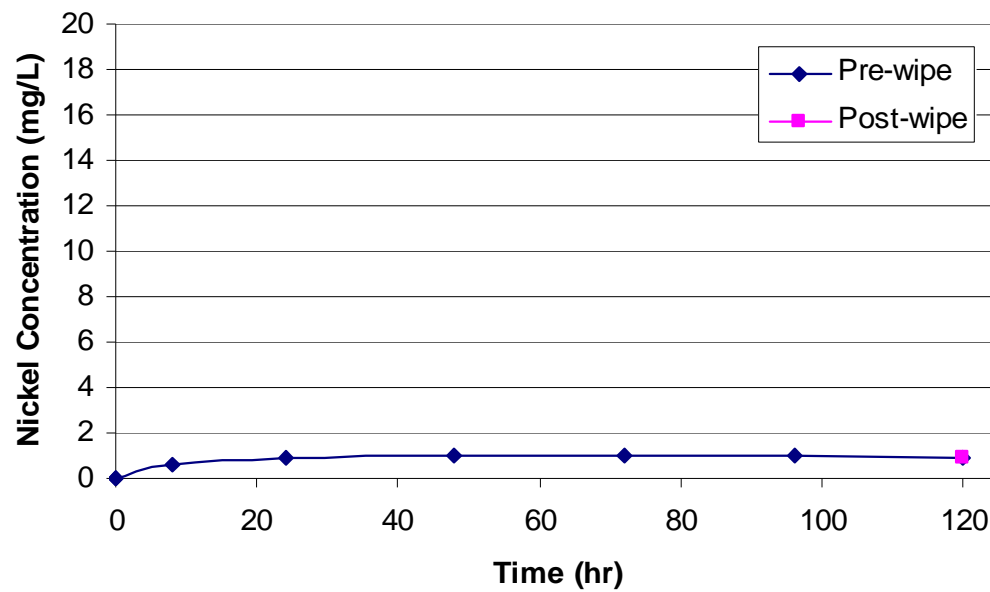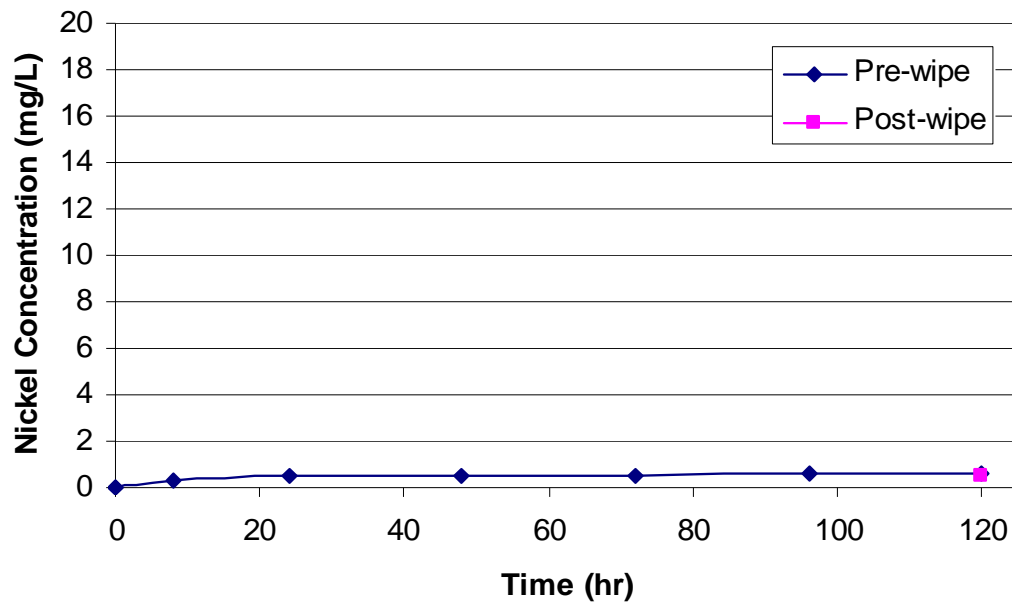| Time (hr)	Nickel Concentration (mg/L)
0	0.295
0.08	0.319
8	0.303
24	0.311
48	0.34
72	0.394
96	0.399
120	0.415
120W	0.416
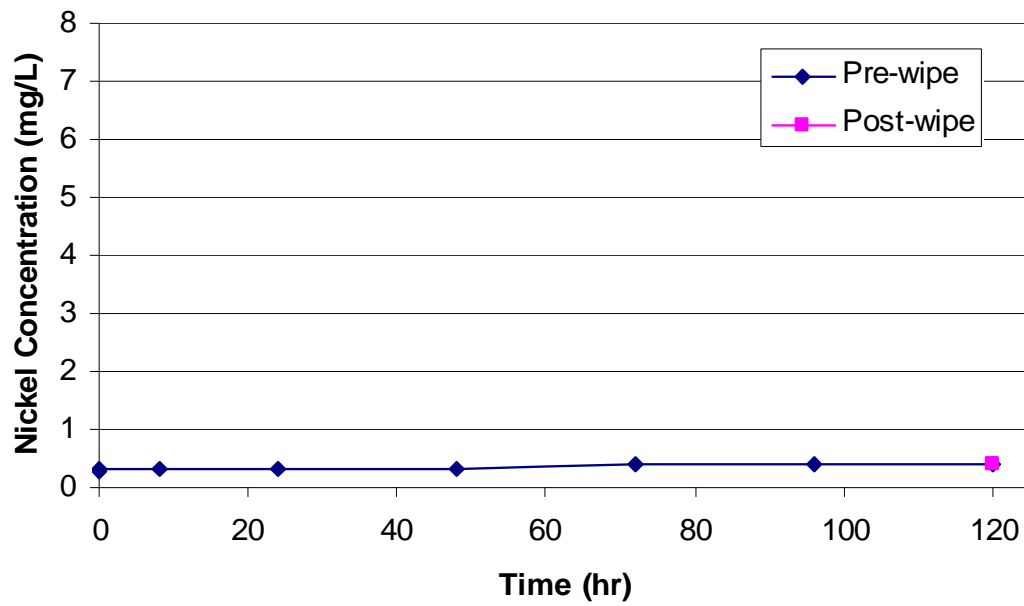
Figure 5.26 Time versus concentration plot for N-.25-W-1-120

Table 5.19 Nickel concentrations for samples from specimen N-.085-W-1-120

| Time (hr)	Nickel Concentration (mg/L)
0	0.266
0.08	0.285
8	0.243
24	0.26
48	0.265
72	0.271
96	0.239
120	0.255
120W	0.279
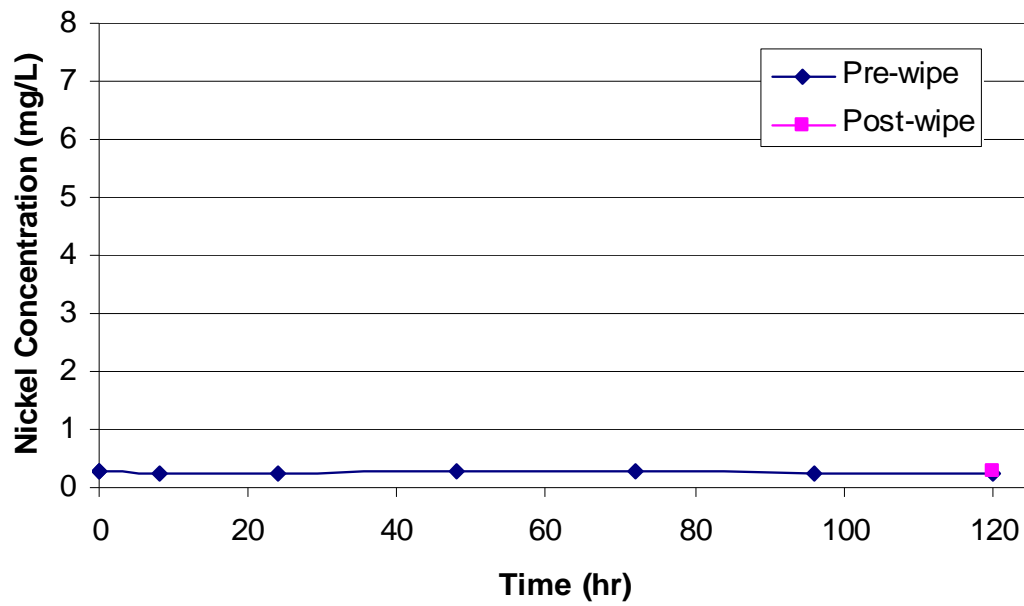
Figure 5.27 Time versus concentration plot for N-.085-W-1-120
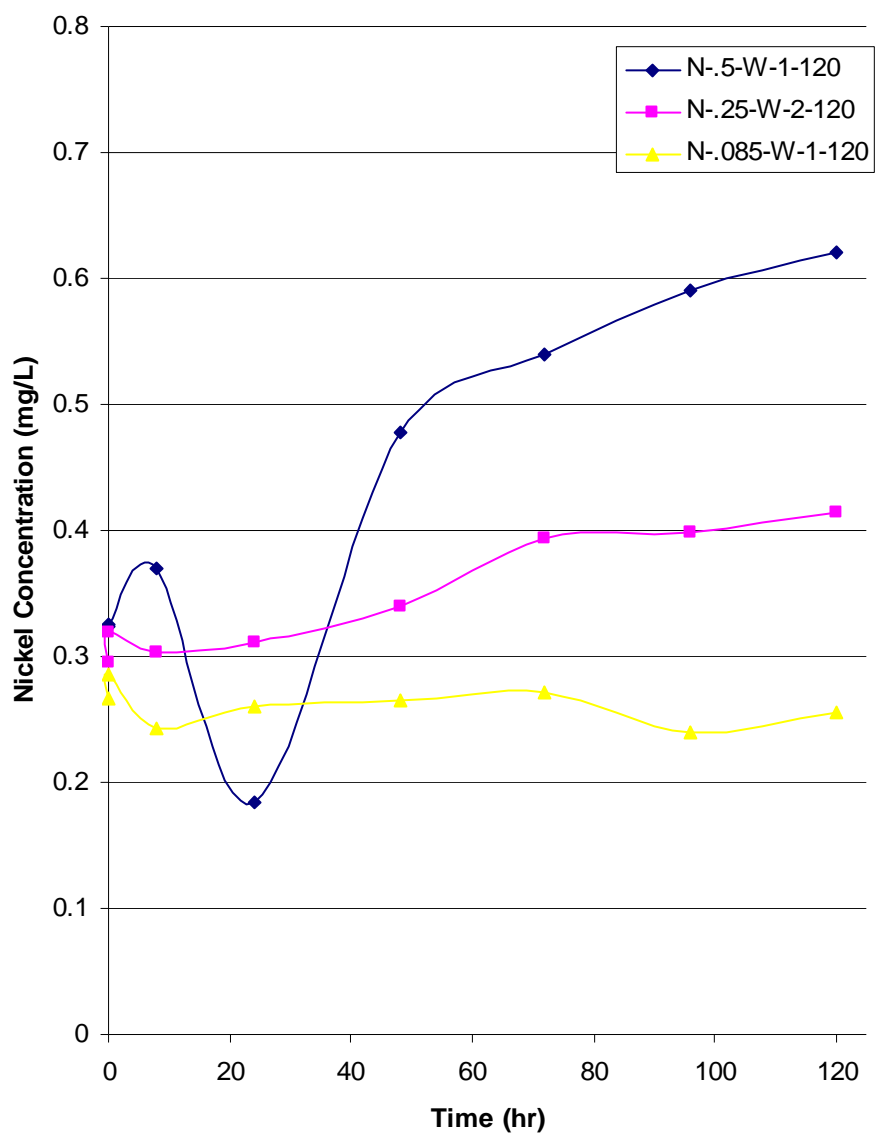
Figure 5.28 Time versus concentration plots for all nitinol specimens in seawater

5.3.5 Direct Comparison

AAS results indicate high iron concentrations in solutions used to corrode steel, and low nickel concentrations in solutions used to corrode nitinol. However, the raw lab results should not be compared directly, because specimens vary in size. A large specimen yields higher concentrations than a smaller specimen, simply because there is more exposed surface area to be corroded. Therefore results should be normalized to account for size disparities. To accomplish this goal, concentrations can be multiplied by solution volume to surface area ratios, found in Table 3.2, to get a ratio of element mass loss to surface area in mg/in^2. Before making this calculation, the initial concentration within a solution should be subtracted from all other values, to eliminate the amount of iron or nickel that already existed within the solution. An example of these calculations can be seen in Table 5.20, which converts the AAS measured concentrations to element mass loss per surface area for specimen S-W-A-2-120.

Table 5.20 Element mass loss per surface area for S-W-A-2-120

Time (hr)	Measured Concentration (mg/L)	Concentration without Initial (mg/L)	Element Mass Loss / Surface Area Corroded (mg/in^2)
0	0.002	0.000	0.00
0.08	0.377	0.375	0.04
8	5.253	5.251	0.62
24	7.872	7.870	0.93
48	6.957	6.955	0.82
72	6.363	6.361	0.75
96	5.535	5.533	0.65
120	4.905	4.903	0.58
120W	170.01	170.01	20.00

Since the ratio of solution volume to surface area for specimen S-W-A-2-120 is 117.6 mL/in^2, the following formula is used to calculate the mass loss per surface area corroded ratio:

ratio = [(0.377 mg/L) – (0.002 mg/L)] x (.1176 L/in^2) = .0441 mg/in^2

where "ratio" refers to element mass loss per surface area corroded. Following the same calculation procedure, normalized results can be plotted for direct comparison. A comparison between one of each size specimen over five days of corrosion in sulfuric acid is shown in Figure 5.29. The figure shows that iron loss per surface area is higher than nickel loss per surface area, even for values recorded prior to wiping the corrosion product.

Figure 5.30 makes the same comparison for specimens in seawater. Values for specimen S-F-W-1-120 actually dip below values for the nitinol specimens. However, the total iron mass loss, recorded by the post-wipe solution sample, is still much higher than nickel mass loss for the nitinol specimens. Table 5.21 compares the concentrations of the post-wipe solution samples and the normalized results for each specimen.

Upon review of the results in Table 5.21, it is apparent that there is a great deal of variation between element mass loss in different specimens, even for specimens of the same material and size. Despite the wide range of values, iron mass loss for steel specimens is consistently higher than nickel mass loss for nitinol specimens. Even the lowest value for iron mass loss is nearly 9 times more than the highest value for nickel loss. The higher iron mass loss values are hundreds of times more than nickel mass loss values. Since nickel accounts for just half of nitinol, the total nitinol mass loss due to

corrosion could be double the amount of measured nickel loss. Still, iron mass loss

values are significantly higher than total nitinol mass loss.
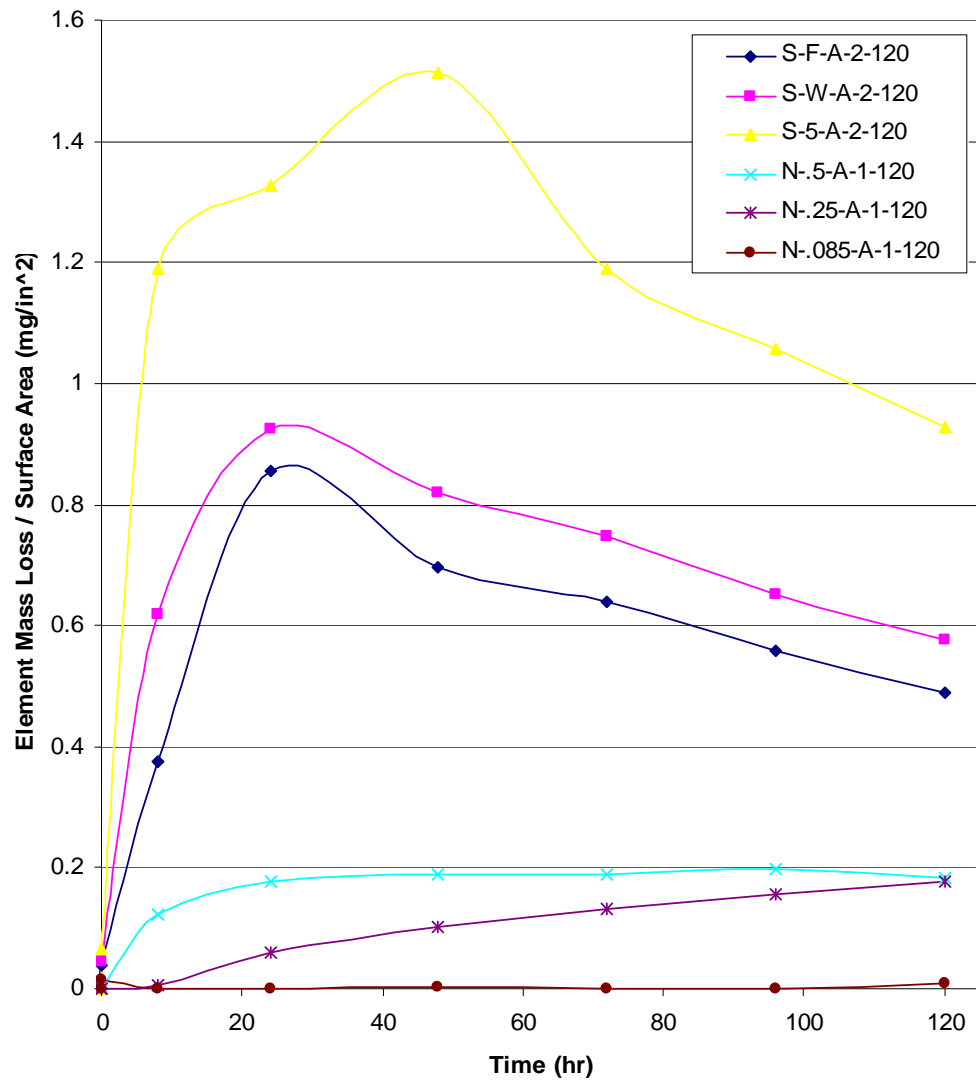
Figure 5.29 Normalized comparison of element mass loss per surface area for each
specimen type in sulfuric acid
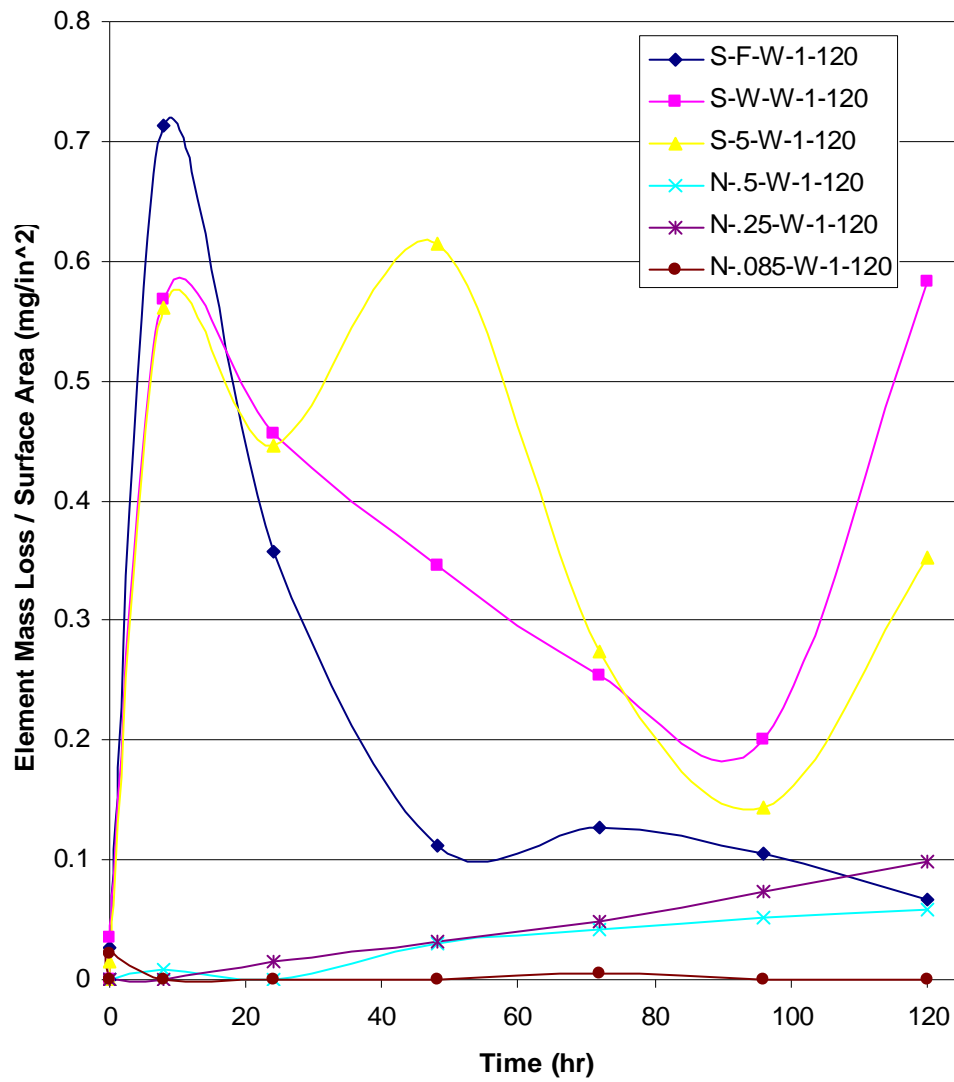
Figure 5.30 Normalized comparison of element mass loss per surface area for each specimen type in seawater

Table 5.21 Normalized results for the final solution sample from each corrosion test

Sample	Measured Concentration (mg/L)	Element Mass Loss / Surface Area Corroded (mg/in^2)
S-F-A-1-120W	21.36	2.3
S-F-A-2-120W	229.32	24.3
S-W-A-1-120W	36.90	4.3
S-W-A-2-120W	170.01	20.0
S-5-A-1-120W	14.31	1.6
S-5-A-2-120W	41.58	4.5
N-.5-A-1-120W	0.94	0.2
N-.5-A-2-120W	0.52	0.1
N-.25-A-1-120W	0.45	0.2
N-.25-A-2-120W	0.27	0.1
N-.085-A-1-120W	0.01	0.01
N-.085-A-2-120W	0.01	0.01
S-F-W-1-120W	106.68	11.3
S-W-W-1-120W	94.74	11.1
S-5-W-1-120W	130.77	14.3
N-.5-W-1-120W	0.62	0.06
N-.25-W-1-120W	0.27	0.10
N-.085-W-1-120W	0.28	0.01

5.4 Tension Testing Results

Tension testing proved to be inconclusive and problematic. Several nitinol specimens failed prematurely because the grips dug into the surface and caused brittle failure at the affected cross section. This occurrence exposes nitinol's high notch-sensitivity, but does not contribute to data regarding the effects of corrosion. The brittle failure occurred for uncorroded specimens as well as for corroded specimens, eliminating the possibility that the failure was related to corrosion.

The .085 inch diameter nitinol specimens were held with grips made for flat specimens, because they were too small to fit in the grips made for round specimens. The

flat grips were less detrimental to the nitinol, and these specimens did not experience early failure due to notch-sensitivity. Therefore, ultimate tensile strengths could be determined for these specimens. Unfortunately, the grips allowed the specimens to slip significantly during testing, which means that the strain values are inaccurate. The general shapes of the stress versus strain diagrams are correct, but they are disproportionate due to the inaccurate strain values. Still, the ultimate tensile strengths of the five specimens can be read from the diagrams, which are shown on the same plot in Figure 5.31. Note that the strengths of all five samples are nearly identical, indicating that the specimens were not adversely affected by the five-day corrosion period.

Tension tests were performed on all steel specimens without incident. Though some corroded specimens have slightly lower strengths than uncorroded specimens, the difference is within the dispersion that would be expected for a group of uncorroded steel specimens. In fact, many of the corroded specimens have higher strengths than the uncorroded specimens. For every specimen, the failure occurred within the corroded portion of the steel as opposed to the uncorroded portion that protruded through the top of the kettle. However, this may simply be a function of the length of the corroded portion that was between the crosshead grips, and does not necessarily indicate that the corroded portion of the steel was significantly weaker. Yield strength, determined by the .2% offset method, and ultimate strength are listed for each specimen in Table 5.22.
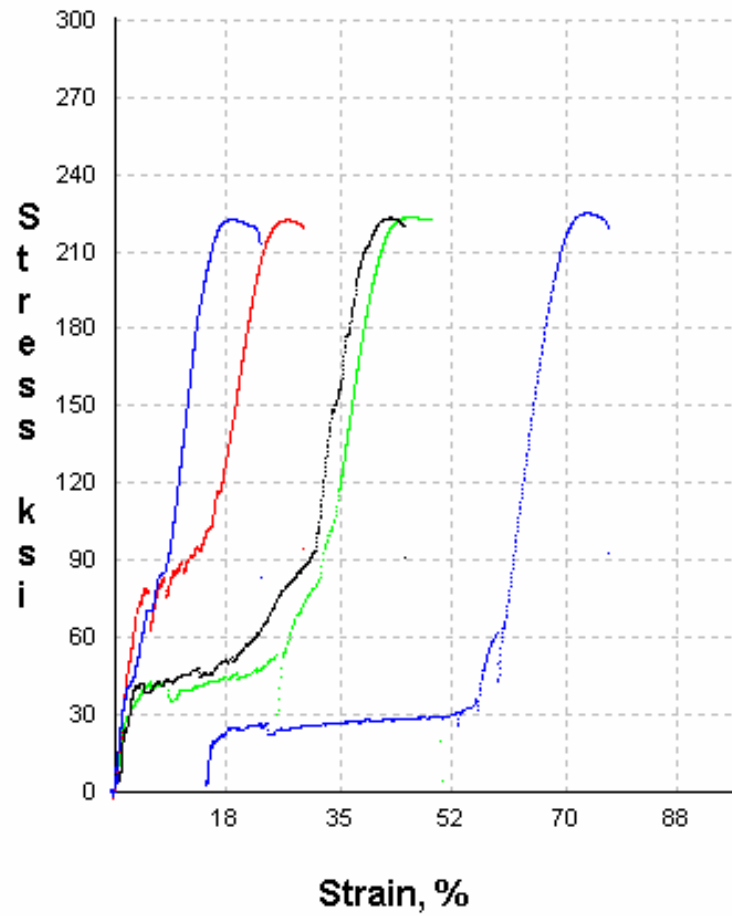
Figure 5.31 Stress-strain diagrams for .085 inch diameter nitinol specimens. From left to right at failure point: N-.085-W-1-120, N-.085-A-1-120, N-.085-A-2-120, N-.085-0-1-0, N-.085-0-2-0.

Table 5.22 Strengths of steel specimens

Specimen	Yield Strength (ksi)	Ultimate Strength (ksi)
S-F-0-1-0	55.7	69.3
S-F-0-2-0	55.6	69.2
S-F-A-1-120	55.1	69.1
S-F-A-2-120	54.1	69.2
S-F-W-1-120	53.7	69.1
S-W-0-1-0	62.7	74.3
S-W-0-2-0	58.5	72.5
S-W-A-1-120	59.4	73.0
S-W-A-2-120	60.4	72.4
S-W-W-1-120	60.1	72.9
S-5-0-1-0	58.9	80.1
S-5-0-2-0	57.5	80.4
S-5-A-1-120	58.3	80.7
S-5-A-2-120	58.9	79.9
S-5-W-1-120	59.1	80.0

It is apparent from the results that tension testing of the specimens after five days of exposure to a corrosive solution was not an effective method of measuring the detrimental effects of corrosion. The specimens were not corroded sufficiently to cause a large enough strength decrease to distinguish it from the common inconsistency in strength data for the uncorroded specimens. Tension testing did show that nitinol did not lose strength during the corrosion period, but since steel did not show an appreciable strength decrease either, a decisive difference between the two metals cannot be distinguished for the short corrosion times studied here.

Stress-strain diagrams for all steel specimens are given in Appendix C. The strain values were affected by the grips settling into the test frame, but the steel specimens did

not slip as much as the nitinol specimens did. Therefore, the general shape of the

diagrams is correct, and the strength values are accurate, even though the elastic modulus

and strain values are not those commonly measured for these grades of steel.

5.5 Mass Loss Testing Results

Mass measurements are listed in Table 5.23. The mass of the three nitinol

specimens showed no change after five days in the solutions. Though these results

cannot be used alone to prove nitinol's corrosion performance, they supplement all other

data that indicates that nitinol has excellent corrosion resistance compared to A992 and

A588 steel. Since no corrosion product was visible on the surface of the specimens, there

is no reason to believe that there was any mass gain to offset nickel mass loss. Instead, it

appears that the nickel mass loss was simply too low to change the mass of the specimen

by a measurable amount.

Table 5.23 Mass Results

Specimen	Starting Mass (g)	Ending Mass (g)
N-.085-A-1-120	7.066	7.066
N-.085-A-2-120	7.292	7.292
N-.085-W-1-120	6.972	6.972

CHAPTER 6 – CONCLUSIONS AND RECOMMENDATIONS

6.1 Conclusions

The testing procedures used for this research varied in effectiveness. AAS testing provided the most productive results whereas tension testing proved to show little effect from the five-day corrosion duration investigated herein. Visual evaluation, pH testing, and mass measurements helped reinforce findings from AAS testing. Based on the results of this research, it can be concluded that nitinol has far less potential for corrosion than does typical structural steel of grade A992, when exposed to marine and industrial environments. Furthermore, this research proves that nitinol resists corrosion better than grade A588 steel, which is designed to be a corrosion-resistant steel. Ultimately, based on the limited data collected for this project, it appears that nitinol can be deemed a safe material for structural engineering in terms of its corrosion resistance.

6.2 Recommendations for the Use of Nitinol

Since, in the preliminary testing reported here, nitinol appeared to resist corrosion better than steel, it is reasonable to project that nitinol can be used in the same environments as those in which steel is currently employed, without risk of corrosion problems. However, tension testing for this research inadvertently demonstrated nitinol's potential for brittle failure, presumably due to notch sensitivity. This phenomenon has been the topic of some research (Labossiere 2004), but is not always considered in research concerning nitinol devices. Therefore, it is recommended that nitinol devices,

such as those discussed in the literature review of this research, can be employed in any structure in which steel is exposed to the environment, provided that the designer understands nitinol's limitations with respect to notch sensitivity and takes necessary precautions to avoid its detrimental effects. Additionally, based on results of the preliminary data gathered in this study, it is suggested that nitinol is safe for more corrosive environments than those in which corrosion-resistant steel is normally used.

It seems reasonable to deduce that nitinol painted with a protective coating would withstand corrosion as well as steel painted with the same coating. However, it is recommended that this option be researched prior to implementation, in order to ensure that particular coatings are not harmful to nitinol. Alternatively, nitinol's superior performance demonstrated in this study provides reason to speculate that nitinol might resist corrosion well enough to perform favorably in its uncoated condition in many environments typical of civil structures. This option may be of interest for future research projects.

6.3 Recommendations for Future Testing

Aside from evaluating nitinol's corrosion performance, this research also exposed problems associated with corrosion testing and led to suggestions for future testing. The most obvious lesson learned from this research is that a five-day corrosion period is not long enough to cause significant degradation in mechanical properties of steel and nitinol, even with harsh solutions such as sulfuric acid. A more appropriate time period would be on the order of several weeks or even months in a highly corrosive solution. The five-day accelerated corrosion test was sufficient for pH and AAS testing, but longer corrosion periods should be used if comparison of mechanical properties is desired.

Tension testing also showed that nitinol can fail below its yield strength in a brittle manner. Since notch sensitivity was not the focus of this research, only anecdotal evidence can be offered to contribute to the investigation of this failure mode. However, based on the occurrence of brittle failure observed, it is recommended that nitinol's notch sensitivity be explored further.

AAS results indicated that nickel concentrations from the .25 inch nitinol specimens grew almost linearly, whereas nickel concentrations from other specimens reached a plateau. Nickel concentrations were still very low compared to iron concentrations from steel specimens, but the lack of a plateau gives reason to believe that the .25 inch specimens could corrode more than the other sizes. Since the .25 inch specimens were the only specimens to be hot rolled instead of cold drawn, the slight difference in corrosion resistance may be related to processing and surface finishing. Therefore, research concerning the effect of processing and surface finishing on corrosion resistance of nitinol is warranted.

As previously mentioned, nitinol's outstanding corrosion resistance demonstrated in this study provides reason to speculate that nitinol may be able to resist corrosion in many environments without a protective coating. It is recommended that research be performed which compares the corrosion resistance of uncoated nitinol and painted steel in highly corrosive environments over a long-term corrosion period. If nitinol resists corrosion similarly to painted steel, it could be used in any environment typical of civil structures without any undue risk of corrosion problems or maintenance requirements.

Since most structural applications of nitinol involve coupling it with steel, it is important that the corrosion resistance of the two metals be studied in combination.

When two dissimilar metals are in contact with each other, they can affect one another's corrosion resistance by allowing ions to flow from one metal to the other. This study showed that nitinol resists corrosion better than A992 and A588 steel when all are subjected singly to the same corrosive solutions, but did not address the affect that nitinol could have on steel if the two metals are coupled.

Aside from uniform corrosion, there are other durability issues associated with structural engineering materials, such as the effects of pitting, stress corrosion, crevice corrosion, and embrittlement. Additionally, the durability of structural engineering materials can be compromised by de-icing salts. In order to gain a complete understanding of the durability of nitinol, it is recommended that these issues be studied

REFERENCES

AISC (2001). <u>LRFD Manual of Steel Construction</u>, American Institute of Steel Construction.

Aizawa, S., T. Kakizawa and M. Higasino (1998). "Case studies of smart materials for civil structures." <u>Smart Materials and Structures</u>(5): 617-626.

ASTM (1972). Standard Practice for Laboratory Immersion Corrosion Testing of Metals (G 31 - 72, Reapproved 2004). <u>Annual Book of ASTM Standards</u>. West Conshohocken, PA, ASTM International. **03.02**.

ASTM (1976). Standard Practice for Conducting Atmospheric corrosion Tests on Metals (G 50 - 76, Reapproved 2003). <u>Annual Book of ASTM Standards</u>. West Conshohocken, PA, ASTM International. **03.02**.

ASTM (2004). Standard Test Methods for Tension Testing of Metallic Materials (E 8 – 04). <u>Annual Book of ASTM Standards</u>. West Conshohocken, PA, ASTM International. **03.01**.

Carroll, W. M. and M. J. Kelly (2003). "Corrosion behavior of nitinol wires in body fluid environments." <u>Journal of Biomedical Materials Research Part A</u> **67A**(4): 1123-1130.

Cattan, J. (1999). "Steel Industry Embraces A992." <u>Modern Steel Construction</u>. April, 1999.

Cross, W. B., A. H. Kariotis and F. J. Stimler (1969). Nitinol Characterization Study. Akron, OH, Langley Research Center.

DesRoches, R. and M. Delemont (2002). "Seismic retrofit of simply supported bridges using shape memory alloys." <u>Engineering Structures</u> **24**(3): 325-332.

DesRoches, R., J. McCormick and M. Delemont (2004). "Cyclic Properties of Superelastic Shape Memory Alloy Wires and Bars." <u>Journal of Structural Engineering</u> **130**(1): 38-46.

Diamant, R. M. E. (1970). <u>The Chemistry of Building Materials</u>. London, Business Books Limited.

Dolce, M., D. Cardone and R. Marnetto (2000). "Implementation and testing of passive control devices based on shape memory alloys." Earthquake Engineering and Structural Dynamics **29**: 945-968.

Dolce, M. and D. Cardone (2001). "Mechanical Behaviour of Shape Memory Alloys for Seismic Applications." International Journal of Mechanical Sciences **43**: 2631-2656.

Duerig, T. W., K. N. Melton, D. Stockel and C. M. Wayman(1990). Engineering Aspects of Shape Memory Alloys. London, Butterworth Heinemann Ltd.

Duerig, T., A. Pelton and D. Stockel (1999). "An overview of nitinol medical applications." Materials Science and Engineering A **273-275**: 149-160.

FHWA (1989). Uncoated Weathering Steel in Structures (T 5140.22). U.S. Department of Transportation, Federal Highway Administration.

Flinn, R. A. and P. K. Trojan (1981). Engineering Materials and Their Applications. Boston, Houghton Mifflin Company.

Ford, D. S. and S. R. White (1996). "Thermomechanical behavior of 55Ni45Ti nitinol." Acta Materialia **44**(6): 2295-2307.

Hibbeler, R. C. (2000). Mechanics of Materials. Upper Saddle River, NJ, Prentice Hall, Inc.

Jackson, C. M., H. J. Wagner and R. J. Wasilewski (1972). 55-Nitinol - The Alloy with a Memory: Its Physical Metallurgy, Properties, and Applications, Battelle Memorial Institute.

Johnson, A. D. (1988). "Shape memory metals." Potentials, IEEE **7**(3): 17-19.

Kauffman, G. B. and I. Mayo (1997). "The Story of Nitinol: The Serendipitous Discovery of the Memory Metal and Its Application." The Chemical Educator **2**(2).

Knofel, D (1978). Corrosion of Building Materials. New York, NY, Van Nostrand Reinhold Company.

Kulisic, I., G. L. Gray and S. E. Mohney (1998). Shape memory alloy coil-shaped clamp for enhanced normal force in electrical connectors. Electrical Contacts, 1998., Proceedings of the Forty-fourth IEEE Holm Conference on.

Labossiere, P., K. Perry (2004). "The Effects of Notches and Grain Size on Transformations in Nitinol." Echobio. May 11, 2006. <http://www2.echobio.com:8008/echobio/gallery.html>

Leygraf, C., T. Graedel (2000). Atmospheric Corrosion. New York, NY, John Wiley & Sons, Inc.

Li, H., M. Liu and J. Ou (2004). "Vibration Mitigation of a Stay Cable with One Shape Memory Alloy Damper." Structural Control and Health Monitoring **11**: 21-36.

Liu, Y., Z. Xie and J. Van Humbeeck (1999). "Cyclic deformation of NiTi shape memory alloys." Materials Science and Engineering A **273-275**: 673-678.

Kross, Brian (2006). Jefferson Lab. January 18, 2006. Thomas Jefferson National Accelerator Facility. <http://education.jlab.org/qa/meltingpoint_01.html>.

McCormac, J. C. and J. James K. Nelson (2003). Structural Steel Design: LRFD Method. Upper Saddle River, NJ, Pearson Education, Inc.

McCuen, R. and P. Albrecht (2005). "Effect of Alloy Composition on Atmospheric Corrosion of Weathering Steel." Journal of Materials in Civil Engineering **17**(2): 117-125.

Morgan, N. B. (2004). "Medical shape memory alloy applications--the market and its products." Materials Science and Engineering A **378**(1-2): 16-23.

Rondelli, G. (1996). "Corrosion resistance tests on NiTi shape memory alloy." Biomaterials **17**(20): 2003-2008.

Schuerch, H. U. (1968). Certain Physical Properties and Applications of Nitinol. Santa Barbara, CA, Astro Research Corporation.

Schweitzer, P. A. (1997). Environmental Degradation of Engineering Materials. Handbook of Materials Selection for Engineering Applications. G. T. Murray. San Luis Obispo, CA, Marcel Dekker, Inc.

Schweitzer, P. A. (1999). Atmospheric Degradation and Corrosion Control. New York, NY, Marcel Dekker, Inc.

Shabalovskaya, S., G. Rondelli, J. Anderegg, B. Simpson and S. Budko (2003). "Effect of chemical etching and aging in boiling water on the corrosion resistance of nitinol wires with black oxide resulting from manufacturing process." Journal of Biomedical Materials Research Part B: Applied Biomaterials **66B**(1): 331-340.

Special Metals (2006). Shape Memory Alloy Division. January 27, 2006. <http://www.shape-memory-alloys.com/data_nitinol.htm>.

Tamai, H. and Y. Kitagawa (2002). "Pseudoelastic behavior of shape memory alloy wire and its application to seismic resistance member for building." <u>Computational Materials Science</u> **25**(1-2): 218-227.

Tedesco, J. W., W. G. McDougal and C. A. Ross (1999). <u>Structural Dynamics Theory and Applications</u>. Menlo Park, CA, Addison Wesley Longman, Inc.

Thomson, P., G. J. Balas and P. H. Leo (1995). "The use of shape memory alloys for passive structural damping." <u>Smart Materials and Structures</u>(1): 36-41.

Van Humbeeck, J. (2001). "Shape memory alloys: A material and a technology." <u>Advanced Engineering Materials</u> **3**(11): 837-850.

Wranglen, G. (1985). <u>An Introduction to Corrosion and Protection of Metals</u>. New York, NY, Chapman and Hall.

APPENDICES

Appendix A

Nitinol Test Certificates

SPECIAL METALS

CERTIFICATE OF TEST

NEW HARTFORD, NY 13413-9576
PHONE: (315) 798-2029
FAX: (315) 798-6860

```
                              CERTIFICATION DATE   :  09/22/05

AUBURN UNIVERSITY             CUSTOMER ORDER NUMBER   :  2-12894
ATTN: DAVID McCARTY           SMC ORDER NUMBER        :  AUB-21023
238 HABERT ENGINEERING CENTER ALLOY                   :  NITINOL
CIVIL ENGINEERING             SIZE                    :  0.500" DIAM.
AUBURN UNIVERSITY, AL 36849   HEAT NUMBER             :  C7-8337
                              WEIGHT/LENGTH:      :96 INCHES/8 BARS
```

CERTIFICATION:

UDIMET® NITINOL BAR. 12.7MM (0.50") DIA. X 304MM (12") LONG, AS COLD DRAWN, 30% COLD WORK.

A_S (FULLY ANNEALED) = -25/-13 DEG. C

CHEMICAL ANALYSES:

Element	Wt %
Nickel	55.94
Titanium	Balance
Oxygen	0.05 Maximum
Carbon	0.05 Maximum
Ag, Al, As, Ba, Be, Bi, Ca, Cd,	<0.01
Co, Cr, Cu, Hf, Hg, Mg, Mo,	<0.01
Na, Nb, P, Pb, S, Sb, Se,	<0.01
SI, Sn, Ta, V, W, Zn, Zr	<0.01
Fe	<0.05
B	<0.001

THIS IS TO CERTIFY THAT THE ABOVE VALUES ARE TRUE AND ACCURATE
TO THE BEST OF MY KNOWLEDGE AND BELIEF.

_9, 22, 05_

SUBHASH C. GUPTA
AUTHORIZED SIGNATURE   DATE

PAGE 1 OF 1 - END OF CERTIFICATE

118

SPECIAL METALS

CERTIFICATE OF TEST

NEW HARTFORD, NY 13413-9576
PHONE: (315) 798-2029
FAX: (315) 798-6860

	CERTIFICATION DATE	: 07/22/05
AUBURN UNIVERSITY	CUSTOMER ORDER NUMBER	: P503400
ATTN: DAVIE McCARTY	SMC ORDER NUMBER	: AUB-20584
238 HABERT	ALLOY	: NITINOL
CIVIL ENGINEERING	SIZE	: 0.250" DIAM.
AUBURN UNIVERSITY, AL 36849	HEAT NUMBER	: C5-9198-5
	WEIGHT/LENGTH:	: SAMPLE

CERTIFICATION:

UDIMET® NITINOL BAR. 6.35MM (0.250") DIA. HOT ROLLED, HOT ROLLED OXIDE SURFACE.

A_s (FULLY ANNEALED) = -26 DEG. C

CHEMICAL ANALYSES:

Element	Wt %
Nickel	56.04
Titanium	Balance
Oxygen	0.05 Maximum
Carbon	0.05 Maximum
Ag, Al, As, Ba, Be, Bi, Ca, Cd,	<0.01
Co, Cr, Cu, Hf, Hg, Mg, Mo,	<0.01
Na, Nb, P, Pb, S, Sb, Se,	<0.01
SI, Sn, Ta, V, W, Zn, Zr	<0.01
Fe	<0.05
B	<0.001

THIS IS TO CERTIFY THAT THE ABOVE VALUES ARE TRUE AND ACCURATE
TO THE BEST OF MY KNOWLEDGE AND BELIEF.

SUBHASH C. GUPTA
AUTHORIZED SIGNATURE

7/22/05
DATE

PAGE 1 OF 1 - END OF CERTIFICATE

119

CERTIFICATE OF TEST

NEW HARTFORD, NY 13413-9576
PHONE: (315) 798-2029
FAX: (315) 798-6860

CERTIFICATION DATE	:	07/22/05

AUBURN UNIVERSITY
ATTN: DAVIE McCARTY
238 HABERT
CIVIL ENGINEERING
AUBURN UNIVERSITY, AL 36849

CUSTOMER ORDER NUMBER	:	P503400
SMC ORDER NUMBER	:	AUB-20584
ALLOY	:	NITINOL
SIZE	:	0.085"DIAM.
HEAT NUMBER	:	C7-8352-6
WEIGHT/LENGTH:	:	SAMPLE

CERTIFICATION:
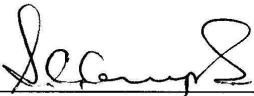
UDIMET® NITINOL REDRAW WIRE, 2.16MM (0.085") DIA., AS COLD DRAWN, 30% COLD WORK, OXIDE FREE SURFACE.

A_s (FULLY ANNEALED) = -30/-22 DEG. C

CHEMICAL ANALYSES:

Element	Wt %
Nickel	55.93
Titanium	Balance
Oxygen	0.05 Maximum
Carbon	0.05 Maximum
Ag, Al, As, Ba, Be, Bi, Ca, Cd,	<0.01
Co, Cr, Cu, Hf, Hg, Mg, Mo,	<0.01
Na, Nb, P, Pb, S, Sb, Se,	<0.01
SI, Sn, Ta, V, W, Zn, Zr	<0.01
Fe	<0.05
B	<0.001

THIS IS TO CERTIFY THAT THE ABOVE VALUES ARE TRUE AND ACCURATE
TO THE BEST OF MY KNOWLEDGE AND BELIEF.

(signature)   7, 22, 05

SUBHASH C. GUPTA
AUTHORIZED SIGNATURE   DATE

PAGE 1 OF 1 - END OF CERTIFICATE

120

Appendix B

AAS Testing Printouts

Analyst	DAVID	
Date Started	11:24 AM 4/18/06	
Worksheet	S-F-A-1	
Comment		
Methods	Fe	

Method: Fe (Flame)

Sample ID	Conc mg/L	%Prec	Mean Abs	Replicates		
CAL ZERO	0.000	0.0	-0.0003	-0.0003	4/18/06	:30:02 AM
STANDARD 1	2.000	0.7	0.2048	0.2048	4/18/06	:30:20 AM
STANDARD 2	4.000	0.8	0.3347	0.3347	4/18/06	:30:40 AM
STANDARD 3	6.000	1.0	0.4483	0.4483	4/18/06	:31:00 AM

New Rational - Cal. Set 1
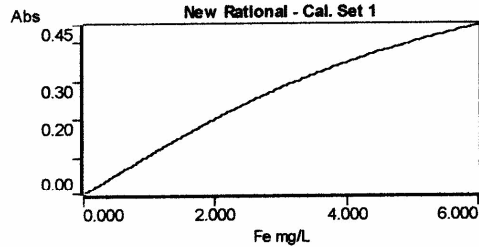
Curve Fit	= New Rational	
Characteristic Conc	= 0.043 mg/L	
r	= 0.9999	
Calculated Conc	= -0.003 2.067 3.801	
Residuals	= 0.003 -0.067 0.199	

Sample ID	Conc mg/L	%Prec	Mean Abs	Replicates		
S-F-A-1-0	0.013	15.7	0.0013	0.0013	4/18/06	:31:32 AM
S-F-A-1-5	0.603	0.9	0.0625	0.0625	4/18/06	:31:52 AM
S-F-A-1-8	5.151	0.4	0.4071	0.4071	4/18/06	:32:12 AM
S-F-A-1-24	5.674	0.4	0.4299	0.4299	4/18/06	:32:32 AM
S-F-A-1-48	4.682	0.3	0.3843	0.3843	4/18/06	:32:50 AM
W0545: Sample result OVER the calibration range						
S-F-A-1-72	OVER	0.2	0.5600	0.5600	4/18/06	:33:08 AM
S-F-A-1-96	4.695	0.3	0.3850	0.3850	4/18/06	:33:26 AM
S-F-A-1-120	4.629	0.4	0.3816	0.3816	4/18/06	:33:42 AM
S-F-A-1-120P	0.356	0.9	0.0369	0.0369	4/18/06	:34:02 AM
4 PPM STANDARD	3.626	1.0	0.3236	0.3236	4/18/06	:34:24 AM

Analyst	DAVID					
Date Started	1:46 PM 4/18/06					
Worksheet	S-F-A-1-72					
Comment						
Methods	Fe					

Method: Fe (Flame)

Sample ID	Conc mg/L	%Prec	Mean Abs	Replicates		
CAL ZERO	0.000	0.0	-0.0012	-0.0012	4/18/06	1:48:44 PM
STANDARD 1	2.000	0.7	0.2106	0.2106	4/18/06	1:49:02 PM
STANDARD 2	4.000	1.0	0.3115	0.3115	4/18/06	1:49:22 PM
STANDARD 3	6.000	0.9	0.4401	0.4401	4/18/06	1:49:48 PM

New Rational - Cal. Set 1
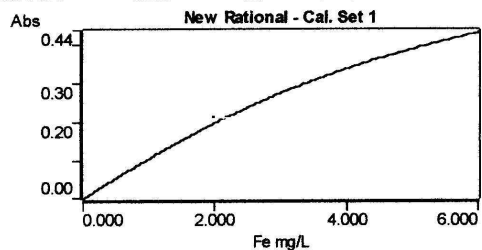
Curve Fit	= New Rational	
Characteristic Conc	= 0.041 mg/L	
r	= 0.9996	
Calculated Conc	= -0.011 2.165 3.558	
Residuals	= 0.011 -0.165 0.442	

S-F-A-1-72	2.133	0.7	0.2080	0.2080	4/18/06	1:50:08 PM

122

Analyst	DAVID	
Date Started	11:46 AM 4/18/06	
Worksheet	S-F-A-2	
Comment		
Methods	Fe	

Method: Fe (Flame)

Sample ID	Conc mg/L	%Prec	Mean Abs	Replicates		
CAL ZERO	0.000	0.0	-0.0007	-0.0007	4/18/06	:52:34 AM
STANDARD 1	2.000	0.9	0.2115	0.2115	4/18/06	:52:52 AM
STANDARD 2	4.000	1.0	0.3374	0.3374	4/18/06	:53:12 AM
STANDARD 3	6.000	1.0	0.4582	0.4582	4/18/06	:53:30 AM

New Rational - Cal. Set 1
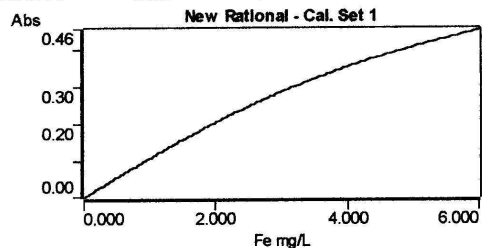
Curve Fit	=	New Rational
Characteristic Conc	=	0.041 mg/L
r	=	0.9999
Calculated Conc	=	-0.006 2.090 3.741
Residuals	=	0.006 -0.090 0.259

Sample ID	Conc mg/L	%Prec	Mean Abs	Replicates		
S-F-A-2-0	-0.017	0.0	-0.0018	-0.0018	4/18/06	:54:02 AM
S-F-A-2-5	0.364	1.0	0.0389	0.0389	4/18/06	:54:24 AM
S-F-A-2-8	1.818	0.7	0.1867	0.1867	4/18/06	:54:44 AM
S-F-A-2-24	2.693	0.3	0.2624	0.2624	4/18/06	:55:00 AM
S-F-A-2-48	2.197	0.5	0.2209	0.2209	4/18/06	:55:18 AM
S-F-A-2-72	2.017	0.6	0.2050	0.2050	4/18/06	:55:36 AM
S-F-A-2-96	1.759	0.7	0.1812	0.1812	4/18/06	:55:52 AM
S-F-A-2-120	1.542	0.7	0.1604	0.1604	4/18/06	:56:08 AM
S-F-A-2-120P	3.822	0.6	0.3425	0.3425	4/18/06	:56:24 AM
4 PPM STANDARD	3.306	0.9	0.3083	0.3083	4/18/06	:56:46 AM

Analyst	DAVID
Date Started	12:08 PM 4/18/06
Worksheet	S-W-A-1
Comment	
Methods	Fe

Method: Fe (Flame)

Sample ID	Conc mg/L	%Prec	Mean Abs	Replicates		
CAL ZERO	0.000	0.0	-0.0001	-0.0001	4/18/06	2:13:50 PM
STANDARD 1	2.000	0.7	0.2041	0.2041	4/18/06	2:14:08 PM
STANDARD 2	4.000	1.0	0.3309	0.3309	4/18/06	2:14:30 PM
STANDARD 3	6.000	0.9	0.4422	0.4422	4/18/06	2:14:48 PM

New Rational - Cal. Set 1
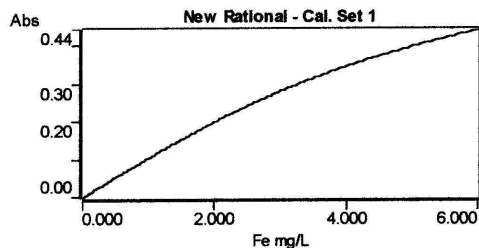
Curve Fit	= New Rational
Characteristic Conc	= 0.043 mg/L
r	= 0.9999
Calculated Conc	= -0.001 2.070 3.791
Residuals	= 0.001 -0.070 0.209

Sample ID	Conc mg/L	%Prec	Mean Abs	Replicates		
S-W-A-1-0	-0.026	0.0	-0.0026	-0.0026	4/18/06	2:15:20 PM
S-W-A-1-5	0.514	1.0	0.0532	0.0532	4/18/06	2:15:38 PM
S-W-A-1-8	2.514	0.7	0.2413	0.2413	4/18/06	2:15:58 PM
S-W-A-1-24	2.586	0.5	0.2470	0.2470	4/18/06	2:16:16 PM
S-W-A-1-48	2.550	0.5	0.2442	0.2442	4/18/06	2:16:34 PM
S-W-A-1-72	2.844	0.5	0.2668	0.2668	4/18/06	2:16:52 PM
S-W-A-1-96	3.374	0.4	0.3044	0.3044	4/18/06	2:17:10 PM
S-W-A-1-120	2.492	0.6	0.2395	0.2395	4/18/06	2:17:30 PM
S-W-A-1-120P	0.410	1.0	0.0423	0.0423	4/18/06	2:17:50 PM
4 PPM STANDARD	3.469	1.0	0.3106	0.3106	4/18/06	2:18:14 PM

124

Analyst	DAVID
Date Started	12:30 PM 4/18/06
Worksheet	S-W-A-2
Comment	
Methods	Fe

Method: Fe (Flame)

Sample ID	Conc mg/L	%Prec	Mean Abs	Replicates		
CAL ZERO	0.000	50.8	0.0003	0.0003	4/18/06	2:35:12 PM
STANDARD 1	2.000	0.7	0.2094	0.2094	4/18/06	2:35:32 PM
STANDARD 2	4.000	1.0	0.3293	0.3293	4/18/06	2:35:52 PM
STANDARD 3	6.000	1.0	0.4438	0.4438	4/18/06	2:36:12 PM

New Rational - Cal. Set 1
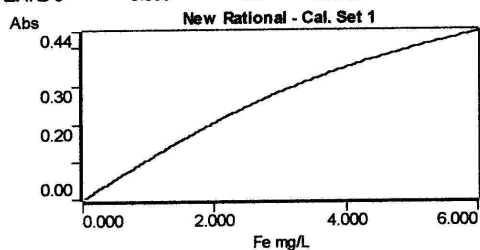
Curve Fit	= New Rational
Characteristic Conc	= 0.042 mg/L
r	= 0.9998
Calculated Conc	= 0.003 2.094 3.724
Residuals	= -0.003 -0.094 0.276

Sample ID	Conc mg/L	%Prec	Mean Abs	Replicates		
S-W-A-2-0	0.002	29.6	0.0002	0.0002	4/18/06	2:36:40 PM
S-W-A-2-5	0.377	1.0	0.0399	0.0399	4/18/06	2:37:00 PM
S-W-A-2-8	1.751	0.6	0.1786	0.1786	4/18/06	2:37:16 PM
S-W-A-2-24	2.624	0.4	0.2532	0.2532	4/18/06	2:37:34 PM
S-W-A-2-48	2.319	0.5	0.2286	0.2286	4/18/06	2:37:52 PM
S-W-A-2-72	2.121	0.6	0.2117	0.2117	4/18/06	2:38:10 PM
S-W-A-2-96	1.845	0.7	0.1872	0.1872	4/18/06	2:38:28 PM
S-W-A-2-120	1.635	0.7	0.1678	0.1678	4/18/06	2:38:46 PM
S-W-A-2-120P	1.889	0.7	0.1912	0.1912	4/18/06	2:39:02 PM
4 PPM STANDARD	3.427	1.0	0.3106	0.3106	4/18/06	2:39:26 PM

Analyst	DAVID
Date Started	12:49 PM 4/18/06
Worksheet	S-5-A-1
Comment	
Methods	Fe

Method: Fe (Flame)

Sample ID	Conc mg/L	%Prec	Mean Abs	Replicates		
CAL ZERO	0.000	0.0	-0.0005	-0.0005	4/18/06	2:52:56 PM
STANDARD 1	2.000	0.5	0.2027	0.2027	4/18/06	2:53:16 PM
STANDARD 2	4.000	1.0	0.3241	0.3241	4/18/06	2:53:38 PM
STANDARD 3	6.000	1.0	0.4329	0.4329	4/18/06	2:54:00 PM

New Rational - Cal. Set 1
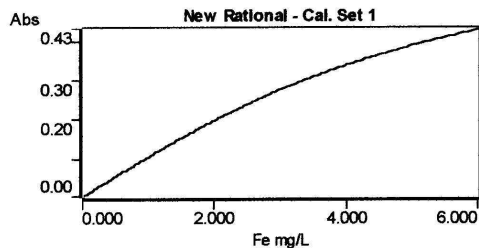
Curve Fit	= New Rational
Characteristic Conc	= 0.043 mg/L
r	= 0.9999
Calculated Conc	= -0.005 2.078 3.766
Residuals	= 0.005 -0.078 0.234

Sample ID	Conc mg/L	%Prec	Mean Abs	Replicates		
S-5-A-1-0	-0.010	0.0	-0.0010	-0.0010	4/18/06	2:54:30 PM
S-5-A-1-5	0.327	1.0	0.0336	0.0336	4/18/06	2:54:50 PM
S-5-A-1-8	1.740	0.5	0.1729	0.1729	4/18/06	2:55:06 PM
S-5-A-1-24	2.246	0.4	0.2168	0.2168	4/18/06	2:55:22 PM
S-5-A-1-48	2.789	0.4	0.2594	0.2594	4/18/06	2:55:40 PM
S-5-A-1-72	3.059	0.6	0.2787	0.2787	4/18/06	2:55:56 PM
S-5-A-1-96	3.023	0.5	0.2762	0.2762	4/18/06	2:56:14 PM
S-5-A-1-120	2.247	0.4	0.2170	0.2170	4/18/06	2:56:30 PM
S-5-A-1-120P	0.159	1.0	0.0163	0.0163	4/18/06	2:56:56 PM
4 PPM STANDARD	3.474	0.8	0.3062	0.3062	4/18/06	2:57:14 PM

126

Analyst	DAVID
Date Started	1:10 PM 4/18/06
Worksheet	S-5-A-2
Comment	
Methods	Fe

Method: Fe (Flame)

Sample ID	Conc mg/L	%Prec	Mean Abs	Replicates		
CAL ZERO	0.000	80.5	0.0002	0.0002	4/18/06	1:14:30 PM
STANDARD 1	2.000	0.8	0.2122	0.2122	4/18/06	1:14:52 PM
STANDARD 2	4.000	0.9	0.3188	0.3188	4/18/06	1:15:12 PM
STANDARD 3	6.000	1.0	0.4328	0.4328	4/18/06	1:15:32 PM

New Rational - Cal. Set 1
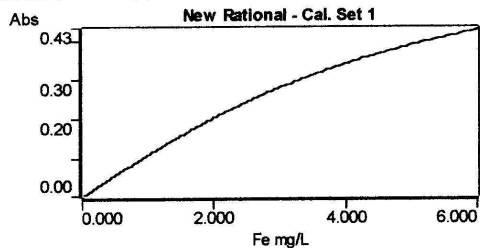
Curve Fit	= New Rational
Characteristic Conc	= 0.041 mg/L
r	= 0.9997
Calculated Conc	= 0.002 2.128 3.627
Residuals	= -0.002 -0.128 0.373

Sample ID	Conc mg/L	%Prec	Mean Abs	Replicates		
S-5-A-2-0	-0.005	0.0	-0.0005	-0.0005	4/18/06	1:16:04 PM
S-5-A-2-5	0.600	0.9	0.0643	0.0643	4/18/06	1:16:22 PM
S-5-A-2-8	3.629	0.3	0.3189	0.3189	4/18/06	1:16:40 PM
S-5-A-2-24	4.044	0.4	0.3421	0.3421	4/18/06	1:16:58 PM
S-5-A-2-48	4.616	0.4	0.3703	0.3703	4/18/06	1:17:16 PM
S-5-A-2-72	3.622	0.5	0.3185	0.3185	4/18/06	1:17:34 PM
S-5-A-2-96	3.223	0.5	0.2938	0.2938	4/18/06	1:17:50 PM
S-5-A-2-120	2.830	0.6	0.2670	0.2670	4/18/06	1:18:06 PM
S-5-A-2-120P	0.693	1.0	0.0741	0.0741	4/18/06	1:18:24 PM
4 PPM STANDARD	3.368	1.0	0.3031	0.3031	4/18/06	1:18:44 PM

127

Analyst	DAVID
Date Started	1:52 PM 4/18/06
Worksheet	S-F-W-1
Comment	
Methods	Fe

Method: Fe (Flame)

Sample ID	Conc mg/L	%Prec	Mean Abs	Replicates		
CAL ZERO	0.000	0.0	-0.0001	-0.0001	4/18/06	1:58:02 PM
STANDARD 1	2.000	0.5	0.1799	0.1799	4/18/06	1:58:18 PM
STANDARD 2	4.000	0.3	0.3410	0.3410	4/18/06	1:58:34 PM
STANDARD 3	6.000	0.4	0.4705	0.4705	4/18/06	1:58:50 PM

New Rational - Cal. Set 1
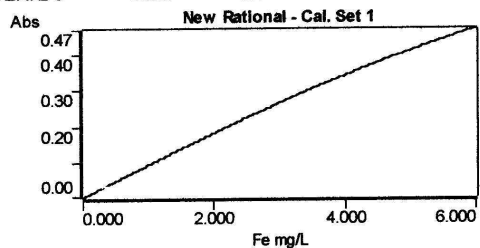
Curve Fit	= New Rational	
Characteristic Conc	= 0.049 mg/L	
r	= 1.0000	
Calculated Conc	= -0.002 2.001 3.999	
Residuals	= 0.002 -0.001 0.001	

Sample ID	Conc mg/L	%Prec	Mean Abs	Replicates		
S-F-W-1-0	0.315	1.0	0.0285	0.0285	4/18/06	1:59:18 PM
S-F-W-1-5	0.566	1.0	0.0512	0.0512	4/18/06	1:59:38 PM
W0545: Sample result OVER the calibration range						
S-F-W-1-8	OVER	0.4	0.4957	0.4957	4/18/06	1:59:54 PM
S-F-W-1-24	3.695	0.5	0.3185	0.3185	4/18/06	2:00:14 PM
S-F-W-1-48	1.374	0.5	0.1243	0.1243	4/18/06	2:00:32 PM
S-F-W-1-72	1.517	0.5	0.1371	0.1371	4/18/06	2:00:48 PM
S-F-W-1-96	1.314	0.7	0.1190	0.1190	4/18/06	2:01:04 PM
S-F-W-1-120	0.948	0.7	0.0859	0.0859	4/18/06	2:01:20 PM
S-F-W-1-120P	3.556	0.5	0.3079	0.3079	4/18/06	2:01:36 PM
4 PPM STANDARD	4.010	0.4	0.3419	0.3419	4/18/06	2:01:54 PM

Analyst	DAVID
Date Started	2:04 PM 4/18/06
Worksheet	S-F-W-1-8
Comment	
Methods	Fe

Method: Fe (Flame)

Sample ID	Conc mg/L	%Prec	Mean Abs	Replicates		
CAL ZERO	0.000	59.1	0.0003	0.0003	4/18/06	2:07:52 PM
STANDARD 1	2.000	0.7	0.1754	0.1754	4/18/06	2:08:06 PM
STANDARD 2	4.000	0.4	0.3394	0.3394	4/18/06	2:08:24 PM
STANDARD 3	6.000	0.3	0.4646	0.4646	4/18/06	2:08:40 PM

New Rational - Cal. Set 1
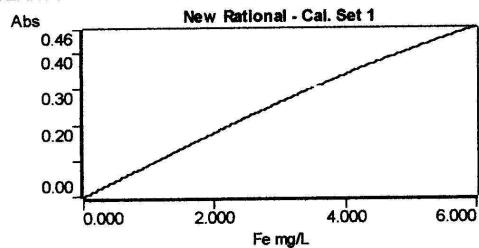
Curve Fit	= New Rational
Characteristic Conc	= 0.050 mg/L
r	= 1.0000
Calculated Conc	= 0.003 1.986 4.035 5.977
Residuals	= -0.003 0.014 -0.035 0.023

S-F-W-1-8	3.528	0.4	0.3016	0.3016	4/18/06	2:09:00 PM
4 PPM STANDARD	3.979	0.4	0.3354	0.3354	4/18/06	2:09:18 PM

Analyst	DAVID
Date Started	9:54 AM 4/18/06
Worksheet	IRON
Comment	
Methods	Fe

Method: Fe (Flame)

Sample ID	Conc mg/L	%Prec	Mean Abs	Replicates		
CAL ZERO	0.000	0.0	-0.0005	-0.0005	4/18/06	1:04:40 AM
STANDARD 1	2.000	0.5	0.1720	0.1720	4/18/06	1:04:58 AM
STANDARD 2	4.000	0.4	0.3320	0.3320	4/18/06	1:05:18 AM
STANDARD 3	6.000	0.2	0.4483	0.4483	4/18/06	1:05:38 AM

New Rational - Cal. Set 1
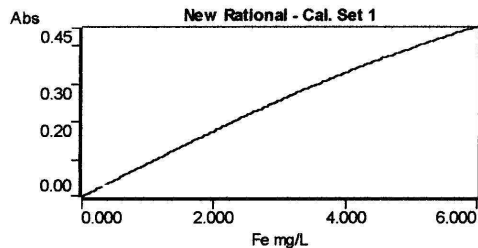
Curve Fit	= New Rational
Characteristic Conc	= 0.051 mg/L
r	= 1.0000
Calculated Conc	= -0.006 1.982 4.047 5.967
Residuals	= 0.006 0.018 -0.047 0.033

Sample ID	Conc mg/L	%Prec	Mean Abs	Replicates		
S-W-W-1-0	0.331	1.0	0.0286	0.0286	4/18/06	1:06:04 AM
S-W-W-1-5	0.630	1.0	0.0547	0.0547	4/18/06	1:06:22 AM
S-W-W-1-8	5.160	0.5	0.4032	0.4032	4/18/06	1:06:46 AM
S-W-W-1-24	4.204	0.5	0.3427	0.3427	4/18/06	1:07:04 AM
S-W-W-1-48	3.275	0.3	0.2761	0.2761	4/18/06	1:07:24 AM
S-W-W-1-72	2.493	0.5	0.2146	0.2146	4/18/06	1:07:40 AM
S-W-W-1-96	2.033	0.8	0.1763	0.1763	4/18/06	1:07:58 AM
S-W-W-1-120	5.282	0.5	0.4104	0.4104	4/18/06	1:08:16 AM
S-W-W-1-120P	3.158	0.4	0.2672	0.2672	4/18/06	1:08:32 AM
4 PPM SOLUTION	3.982	0.3	0.3275	0.3275	4/18/06	1:08:56 AM

Analyst	David
Date Started	9:32 AM 4/18/06
Worksheet	Fe
Comment	
Methods	Fe

Method: Fe (Flame)

3

Sample ID	Conc mg/L	%Prec	Mean Abs	Replicates		
CAL ZERO	0.000	16.9	0.0008	0.0008	4/18/06	1:47:32 AM
STANDARD 1	2.000	0.3	0.1667	0.1667	4/18/06	1:47:56 AM
STANDARD 2	4.000	0.4	0.3181	0.3181	4/18/06	1:48:12 AM
STANDARD 3	6.000	0.4	0.4452	0.4452	4/18/06	1:48:30 AM

Abs — New Rational - Cal. Set 1
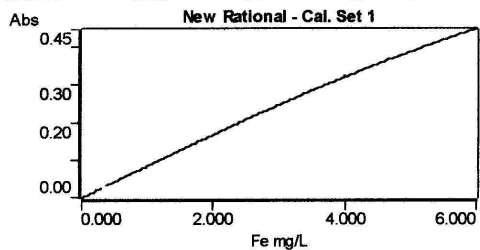
Curve Fit	= New Rational
Characteristic Conc	= 0.053 mg/L
r	= 1.0000
Calculated Conc	= 0.009 2.003 3.993
Residuals	= -0.009 -0.003 0.007

Sample ID	Conc mg/L	%Prec	Mean Abs	Replicates		
S-5-W-1-0	0.334	1.0	0.0279	0.0279	4/18/06	1:48:52 AM
S-5-W-1-5	0.470	1.0	0.0393	0.0393	4/18/06	1:49:16 AM
S-5-W-1-8	5.465	0.3	0.4138	0.4138	4/18/06	1:49:38 AM
S-5-W-1-24	4.413	0.4	0.3469	0.3469	4/18/06	1:49:56 AM
S-5-W-1-48	5.957	0.3	0.4426	0.4426	4/18/06	1:50:14 AM
S-5-W-1-72	2.846	0.5	0.2335	0.2335	4/18/06	1:50:34 AM
S-5-W-1-96	1.654	0.7	0.1381	0.1381	4/18/06	1:50:50 AM
S-5-W-1-120	3.560	0.4	0.2871	0.2871	4/18/06	1:51:20 AM
S-5-W-1-120P	4.359	0.5	0.3432	0.3432	4/18/06	1:51:38 AM
4PPM STANDARD	4.017	0.3	0.3197	0.3197	4/18/06	1:52:00 AM

Analyst	DAVID
Date Started	9:32 AM 4/26/06
Worksheet	N-.5-A-1
Comment	
Methods	Ni

Method: Ni (Flame)

Sample ID	Conc mg/L	%Prec	Mean Abs	Replicates		
CAL ZERO	0.000	11.4	0.0018	0.0018	4/26/06	1:37:34 AM
STANDARD 1	2.000	1.0	0.1654	0.1654	4/26/06	1:37:52 AM
STANDARD 2	4.000	1.0	0.2677	0.2677	4/26/06	1:38:12 AM
STANDARD 3	6.000	0.7	0.3405	0.3405	4/26/06	1:38:28 AM

Abs   New Rational - Cal. Set 1
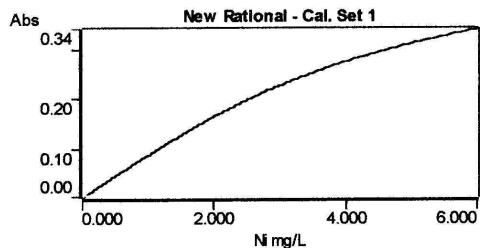
Curve Fit	= New Rational
Characteristic Conc	= 0.053 mg/L
r	= 1.0000
Calculated Conc	= 0.022 2.038 3.867
Residuals	= -0.022 -0.038 0.133

Sample ID	Conc mg/L	%Prec	Mean Abs	Replicates		
N-.5-A-1-0	0.022	6.3	0.0018	0.0018	4/26/06	1:38:54 AM
N-.5-A-1-5	0.004	11.2	0.0003	0.0003	4/26/06	1:39:20 AM
N-.5-A-1-8	0.635	1.0	0.0538	0.0538	4/26/06	1:39:36 AM
N-.5-A-1-24	0.908	1.0	0.0770	0.0770	4/26/06	1:40:00 AM
N-.5-A-1-48	0.966	0.9	0.0819	0.0819	4/26/06	1:40:20 AM
N-.5-A-1-72	0.962	1.0	0.0816	0.0816	4/26/06	1:40:36 AM
N-.5-A-1-96	1.007	0.8	0.0854	0.0854	4/26/06	1:40:52 AM
N-.5-A-1-120	0.937	0.7	0.0794	0.0794	4/26/06	1:41:08 AM
N-.5-A-1-120P	0.935	0.9	0.0792	0.0792	4/26/06	1:41:26 AM
4 PPM STANDARD	3.756	1.0	0.2628	0.2628	4/26/06	1:41:46 AM

Analyst	DAVID
Date Started	12:01 PM 4/26/06
Worksheet	N-.5-A-2
Comment	
Methods	Ni

Method: Ni (Flame)

Sample ID	Conc mg/L	%Prec	Mean Abs	Replicates		
CAL ZERO	0.000	48.7	0.0006	0.0006	4/26/06	2:07:58 PM
STANDARD 1	2.000	1.0	0.1637	0.1637	4/26/06	2:08:14 PM
STANDARD 2	4.000	0.9	0.2743	0.2743	4/26/06	2:08:32 PM
STANDARD 3	6.000	0.9	0.3555	0.3555	4/26/06	2:08:52 PM

Abs   New Rational - Cal. Set 1
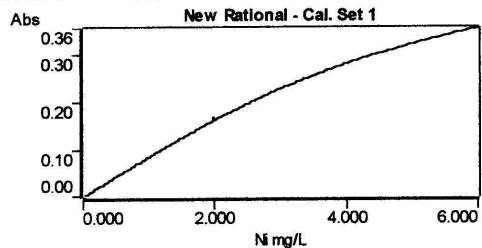
Curve Fit	= New Rational
Characteristic Conc	= 0.053 mg/L
r	= 1.0000
Calculated Conc	= 0.007 2.033 3.894
Residuals	= -0.007 -0.033 0.106

Sample ID	Conc mg/L	%Prec	Mean Abs	Replicates		
N-.5-A-2-0	-0.012	0.0	-0.0010	-0.0010	4/26/06	2:09:16 PM
N-.5-A-2-5	-0.013	0.0	-0.0011	-0.0011	4/26/06	2:09:42 PM
N-.5-A-2-8	0.285	1.0	0.0236	0.0236	4/26/06	2:10:06 PM
N-.5-A-2-24	0.454	1.0	0.0378	0.0378	4/26/06	2:10:24 PM
N-.5-A-2-48	0.547	1.0	0.0456	0.0456	4/26/06	2:10:42 PM
N-.5-A-2-72	0.547	1.0	0.0456	0.0456	4/26/06	2:10:58 PM
N-.5-A-2-96	0.567	1.0	0.0473	0.0473	4/26/06	2:11:18 PM
N-.5-A-2-120	0.594	1.0	0.0495	0.0495	4/26/06	2:11:34 PM
N-.5-A-2-120P	0.523	1.0	0.0435	0.0435	4/26/06	2:11:50 PM
4 PPM STANDARD	3.931	1.0	0.2761	0.2761	4/26/06	2:12:08 PM

133

Analyst	DAVID
Date Started	12:13 PM 4/26/06
Worksheet	N-.25-A-1
Comment	
Methods	Ni

Method: Ni (Flame)

Sample ID	Conc mg/L	%Prec	Mean Abs	Replicates		
CAL ZERO	0.000	10.8	0.0025	0.0025	4/26/06	2:18:08 PM
STANDARD 1	2.000	1.0	0.1570	0.1570	4/26/06	2:18:28 PM
STANDARD 2	4.000	1.0	0.2585	0.2585	4/26/06	2:18:46 PM
STANDARD 3	6.000	1.0	0.3354	0.3354	4/26/06	2:19:04 PM

New Rational - Cal. Set 1
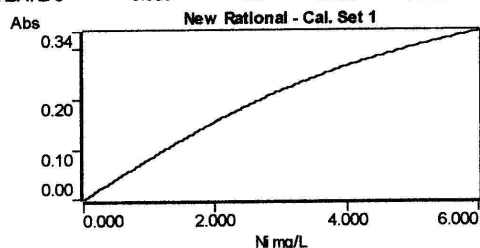
Curve Fit	= New Rational
Characteristic Conc	= 0.056 mg/L
r	= 1.0000
Calculated Conc	= 0.032 2.042 3.863
Residuals	= -0.032 -0.042 0.137

Sample ID	Conc mg/L	%Prec	Mean Abs	Replicates		
N-.25-A-1-0	-0.031	>100	-0.0025	-0.0025	4/26/06	2:19:32 PM
N-.25-A-1-5	-0.028	90.4	-0.0022	-0.0022	4/26/06	2:19:58 PM
N-.25-A-1-8	0.015	5.9	0.0012	0.0012	4/26/06	2:20:22 PM
N-.25-A-1-24	0.155	1.7	0.0123	0.0123	4/26/06	2:20:46 PM
N-.25-A-1-48	0.259	1.0	0.0206	0.0206	4/26/06	2:21:10 PM
N-.25-A-1-72	0.335	1.0	0.0267	0.0267	4/26/06	2:21:32 PM
N-.25-A-1-96	0.396	1.0	0.0315	0.0315	4/26/06	2:21:50 PM
N-.25-A-1-120	0.453	1.0	0.0361	0.0361	4/26/06	2:22:08 PM
N-.25-A-1-120P	0.450	1.0	0.0359	0.0359	4/26/06	2:22:30 PM
4 PPM STANDARD	3.791	1.0	0.2553	0.2553	4/26/06	2:22:48 PM

Analyst	DAVID
Date Started	12:25 PM 4/26/06
Worksheet	N-.25-A-2
Comment	
Methods	Ni

Method: Ni (Flame)

Sample ID	Conc mg/L	%Prec	Mean Abs	Replicates		
CAL ZERO	0.000	0.0	-0.0000	-0.0000	4/26/06	2:30:08 PM
STANDARD 1	2.000	1.0	0.1617	0.1617	4/26/06	2:30:26 PM
STANDARD 2	4.000	1.0	0.2564	0.2564	4/26/06	2:30:44 PM
STANDARD 3	6.000	1.0	0.3265	0.3265	4/26/06	2:31:00 PM

New Rational - Cal. Set 1
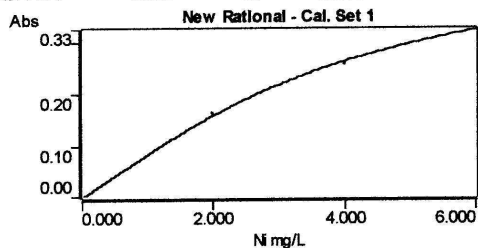
Curve Fit	= New Rational
Characteristic Conc	= 0.054 mg/L
r	= 0.9999
Calculated Conc	= -0.001 2.049 3.828
Residuals	= 0.001 -0.049 0.172

Sample ID	Conc mg/L	%Prec	Mean Abs	Replicates		
N-.25-A-2-0	0.020	18.1	0.0016	0.0016	4/26/06	2:31:24 PM
N-.25-A-2-5	0.010	33.1	0.0008	0.0008	4/26/06	2:31:50 PM
N-.25-A-2-8	0.020	13.1	0.0017	0.0017	4/26/06	2:32:16 PM
N-.25-A-2-24	0.059	4.8	0.0048	0.0048	4/26/06	2:32:40 PM
N-.25-A-2-48	0.102	2.9	0.0083	0.0083	4/26/06	2:33:04 PM
N-.25-A-2-72	0.145	2.1	0.0118	0.0118	4/26/06	2:33:30 PM
N-.25-A-2-96	0.207	1.4	0.0170	0.0170	4/26/06	2:33:54 PM
N-.25-A-2-120	0.273	1.1	0.0224	0.0224	4/26/06	2:34:18 PM
N-.25-A-2-120P	0.271	1.1	0.0223	0.0223	4/26/06	2:34:44 PM
4 PPM STANDARD	3.661	1.0	0.2494	0.2494	4/26/06	2:35:00 PM

Analyst	DAVID
Date Started	12:36 PM 4/26/06
Worksheet	N-.085-A-1
Comment	
Methods	Ni

Method: Ni (Flame)

Sample ID	Conc mg/L	%Prec	Mean Abs	Replicates		
CAL ZERO	0.000	0.0	-0.0001	-0.0001	4/26/06	2:40:54 PM
STANDARD 1	2.000	1.0	0.1556	0.1556	4/26/06	2:41:12 PM
STANDARD 2	4.000	1.0	0.2552	0.2552	4/26/06	2:41:30 PM
STANDARD 3	6.000	0.9	0.3339	0.3339	4/26/06	2:41:48 PM

Abs — New Rational - Cal. Set 1 — Ni mg/L
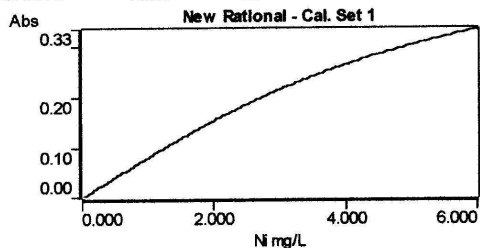
Curve Fit	=	New Rational
Characteristic Conc	=	0.056 mg/L
r	=	1.0000
Calculated Conc	=	-0.002 2.050 3.843
Residuals	=	0.002 -0.050 0.157

Sample ID	Conc mg/L	%Prec	Mean Abs	Replicates		
N-.085-A-1-0	-0.002	0.0	-0.0002	-0.0002	4/26/06	2:42:14 PM
N-.085-A-1-5	0.014	25.0	0.0011	0.0011	4/26/06	2:42:38 PM
N-.085-A-1-8	-0.006	0.0	-0.0005	-0.0005	4/26/06	2:43:04 PM
N-.085-A-1-24	-0.007	0.0	-0.0006	-0.0006	4/26/06	2:43:28 PM
N-.085-A-1-48	0.003	>100	0.0003	0.0003	4/26/06	2:43:54 PM
N-.085-A-1-72	-0.014	0.0	-0.0011	-0.0011	4/26/06	2:44:18 PM
N-.085-A-1-96	-0.003	0.0	-0.0003	-0.0003	4/26/06	2:44:42 PM
N-.085-A-1-120	0.008	49.9	0.0006	0.0006	4/26/06	2:45:08 PM
N-.085-A-1-120P	0.010	38.1	0.0008	0.0008	4/26/06	2:45:32 PM
4 PPM STANDARD	3.493	1.0	0.2390	0.2390	4/26/06	2:45:50 PM

136

Analyst	DAVID
Date Started	1:05 PM 4/26/06
Worksheet	N-.085-A-2
Comment	
Methods	Ni

Method: Ni (Flame)

Sample ID	Conc mg/L	%Prec	Mean Abs	Replicates		
CAL ZERO	0.000	18.8	0.0014	0.0014	4/26/06	1:10:26 PM
STANDARD 1	2.000	0.9	0.1643	0.1643	4/26/06	1:10:46 PM
STANDARD 2	4.000	0.9	0.2485	0.2485	4/26/06	1:11:04 PM
STANDARD 3	6.000	0.9	0.3215	0.3215	4/26/06	1:11:30 PM

New Rational - Cal. Set 1
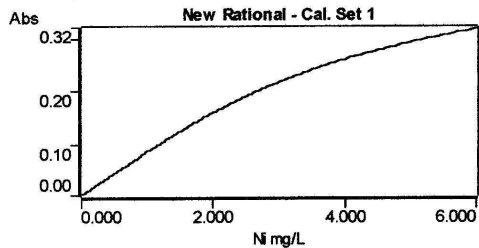
Curve Fit	=	New Rational
Characteristic Conc	=	0.053 mg/L
r	=	0.9998
Calculated Conc	=	0.017 2.088 3.707
Residuals	=	-0.017 -0.088 0.293

Sample ID	Conc mg/L	%Prec	Mean Abs	Replicates		
N-.085-A-2-0	0.005	12.1	0.0004	0.0004	4/26/06	1:11:58 PM
N-.085-A-2-5	0.010	10.9	0.0008	0.0008	4/26/06	1:12:24 PM
N-.085-A-2-8	-0.009	35.5	-0.0008	-0.0008	4/26/06	1:12:50 PM
N-.085-A-2-24	-0.014	77.3	-0.0011	-0.0011	4/26/06	1:13:16 PM
N-.085-A-2-48	0.009	10.1	0.0008	0.0008	4/26/06	1:13:44 PM
N-.085-A-2-72	-0.002	16.6	-0.0001	-0.0001	4/26/06	1:14:08 PM
N-.085-A-2-96	0.025	7.5	0.0020	0.0020	4/26/06	1:14:34 PM
N-.085-A-2-120	0.028	7.3	0.0024	0.0024	4/26/06	1:14:58 PM
N-.085-A-2-120P	0.012	11.2	0.0010	0.0010	4/26/06	1:15:22 PM
4 PPM STANDARD	3.709	1.0	0.2485	0.2485	4/26/06	1:15:40 PM

137

Analyst	DAVID
Date Started	1:17 PM 4/26/06
Worksheet	N-.5-W-1
Comment	
Methods	Ni

Method: Ni (Flame)

Sample ID	Conc mg/L	%Prec	Mean Abs	Replicates		
CAL ZERO	0.000	6.7	0.0034	0.0034	4/26/06	1:20:56 PM
STANDARD 1	2.000	1.0	0.1499	0.1499	4/26/06	1:21:12 PM
STANDARD 2	4.000	0.9	0.2322	0.2322	4/26/06	1:21:30 PM
STANDARD 3	6.000	1.0	0.3035	0.3035	4/26/06	1:21:46 PM

Abs — New Rational - Cal. Set 1 — Ni mg/L
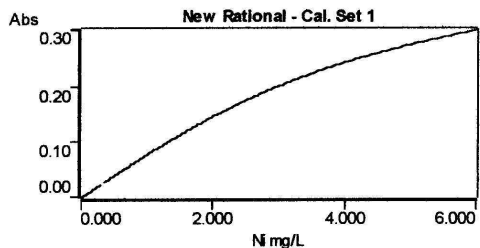
Curve Fit	= New Rational
Characteristic Conc	= 0.058 mg/L
r	= 0.9999
Calculated Conc	= 0.045 2.081 3.738
Residuals	= -0.045 -0.081 0.262

Sample ID	Conc mg/L	%Prec	Mean Abs	Replicates		
N-.5-W-1-0	0.324	1.0	0.0247	0.0247	4/26/06	1:22:08 PM
N-.5-W-1-5	0.326	1.0	0.0248	0.0248	4/26/06	1:22:30 PM
N-.5-W-1-8	0.370	1.0	0.0282	0.0282	4/26/06	1:22:48 PM
N-.5-W-1-24	0.184	1.9	0.0140	0.0140	4/26/06	1:23:20 PM
N-.5-W-1-48	0.477	1.0	0.0365	0.0365	4/26/06	1:23:36 PM
N-.5-W-1-72	0.540	1.0	0.0412	0.0412	4/26/06	1:24:08 PM
N-.5-W-1-96	0.591	1.0	0.0452	0.0452	4/26/06	1:24:24 PM
N-.5-W-1-120	0.621	1.0	0.0475	0.0475	4/26/06	1:24:42 PM
N-.5-W-1-120P	0.621	1.0	0.0475	0.0475	4/26/06	1:25:00 PM
4 PPM STANDARD	4.481	1.0	0.2586	0.2586	4/26/06	1:25:18 PM

Analyst	DAVID
Date Started	1:27 PM 4/26/06
Worksheet	N-.25-W-1
Comment	
Methods	Ni

Method: Ni (Flame)

Sample ID	Conc mg/L	%Prec	Mean Abs	Replicates		
CAL ZERO	0.000	0.0	-0.0001	-0.0001	4/26/06	1:31:00 PM
STANDARD 1	2.000	1.0	0.1536	0.1536	4/26/06	1:31:18 PM
STANDARD 2	4.000	1.0	0.2703	0.2703	4/26/06	1:31:34 PM
STANDARD 3	6.000	0.9	0.3261	0.3261	4/26/06	1:31:50 PM

New Rational - Cal. Set 1
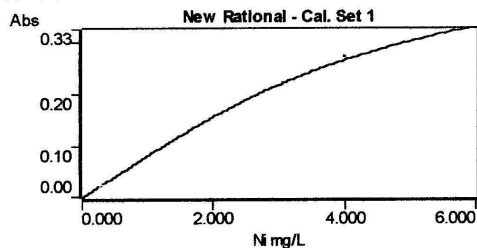
Curve Fit	= New Rational
Characteristic Conc	= 0.057 mg/L
r	= 1.0000
Calculated Conc	= -0.001 1.970 4.124 5.876
Residuals	= 0.001 0.030 -0.124 0.124

Sample ID	Conc mg/L	%Prec	Mean Abs	Replicates		
N-.25-W-1-0	0.295	1.0	0.0231	0.0231	4/26/06	1:32:12 PM
N-.25-W-1-5	0.319	1.0	0.0249	0.0249	4/26/06	1:32:38 PM
N-.25-W-1-8	0.303	1.0	0.0237	0.0237	4/26/06	1:33:02 PM
N-.25-W-1-24	0.311	1.0	0.0243	0.0243	4/26/06	1:33:24 PM
N-.25-W-1-48	0.340	1.0	0.0266	0.0266	4/26/06	1:33:58 PM
N-.25-W-1-72	0.394	1.0	0.0309	0.0309	4/26/06	1:34:20 PM
N-.25-W-1-96	0.399	1.0	0.0313	0.0313	4/26/06	1:34:44 PM
N-.25-W-1-120	0.415	1.0	0.0326	0.0326	4/26/06	1:35:12 PM
N-.25-W-1-120P	0.416	1.0	0.0326	0.0326	4/26/06	1:35:32 PM
4 PPM STANDARD	4.383	0.7	0.2803	0.2803	4/26/06	1:35:48 PM

139

Analyst	DAVID
Date Started	9:10 AM 4/26/06
Worksheet	N-.085-W-1
Comment	
Methods	Ni

Method: Ni (Flame)

Sample ID	Conc mg/L	%Prec	Mean Abs	Replicates		
CAL ZERO	0.000	8.8	0.0027	0.0027	4/26/06	9:22:20 AM
STANDARD 1	2.000	0.9	0.1652	0.1652	4/26/06	9:22:36 AM
STANDARD 2	4.000	1.0	0.2660	0.2660	4/26/06	9:22:54 AM
STANDARD 3	6.000	1.0	0.3494	0.3494	4/26/06	9:23:10 AM

New Rational - Cal. Set 1
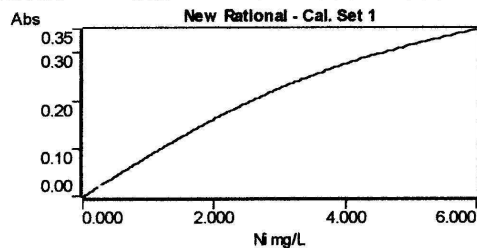
Curve Fit	= New Rational
Characteristic Conc	= 0.053 mg/L
r	= 0.9999
Calculated Conc	= 0.033 2.063 3.802
Residuals	= -0.033 -0.063 0.198

Sample ID	Conc mg/L	%Prec	Mean Abs	Replicates		
N-.085-W-1-0	0.268	1.0	0.0224	0.0224	4/26/06	9:23:34 AM
N-.085-W-1-5	0.285	1.1	0.0239	0.0239	4/26/06	9:24:00 AM
N-.085-W-1-8	0.243	1.0	0.0204	0.0204	4/26/06	9:24:26 AM
N-.085-W-1-24	0.260	1.1	0.0218	0.0218	4/26/06	9:24:52 AM
N-.085-W-1-48	0.265	1.0	0.0221	0.0221	4/26/06	9:25:16 AM
N-.085-W-1-72	0.271	1.0	0.0227	0.0227	4/26/06	9:25:42 AM
N-.085-W-1-96	0.239	1.0	0.0200	0.0200	4/28/06	9:26:06 AM
N-.085-W-1-120	0.255	1.1	0.0214	0.0214	4/26/06	9:26:34 AM
N-.085-W-1-120P	0.279	1.0	0.0234	0.0234	4/26/06	9:26:58 AM
4 PPM STANDARD	3.911	1.0	0.2710	0.2710	4/26/06	9:27:20 AM

140

Appendix C

Stress-Strain Diagrams for Steel Specimens
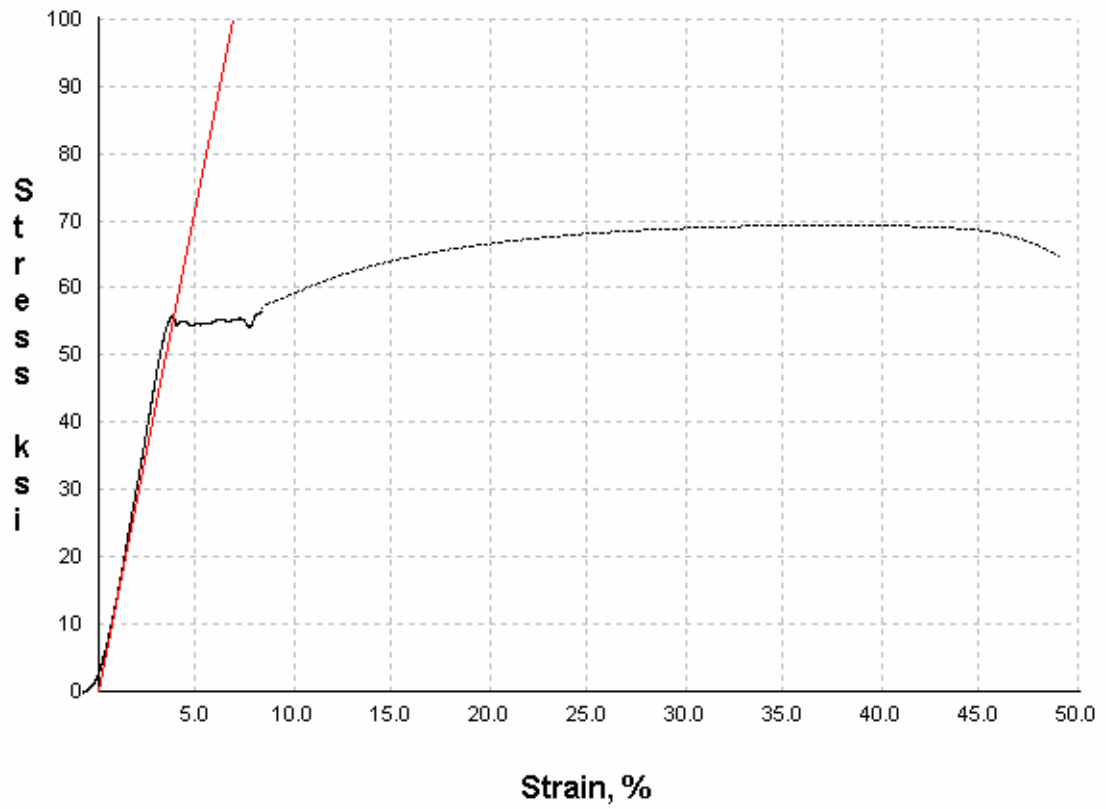
Figure C.1 Stress-strain diagram for specimen S-F-0-1-0
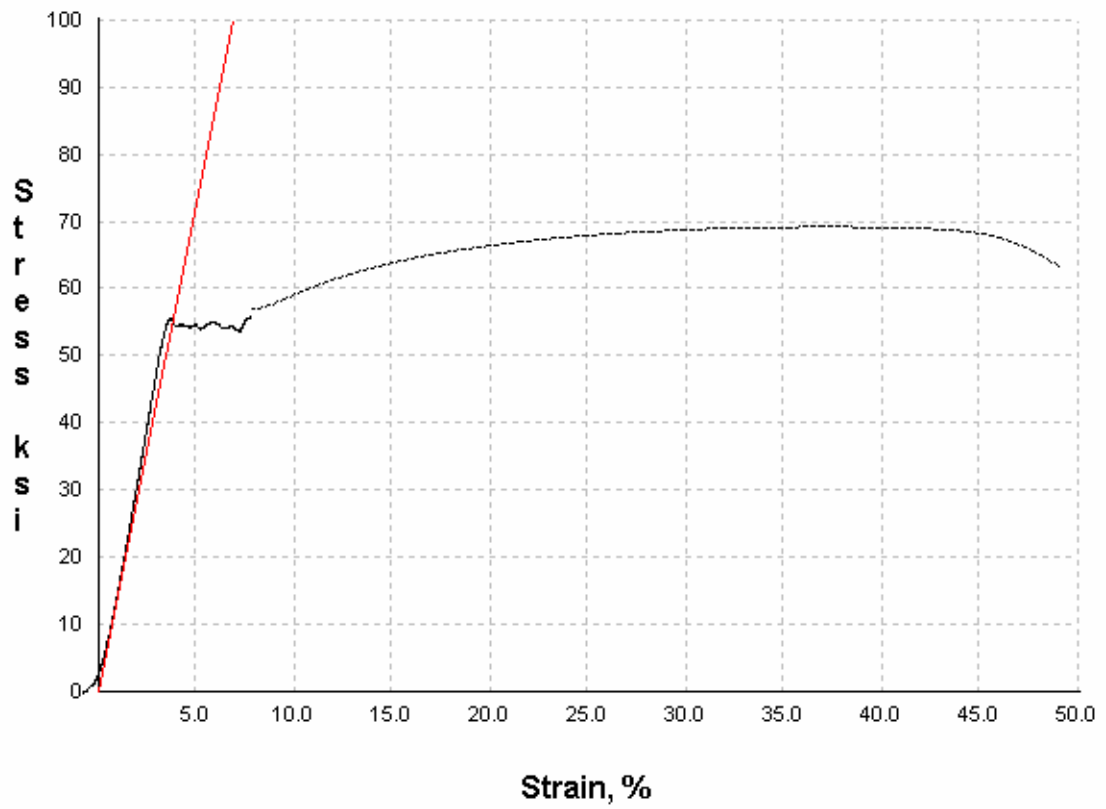
Figure C.2 Stress-strain diagram for specimen S-F-0-2-0
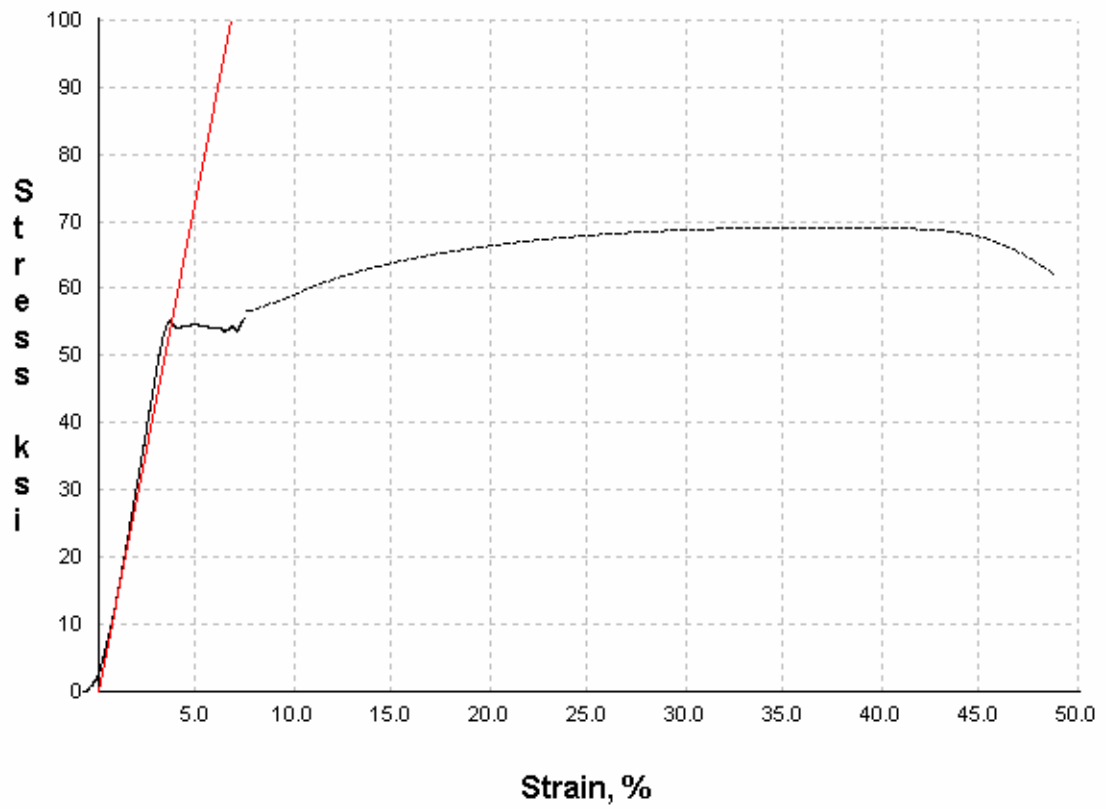
Figure C.3 Stress-strain diagram for specimen S-F-A-1-120
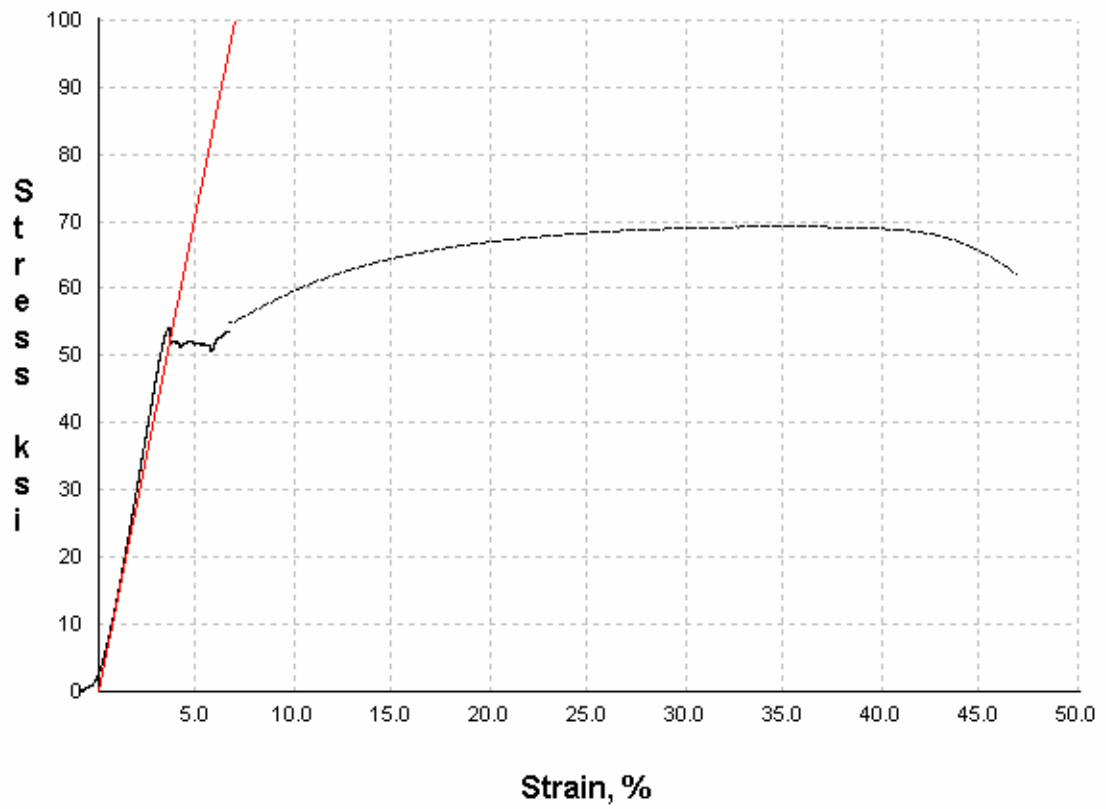
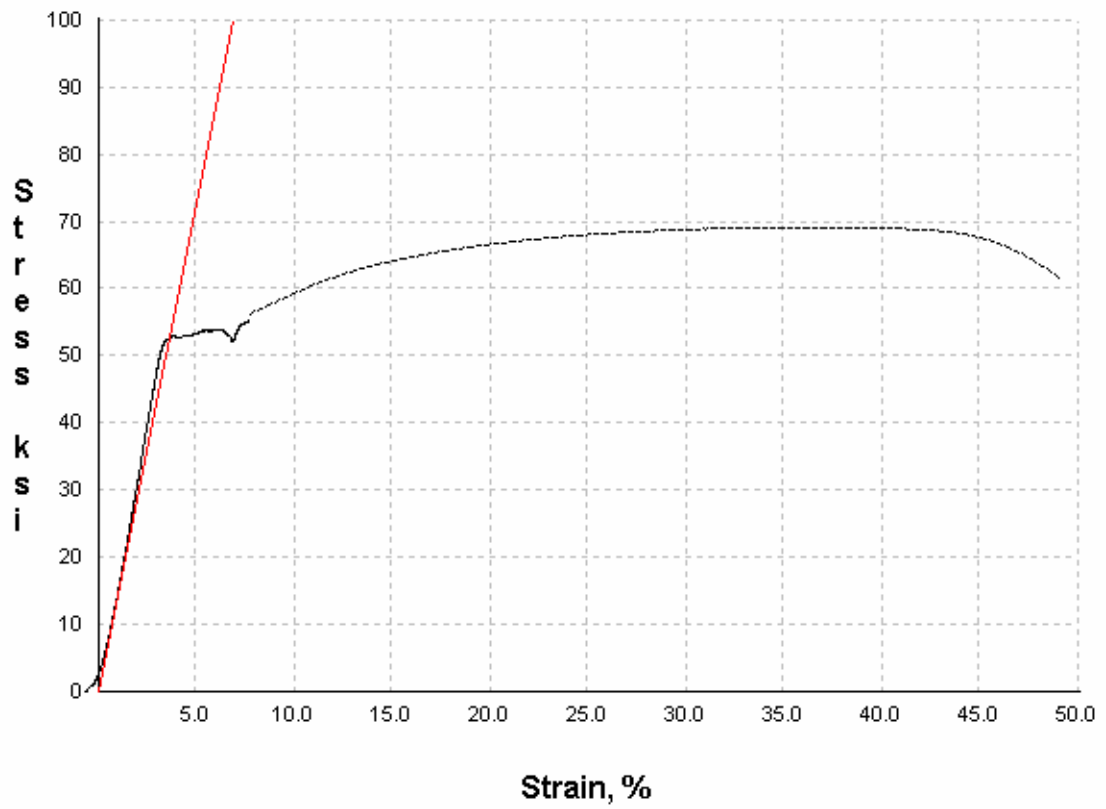Figure C.4 Stress-strain diagram for specimen S-F-A-2-120

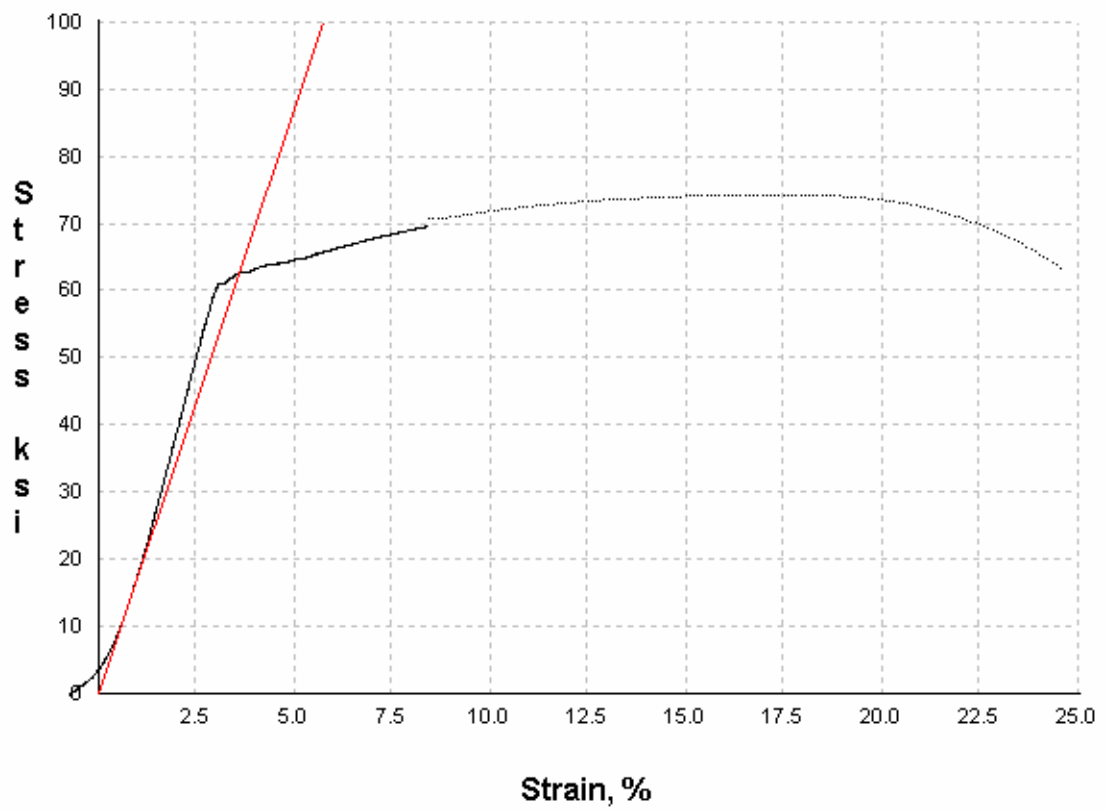Figure C.5 Stress-strain diagram for specimen S-F-W-1-120

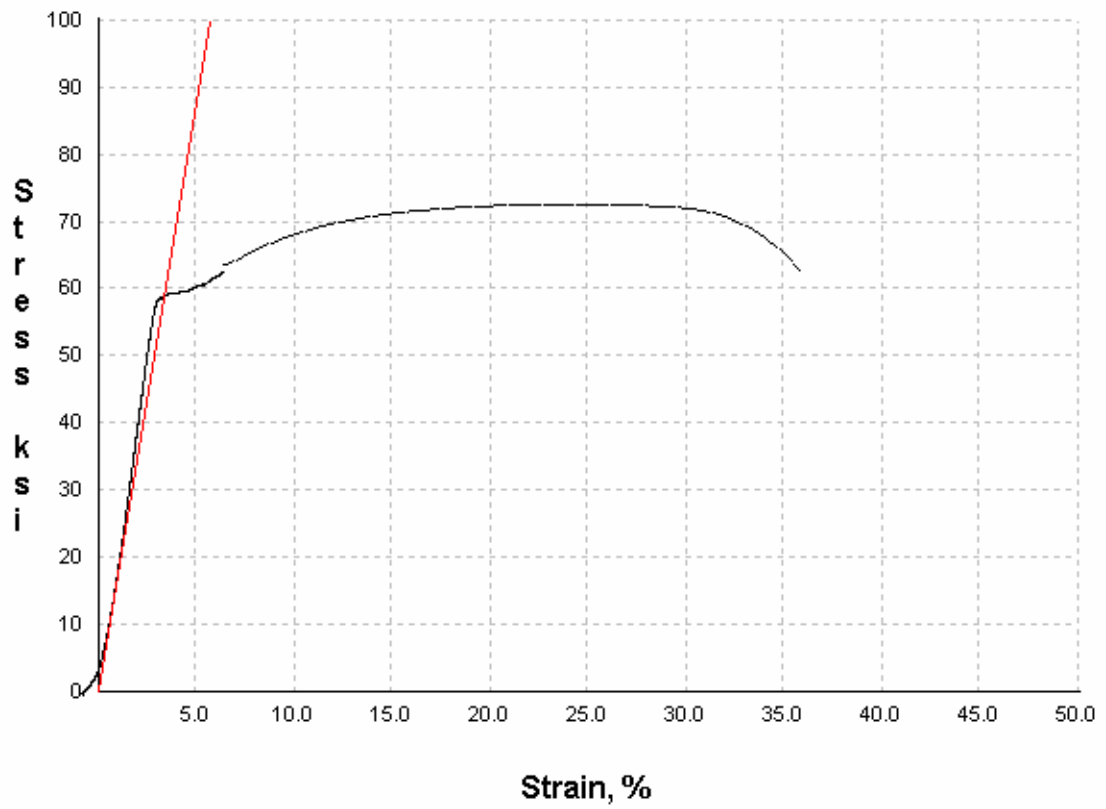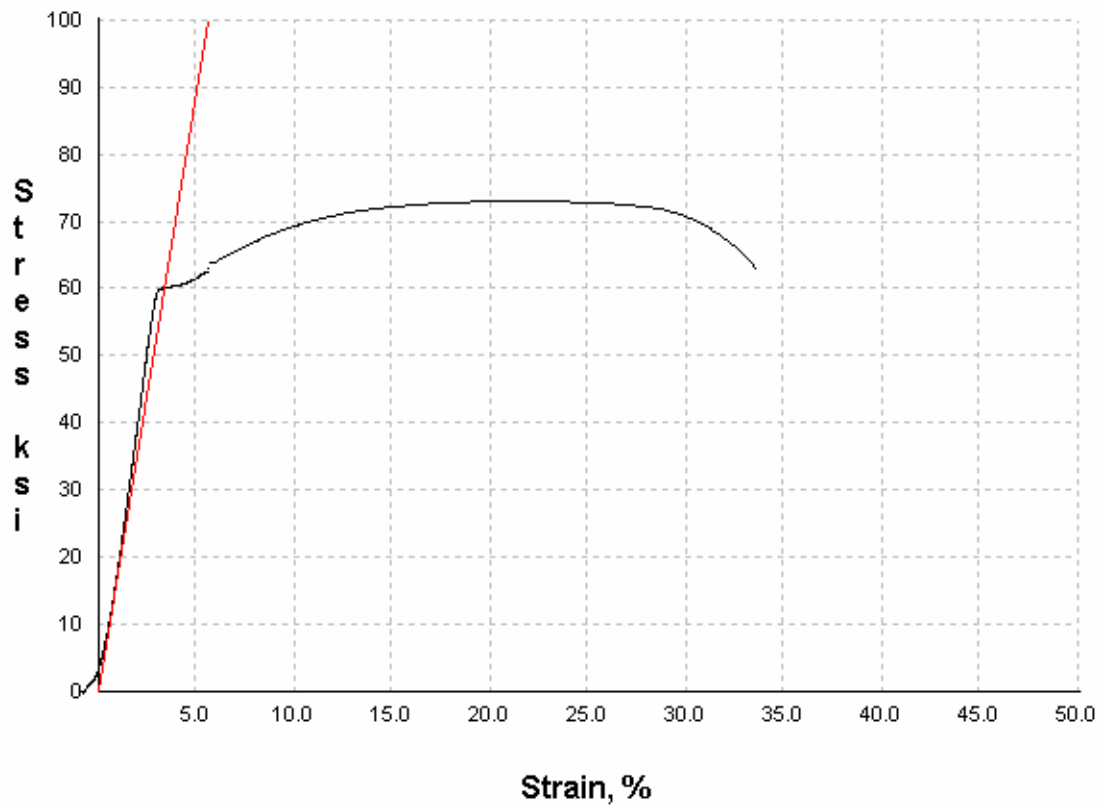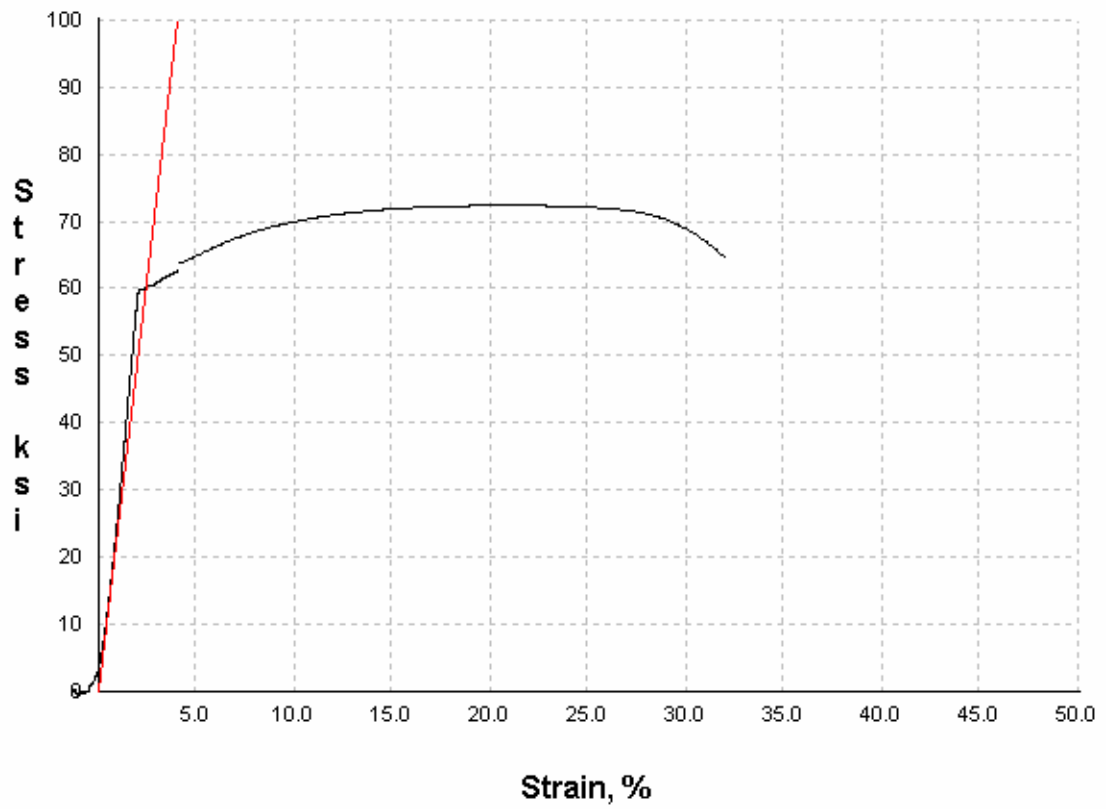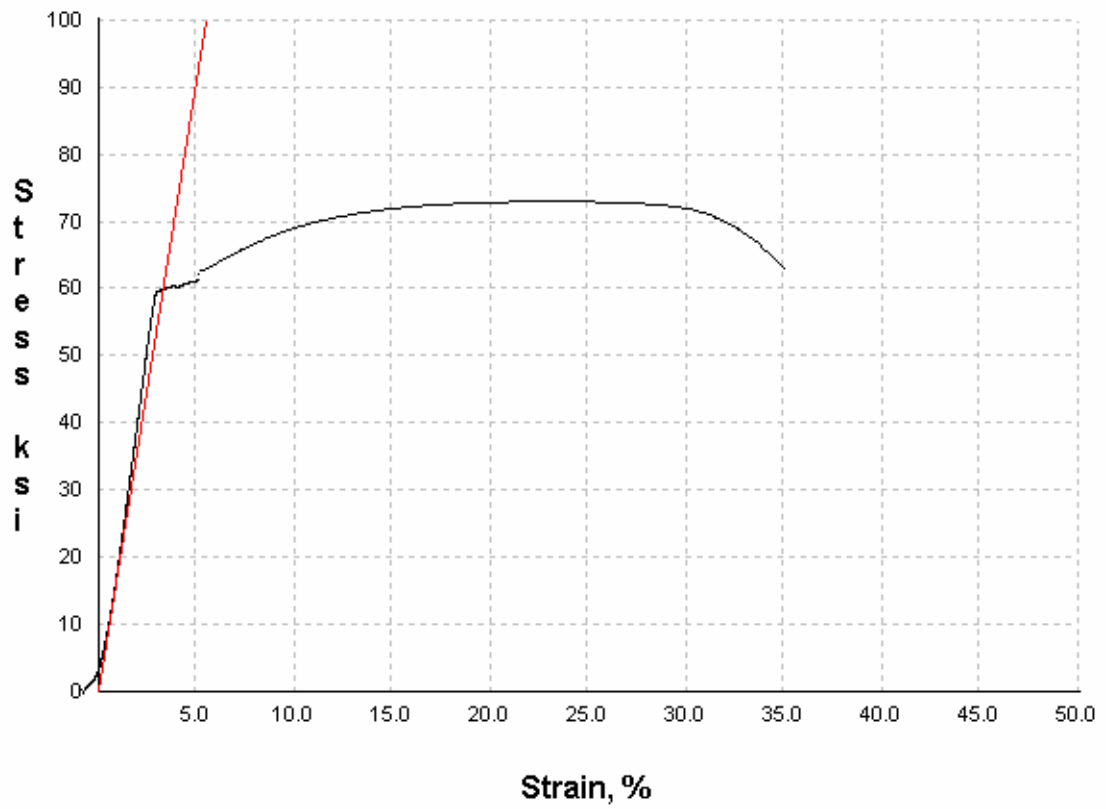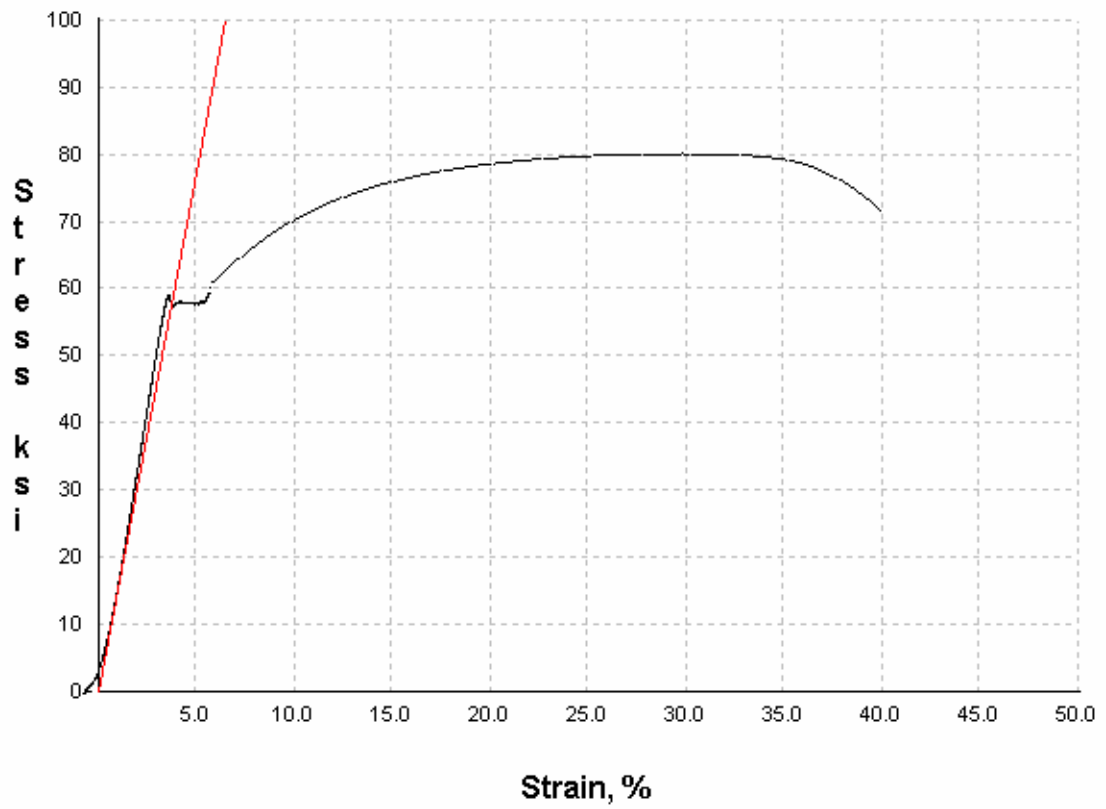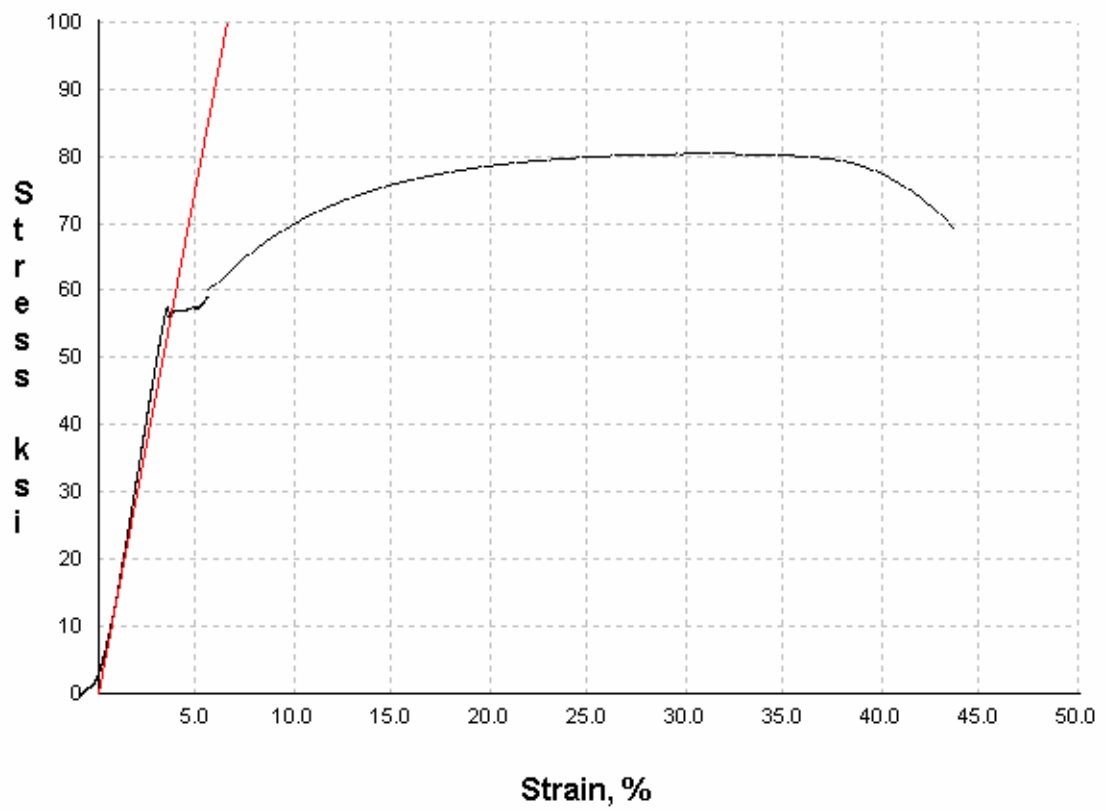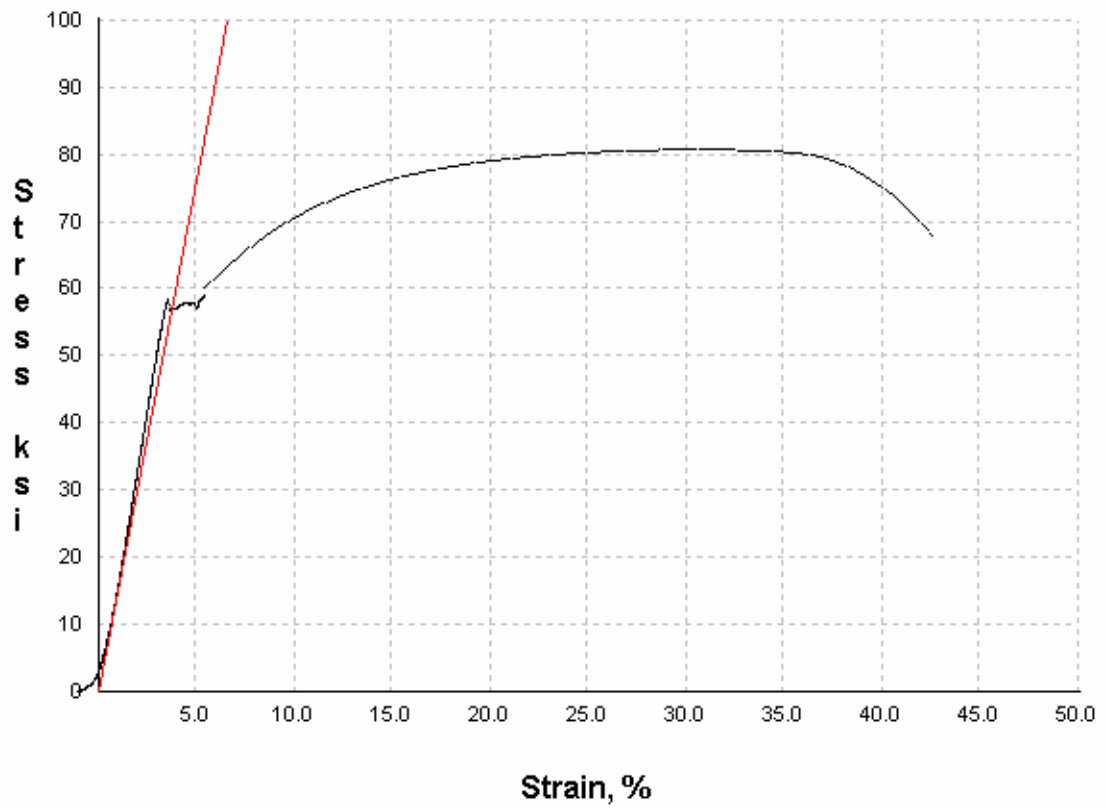Figure C.6 Stress-strain diagram for specimen S-W-0-1-0

Figure C.7 Stress-strain diagram for specimen S-W-0-2-0

Figure C.8 Stress-strain diagram for specimen S-W-A-1-120

Figure C.9 Stress-strain diagram for specimen S-W-A-2-120

Figure C.10 Stress-strain diagram for specimen S-W-W-1-120

Figure C.11 Stress-strain diagram for specimen S-5-0-1-0

Figure C.12 Stress-strain diagram for specimen S-5-0-2-0

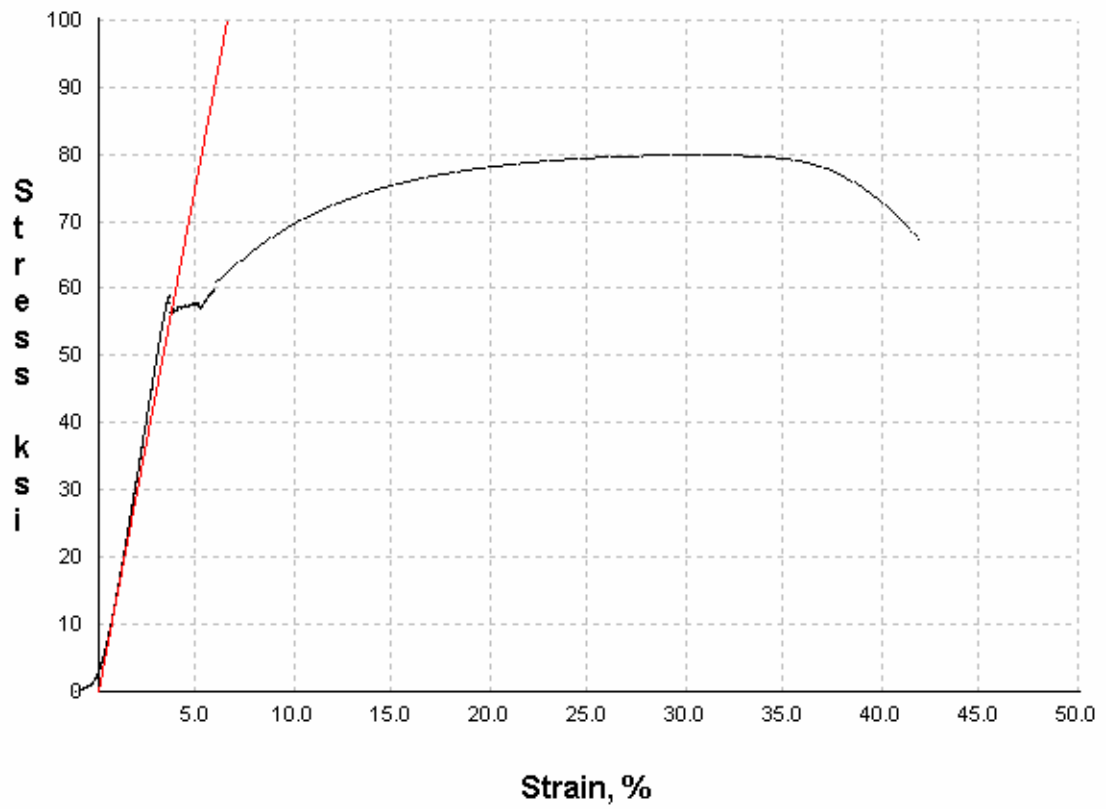Figure C.13 Stress-strain diagram for specimen S-5-A-1-120
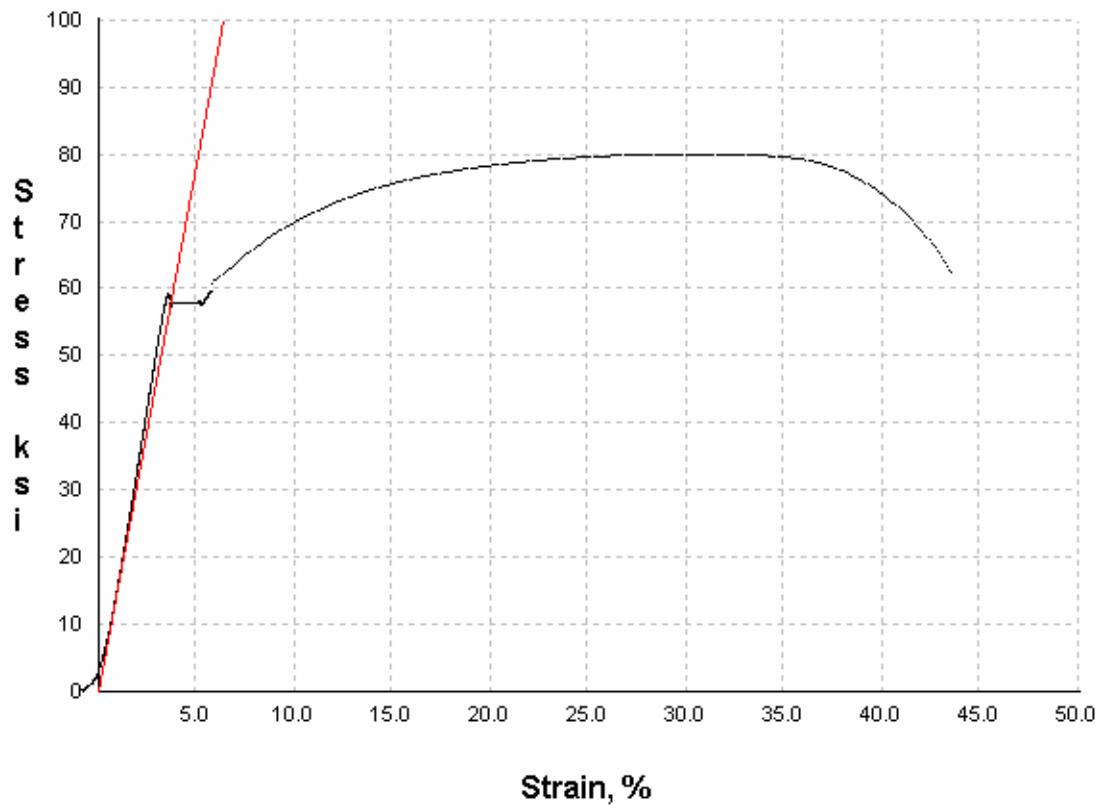
Figure C.14 Stress-strain diagram for specimen S-5-A-2-120

Figure C.15 Stress-strain diagram for specimen S-5-W-1-120